

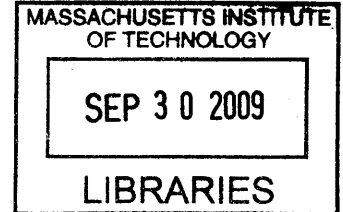
Regulation of Lubricin Gene Expression and Synthesis in Cartilage by  
Mechanical Injury

by

Shuodan Chen

B.S. Electrical Engineering  
Georgia Institute of Technology, 2003

M.S. Electrical Engineering  
Massachusetts Institute of Technology, 2005



SUBMITTED TO THE DEPARTMENT OF  
ELECTRICAL ENGINEERING AND COMPUTER SCIENCE  
IN PARTIAL FULFILLMENT OF THE REQUIREMENTS FOR THE DEGREE OF

DOCTORATE OF PHILOSOPHY IN  
ELECTRICAL ENGINEERING AND COMPUTER SCIENCE

AT THE  
MASSACHUSETTS INSTITUTE OF TECHNOLOGY

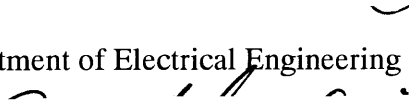
SEPTEMBER 2009

**ARCHIVES**

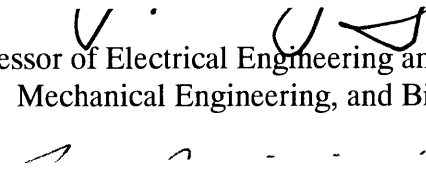
© 2009 Massachusetts Institute of Technology. All rights reserved.

The author hereby grants to MIT permission to reproduce and to distribute publicly paper and  
electronic copies of this thesis document in whole or in part.

Signature of Author: \_\_\_\_\_

  
Shuodan Chen  
Department of Electrical Engineering and Computer Science

Certified by: \_\_\_\_\_

  
Alan J. Grodzinsky  
Professor of Electrical Engineering and Computer Science,  
Mechanical Engineering, and Biological Engineering  
Thesis Supervisor

Accepted by: \_\_\_\_\_

  
Terry Orlando  
Chairman, EECS Department Committee on Graduate Students

# Regulation of Lubricin Gene Expression and Synthesis in Cartilage by Mechanical Injury

by

Shuodan Chen

Submitted to the Department of Electrical Engineering and Computer Science  
On September 4, 2009 in Partial Fulfillment of the Requirements for the Degree of  
Doctorate of Philosophy in Electrical Engineering and Computer Science

## ABSTRACT

Articular cartilage is the connective tissue which lines the bony ends of diarthrodial joints to provide load distribution and frictionless motion. Lubricin, a glycoprotein which concentrates at the superficial layer of the cartilage, contributes to the low friction coefficient. Mechanical injury to cartilage increases the risk of osteoarthritis (OA), characterized by degradation of articular cartilage starting with the articular surface. The objectives of this study were to quantify the effects of injurious compression on the surface mechanical properties of cartilage, and lubricin gene expression and synthesis using an *in vitro* organ culture model. Furthermore, the role of TGF- $\beta$  signaling in the induction of lubricin gene expression and protein secretion from cartilage explants following mechanical injury was analyzed. Cartilage disks with intact superficial zone from the patellofemoral grooves of 1-2 wk old bovine knees were cultured in either free swelling conditions or subjected to injurious compression using a range of applied strains and strain rates. Mechanical injury was found to elevate the friction coefficient of cartilage. Average surface roughness of cartilage superficial zone was increased by the combination of injury and subsequent oscillating shear motion at the surface superimposed on an applied normal strain. RNA extraction and qRT-PCR were conducted sequentially to determine the expression of lubricin and other relevant cartilage genes. Western blotting and ELISA were used to assess protein expression. Lubricin gene expression and secretion increased two days after injury. This finding, plus the fact that injury and TGF- $\beta$  are each known to increase lubricin expression, suggested that the TGF- $\beta$  signaling pathway may be a mechanism through which injury induces lubricin expression. We therefore tested the hypothesis that blocking the TGF- $\beta$  pathway would suppress the increase in lubricin gene expression and protein secretion caused by injurious compression of cartilage. Indeed, lubricin gene expression and protein secretion were reduced after blocking TGF- $\beta$  compared to injury alone. Together, these results show that surface damage caused injury and sliding motion can be ameliorated by the presence of lubricin on the cartilage surface. The TGF- $\beta$  pathway is an important mechanism in regulating the increased lubricin gene expression and secretion that result from injury.

Thesis Supervisor: Dr. Alan J. Grodzinsky

Title: Professor of Electrical Engineering & Computer Science,  
Mechanical Engineering, and Biological Engineering

## Acknowledgements

Going through graduate school is like savoring a piece of dark chocolate with at least 85% cocoa. There are bitter/tangy notes and sweet notes, but the overall experience was rich and creamy. If you consistently eat dark chocolates for about six years, the health benefits are endless. If they are paired with the signature coffee from our lab, you will live a long and happy life. ☺

My deepest gratitude goes to Dr. Alan Grodzinsky, my advisor, for making my graduate experience truly phenomenal and memorable. He inspires us, his students, to conduct quality research while celebrating life and having fun! Anyone who comes through the glass doors to our lab will surely be greeted by sounds of laughter and the smell of coffee as we gather around the table to hear about AI's latest conference trip or his insight on current research. He constantly reassures us of his confidence in our research prospects through his encouragement. His dedication to teaching is only matched by his genuine care for all his students. After each individual or group meeting, I have renewed motivation for our research and respect for AI's acumen regarding everyone's research. Watching his interaction with people is the greatest lesson in professionalism, compassion, diplomacy, and humility.

The three pillars of our lab are Dr. Eliot Frank, Ms. Han-Hwa Hung, and Ms. Linda Bragman. Eliot is our indispensable engineer who built all the necessary machines that made our research possible. He taught me a great deal in mechanical design, assembly, electrical circuitry and other engineering concepts. Han-Hwa is our lab manager who trained me in proper techniques when I joined the lab. I often sought her advice when planning out my experiments. Linda is the genie who removes all the administrative worries from the graduate students so we can concentrate on our work. They brighten the lab with their liveliness and humor! ☺

My labmates, past and present, are the key ingredients to my learning experience in this lab. Delphine offered much wisdom on the EECS graduate student path; Laurel sat next to me and was very motivational during my Master's work; Jon (Fitzy) patiently gave me technical guidance during the initial stage of my research; and Lin introduced me to this lab when we took 6.561 together. Furthermore, I want to thank Berndt, Eric, Paul, Rachel, Yi, Bo Bae, Sanwong, and Hsu-Yi for helping me think through ideas and experiments. I feel extremely privileged to have enjoyed many insightful discussions with them!

Next, I would like to thank my committee members, Dr. Carl Flannery from Wyeth Research and Dr. Dennis Freeman, for their inputs during my research. Carl has been a constant to offer his expertise on lubricin throughout my collaborations with Wyeth, Cornell, and UCSD. Denny offered me excellent advice during my RQE and guidance throughout my doctorate work.

My research would not be as wholesome had it not included the contributions from my collaborators. For the lubricin and injury study, Dr. Aled Jones and Dr. Carl Flannery from Wyeth Research worked with me on the initial lubricin gene and protein expressions. Then, Natalie Galley, Dr. Jason Gleghorn, and Dr. Larry Bonassar from Cornell University teamed with me to evaluate the surface properties of the articular cartilage surface post injury. Finally, Hoa Nyguen and Dr. Bob Sah from UCSD helped me with lubricin ELISA. For my confocal imaging study of chondrocytes, I would like to thank Dr. James Evans in Whitehead Center of Bioimaging for his expertise on fluorescent microscopy and Dr. Eliot Frank for his guidance during the design and assembly of the microscope stage actuator.

Last, but not least, I would like to thank my family for their encompassing love and pep talk, especially to my parents and paternal grandparents. I was first inspired to obtain a PhD when I watched my father receive his doctorate degree in that black velvet regalia with the signature triple bands embroidered on the sleeves. Back then, I only saw the triumph associated with that academic honor. Now, I have a better appreciation for the journey taken to earn that degree. Looking back over the last six years, being a student in this great university has been a fulfilling and humbling experience. It allowed me to develop very valuable academic and research skills, expand my interests, and make some quality, life long friends. The dark chocolate years spent at MIT will be the foundation for me to embrace and explore new frontiers!

# CONTENTS

<b>1</b>	<b>INTRODUCTION .....</b>	<b>8</b>
1.1	CARTILAGE STRUCTURES AND MECHANICAL PROPERTIES .....	8
1.1.1	<i>Aggrecan</i> .....	9
1.1.2	<i>Collagen</i> .....	10
1.1.3	<i>Lubricin</i> .....	11
1.2	MECHANICAL REGULATION OF THE STRUCTURE .....	12
1.3	SIGNIFICANCE OF LUBRICIN TO MECHANICAL LOADING OF CARTILAGE .....	14
1.4	IMPACT OF INJURY .....	14
1.4.1	<i>In vivo Injury Models and Lubricin</i> .....	15
1.4.2	<i>In vitro Injury Model</i> .....	16
1.5	OBJECTIVES .....	16
1.6	BIBLIOGRAPHY.....	18
<b>2</b>	<b>EFFECT OF INJURY ON CARTILAGE SURFACE PROPERTIES.....</b>	<b>21</b>
2.1	INTRODUCTION .....	21
2.1.1	<i>Description of the in vitro injury model</i> .....	21
2.1.2	<i>Boundary Mode Lubrication</i> .....	24
2.2	METHODS.....	25
2.2.1	<i>Harvesting Cartilage Explants</i> .....	25
2.2.2	<i>Injurious compression</i> .....	25
2.2.3	<i>Dynamic Shear</i> .....	26
2.2.4	<i>Friction Test</i> .....	26
2.2.5	<i>Surface Roughness</i> .....	27
2.2.6	<i>Equilibrium Modulus</i> .....	27
2.2.7	<i>Environmental Scanning Electron Microscope (ESEM) Images</i> .....	28
2.2.8	<i>Statistics</i> .....	28
2.3	RESULTS .....	28
2.4	DISCUSSION .....	33
2.5	BIBLIOGRAPHY.....	35
<b>3</b>	<b>EFFECT OF INJURY ON LUBRICIN SYNTHESIS FROM CARTILAGE.....</b>	<b>37</b>
3.1	INTRODUCTION .....	37
3.2	METHODS.....	38
3.2.1	<i>Harvest and Injurious Compression</i> .....	38
3.2.2	<i>Lubricin Gene Expression</i> .....	38
3.2.3	<i>Lubricin Protein Secretion</i> .....	39
3.2.4	<i>Lubricin Retained on the Cartilage Surface</i> .....	39
3.2.5	<i>Lubricin Protein Synthesis</i> .....	39
3.2.6	<i>Friction Test Paradigm</i> .....	39
3.3	RESULTS .....	40
3.4	DISCUSSION .....	44
3.5	BIBLIOGRAPHY.....	47
<b>4</b>	<b>INDUCTION OF LUBRICIN EXPRESSION BY MECHANICAL INJURY THROUGH THE TGF-<math>\beta</math> SIGNALING PATHWAY .....</b>	<b>48</b>
4.1	INTRODUCTION .....	48
4.1.1	<i>Canonical TGF-<math>\beta</math> Signaling Pathway</i> .....	48
4.1.2	<i>TGF-<math>\beta</math> Blocker Selection</i> .....	50
4.2	METHODS.....	50
4.2.1	<i>Tissue Harvest</i> .....	50
4.2.2	<i>Strain Dependence of TGF-<math>\beta</math> Gene and Protein Expression</i> .....	50
4.2.3	<i>Effect of SB431542 on Lubricin Gene and Protein Expression of Injured Tissue</i> .....	51
4.2.4	<i>Sulfate Incorporation Rate Analysis</i> .....	52

4.2.5	<i>RNA Isolation and qRT-PCR</i> .....	52
4.2.6	<i>Statistical Analysis</i> .....	52
4.3	RESULTS .....	53
4.4	DISCUSSION .....	57
4.5	BIBLIOGRAPHY.....	58
<b>5</b>	<b>MICROSCOPE STAGE ACTUATOR DESIGN FOR OBSERVING INTRACELLULAR TRANSIENT BEHAVIOR OF CHONDROCYTES UNDER INJURY</b> .....	<b>60</b>
5.1	INTRODUCTION .....	60
5.2	ACTUATOR DESIGN 1.0.....	62
5.2.1	<i>Mechanical Stage Design</i> .....	62
5.2.2	<i>Electrical Circuit Design</i> .....	64
5.3	ACTUATOR DESIGN 2.0: UPGRADE.....	64
5.4	EXPERIMENTAL SETUP.....	66
5.4.1	<i>Harvest</i> .....	66
5.4.2	<i>Dye Application</i> .....	66
5.4.3	<i>Image Aquisition</i> .....	66
5.5	BIBLIOGRAPHY.....	68
<b>6</b>	<b>CONCLUSION</b> .....	<b>70</b>
<b>A.</b>	<b>ARTHRITIS AND RHEUMATISM JOURNAL PUBLICATION</b> .....	<b>71</b>
<b>B.</b>	<b>GENE EXPRESSIONS DUE TO TGF-B BLOCKER</b> .....	<b>95</b>
<b>C.</b>	<b>DERIVATION FOR HYDRAULIC PERMEABILITY</b> .....	<b>96</b>
<b>D.</b>	<b>SCHEMATIC OF THE SOLENOID OUTPUT CIRCUIT FOR ACTUATOR DESIGN</b> .....	<b>99</b>
<b>E.</b>	<b>ILLUSTRATION OF MECHANICAL ACTUATOR 2.0 PLATFORM</b> .....	<b>100</b>

# FIGURES

FIGURE 1.1. A) DIAGRAM OF THE KNEE JOINT [1] AND B) MAIN CONSTITUENTS WITHIN THE BULK OF THE ARTICULAR CARTILAGE .....	8
FIGURE 1.2. AFM IMAGE OF THE FULL LENGTH AGGREGAN MOLECULE (COURTESY OF HSU-YI LEE) .....	9
FIGURE 1.3. A NEGATIVELY CHARGED REPEATING DISACCHARIDE UNIT ON A CHONDROITIN-4 SULFATE GAG CHAIN..	9
FIGURE 1.4 AFM IMAGE OF THE TRIPLE HELICAL COLLAGEN FIBRILS (COURTESY OF DR. LAUREL NG) .....	10
FIGURE 1.5 COLLAGEN NETWORK ORGANIZATION IN DIFFERENT ZONES OF THE ARTICULAR CARTILAGE. [11] .....	10
FIGURE 1.6. LUBRICIN DISTRIBUTION IN ARTICULAR CARTILAGE USING G35 ANTILUBRICIN STAIN [14] .....	11
FIGURE 1.7 LUBRICIN STRUCTURE AND PRG4 GENE TARGETING IN MICE [21].....	12
FIGURE 1.8. POSSIBLE PROGRESSION FROM HEALTHY HUMAN CARTILAGE TO OA RIDDEN CARTILAGE THROUGH INJURY .....	14
FIGURE 2.1 IN HOUSE INJURIOUS LOADING APPARATUS [1] ALONG WITH THE LOADING PROTOCOL WAVEFORMS .....	21
FIGURE 2.2 A) INCREASING STRAIN WHILE KEEPING RAMP TIME CONSTANT B) DIRECTLY INFLUENCES STRAIN RATE AND THE PEAK STRESS WITHIN CARTILAGE .....	22
FIGURE 2.3. B) THE LOCAL STRAIN ( $E_{zz}$ ) AT 10% COMPRESSION, AND C) CONFINED COMPRESSIVE MODULUS ( $H_{AD}$ ) AS A FUNCTION OF DEPTH FROM THE ARTICULAR SURFACE (N=4). (ONLY OBSERVE THE NEWBORN CALF DATA MARKED BY ▲) [3].....	23
FIGURE 2.4 THE STRIBECK CURVE: SHOWING HOW RELATIONSHIP BETWEEN FRICTION COEFFICIENT ( $\mu$ ), VISCOSITY ( $H$ ), SPEED ( $V$ ), AND $P$ (NORMAL LOAD) VARIES IN THE THREE MODES OF LUBRICITON. (DR. J. GLEGHORN).....	24
FIGURE 2.5. HARVESTING PROCEDURE TO EXTRACT L1 AND L2 CARTILAGE DISKS.....	25
FIGURE 2.6 CUSTOM BUILT FRICTION COEFFICIENT TEST APPARATUS [7].....	26
FIGURE 2.7 A) 3-D OPTICAL PROFILOMETER B) AREA OF THE HEIGHT PROFILE THAT IS SCANNED ON THE CARTILAGE DISK.....	27
FIGURE 2.8. EQUILIBRIUM MODULUS OF L1 AND L2 CARTILAGE DISKS. ....	28
FIGURE 2.9. EQUILIBRIUM FRICTION COEFFICIENT OF L1 AND L2 NORMAL AND INJURED CARTILAGE DISKS (N=6). # $\rightarrow$ $p < 0.05$ COMPARED TO L1 CONTROL.....	29
FIGURE 2.10 AVERAGE SURFACE ROUGHNESS AFTER VARIOUS MECHANICAL TREATMENTS. ....	29
FIGURE 2.11 THE HEIGHT PROFILES OF THE 3D PROFILOMETER SCANS FOR SURFACE ROUGHNESS.....	31
FIGURE 2.12. L1 CARTILAGE SURFACE THAT WERE INJURED AT VARIOUS STRAIN RATES. ....	32
FIGURE 2.13. L1 CARTILAGE DISKS THAT WERE INJURED AND FRICTION TESTED, THUS SUBJECTED TO ADDITIONAL LATERAL MOTION SUPERIMPOSED ON NORMAL LOAD. ....	33
FIGURE 3.1. TIMELINE OF THE STEPS TAKEN IN ANALYZING THE GENE EXPRESSION AND PROTEIN SYNTHESIS.....	38
FIGURE 3.2. THE PARADIGM FOR TESTING THE EFFECT OF LUBRICIN ON FRICTION COEFFICIENT. ....	39
FIGURE 3.3. LUBRICIN GENE EXPRESSION OF L1 AND L2 CARTILAGE DAYS AFTER INJURY (N=3 ANIMALS; MEAN $\pm$ SEM; * $\rightarrow$ $p < 0.05$ ).....	40
FIGURE 3.4. WESTERN BLOT OF A) LUBRICIN PROTEIN SECRETION INTO THE MEDIUM AND B) LUBRICIN EXTRACTED FROM L1 CARTILAGE 2 DAYS AFTER INJURY .....	41
FIGURE 3.5. IMMUNOHISTOCHEMICAL STAIN OF LUBRICIN IN L1 NORMAL AND INJURED CARTILAGE 2 DAYS AFTER INJURY USING G35 ANTILUBRICIN STAIN .....	42
FIGURE 3.6. GAG STAINED WITH SAFRANIN O (SHOWN IN 1 <sup>ST</sup> AND 3 <sup>RD</sup> ROWS) AND COLLAGEN STAINED WITH TRICHROME (SHOWN IN 2 <sup>ND</sup> AND 4 <sup>TH</sup> ROWS) OF L1 AND L2 NORMAL AND INJURED CARTILAGE .....	43
FIGURE 3.7. EFFECT OF ENDOGENOUS AND EXOGENOUS LUBRICIN ON THE FRICTION COEFFICIENT OF NORMAL AND INJURED L1 CARTILAGE .....	44
FIGURE 3.8. RAT OA JOINT AFTER TREATED WITH PBS OR RECOMBINANT LUBRICIN FOR 4 WEEKS [19]. ....	46
FIGURE 4.1 THE CANONICAL TGF-B SIGNALING PATHWAY THROUGH SMAD 2/3 PHOSPHORYLATION [9] .....	49
FIGURE 4.2 CHEMICAL STRUCTURE OF SB431542, SMALL MOLECULE WHICH BLOCKS THE TYPE I RECEPTOR OF TGF-B [14].....	50
FIGURE 4.3 THE EXPERIMENT SCHEME TO TEST THE EFFECT OF THE BLOCKER ON INJURED.....	51
FIGURE 4.4 EFFECT OF STRAIN RATE ON TGF-B GENE EXPRESSION.....	53
FIGURE 4.5 EFFECT OF STRAIN RATE ON TGF-B PROTEIN RELEASE .....	53
FIGURE 4.6 RELATIVE COPY NUMBER OF 18S GENE EXPRESSION.....	54
FIGURE 4.7 THE EFFECT OF BLOCKER ON THE LUBRICIN PROTEIN RELEASE FROM L1 INJURED VERSUS NONINJURED CARTILAGE .....	54

FIGURE 4.8 THE EFFECT OF TGF-B BLOCKER ON LUBRICIN GENE EXPRESSION IN L1 INJURED OR NONINJURED  
 CARTILAGE. ....55

FIGURE 4.9 THE EFFECT OF TGF-B BLOCKER ON TGF-B GENE EXPRESSION IN L1 INJURED OR NONINJURED CARTILAGE  
 .....55

FIGURE 4.10 THE EFFECT OF TGF-B BLOCKER ON IL-1B GENE EXPRESSION IN L1 INJURED OR NONINJURED CARTILAGE  
 .....56

FIGURE 4.11. PEAK STRESS AMONG ALL THE INJURY CONDITIONS ACROSS THE 4 ANIMALS.....56

FIGURE 4.12 EFFECT OF BLOCKER ON SULFATE INCORPORATION RATE .....57

FIGURE 5.1. EXPERIMENTAL CONCEPT OF THE REAL-TIME OBSERVATION OF CELLULAR DEFORMATION AS THE  
 CARTILAGE IS COMPRESSED BY THE APPLICATOR (SHOWN BY THE BLUE ARROW). .....62

FIGURE 5.2. 3-D MODELS OF THE APPLICATOR, THE STAGE, AND THE BRIDGE THAT SECURES THE SOLENOID (LEFT TO  
 RIGHT). .....63

FIGURE 5.3. SETUP OF MECHANICAL SYSTEM WHICH REFLECTS THE CONCEPT ILLUSTRATED IN THE. FIGURE 5.1 .....63

FIGURE 5.4. THE ELECTRONICS EMBEDDED IN THE CIRCUIT BOX. ....64

FIGURE 5.5. MECHANICAL ACTUATOR DEVICE DESIGNED USING SOLIDWORKS (TOP VIEW) .....65

FIGURE 5.6 SIDE VIEW OF MECHANICAL ACTUATOR (SIDE VIEW) .....65

FIGURE 5.7. DIAGRAM OF THE CUSTOM STAGE AND THE CONFOCAL MICROSCOPE SYSTEM .....67

FIGURE 5.8. PICTORIAL CONCEPT OF INTRACELLULAR STRUCTURES PROGRESSING FROM THE DEFORMED STATE (LEFT)  
 TO THE RELAXED STATE (RIGHT) AS INDICATED BY THE DISTRIBUTION OF THE MITOTracker DYE .....67

FIGURE C.1. FLUID FLOW WITH VELOCITY  $V$  ACROSS A NETWORK OF RIGID RODS BOUNDED BY A CUBIC GAUSSIAN  
 SURFACE OF LENGTH  $L$ . .....96

# 1 Introduction

## 1.1 Cartilage Structures and Mechanical Properties

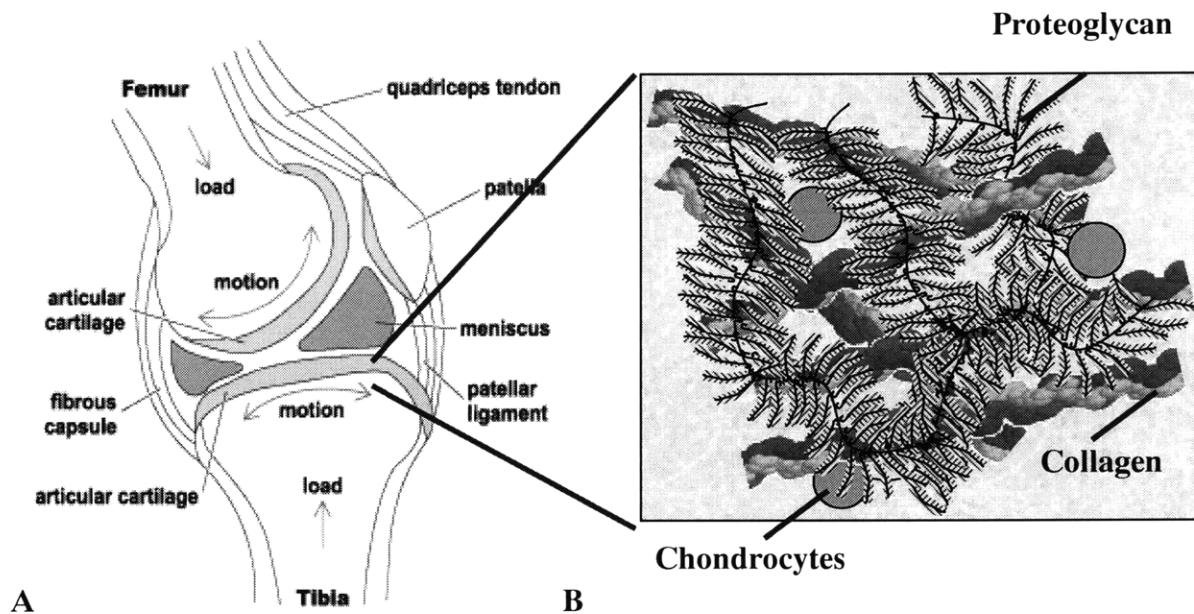


Figure 1.1. A) Diagram of the knee joint [1] and B) main constituents within the bulk of the articular cartilage

Articular cartilage (Figure 1.1) is a smooth, load bearing connective tissue that lines the diarthrodial joint inside the joint capsule filled with synovial fluid. Its opposing frictionless surfaces, spaced apart by a thin film of synovial fluid, allow even distribution of loads from one bone plate to another during motion [2]. The robustness of cartilage is due to extracellular matrix (ECM) being a hydrated gel primarily filled with tightly packed aggregated proteoglycans macromolecules encased in a crosslinked network of collagen fibrils. In addition, 75-80% of the wet weight is water, which enables the poroelastic tissue to withstand high levels of hydrostatic pressurization with little immediate deformation after loading [3-5]. The depth dependent heterogeneous composition of cartilage allows it to withstand loading in both the tangential and axial directions. Near the articular surface and in the synovial fluid is a glycoprotein coded by PRG4, known as lubricin. It is one of the key factors that contribute to the frictionless cartilage surface and smooth articulation between the diarthrodial joints. This chapter will summarize the primary structures of cartilage, their mechanical functions, and how mechanical trauma to the cartilage can eventually lead to secondary osteoarthritis.



### 1.1.1 Aggrecan

Aggrecan and collagen synthesis are two major determinants of cartilage health. The robust framework of cartilage results mostly from the electrostatic repulsion between the polyelectrolyte brushes on the proteoglycans and the incredible tensile strength exhibited by the collagen fibrils [6]. Aggrecan, a member of hyaluronan (HA)-binding proteoglycan family, is the major contributor to cartilage resilience to compression.

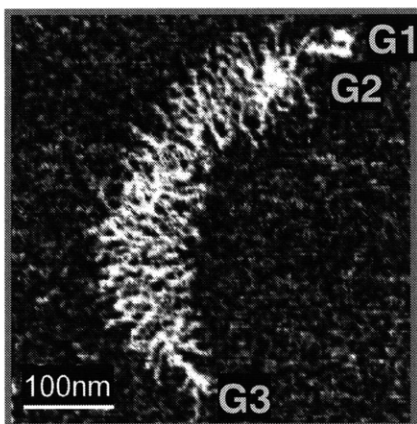


**Figure 1.2.** AFM image of the full length aggrecan molecule (courtesy of Hsu-Yi Lee)

The core protein is divided into three globular domains: G1, G2, and G3 (Figure 1.2). The G1 domain is located near the N-terminal where the aggrecan monomer noncovalently binds to the hyaluronic acid via a link proteins, G2 domain holds most of the keratin sulfate, while G3 domain remains near the C-terminal. Furthermore, there are approximately 100 highly charged chondroitin sulfate (CS) glycosaminoglycan (GAG) chains that covalently bind to the 300 kDa core protein backbone between G2 and G3 [7, 8].

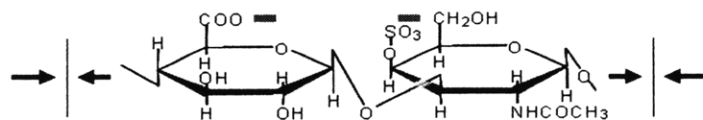


**Figure 1.3.** A negatively charged repeating disaccharide unit on a chondroitin-4 sulfate GAG chain.

The negative sulfate and carboxyl side groups on each of the ~50 repeating GAG disaccharide units contribute to the electric repulsive force that accounts for ~50% of equilibrium compressive modulus in cartilage (Figure 1.3). Moreover, by attracting counter-ions to the fixed charges, PG macromolecules create a local osmotic imbalance. Together, these osmotic and the electrostatic repulsion interaction from the hierarchical arrangement of polyelectrolyte brushes help to counteract against external compressive loading [9].

## 1.1.2 Collagen

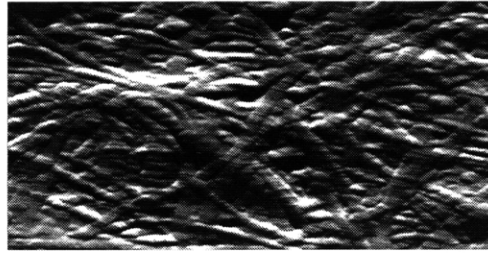


**Figure 1.4** AFM Image of the triple helical collagen fibrils (courtesy of Dr. Laurel Ng)

The collagen network distribution in cartilage is inhomogeneous with depth in this inhomogeneous structure composed of triple helical fibrils is responsible for over two thirds of the dry weight in ECM (Figure 1.4). Among the five major types of collagen (II, VI, IX, XI, and X) in cartilage, type II is the most abundant comprises of 80-85% of total protein. The ECM scaffold is primarily composed of collagen II cross-linked together with type IX and XI interlaced between them [10]. Nevertheless, other collagen types such as III, VI, XII, and XIV all play a minor role in strengthening and stabilizing the developed ECM.

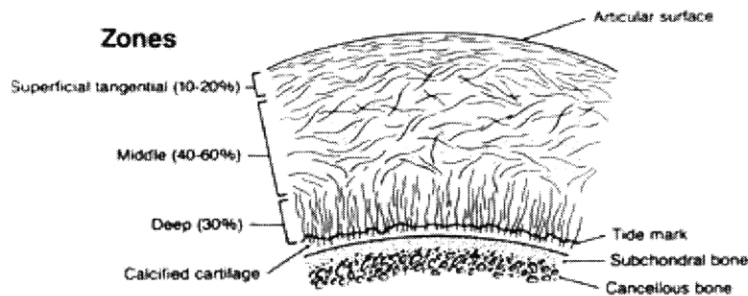


**Figure 1.5** Collagen network organization in different zones of the articular cartilage. [11]

Collagen exhibits a depth dependent architectural arrangement (Figure 1.5). In the superficial zone, the collagen fibers intersect in a plane that runs in parallel to the cartilage surface. Gradually, their orientation becomes more random with increasing depth. In the deep zone, the collagen is aligned almost perpendicular to the surface. The arrangement and alignment of the fibrils when subjected to loading allows the cartilage to withstand tensile and mechanical shear force [12, 13]. The ultrastructure of the collagen fibrils varies as a function of distance away from the chondrocyte. Type XI determines the fibril size and IX facilitates fibril interaction with proteoglycan macromolecules. For instance, the ones that form the pericellular

matrix consist of thin fibrils of type VI, IX, and XI whereas the ones in the ECM are coarser and banded. Moreover, the biochemical evidence that collagen IX can potentially form covalent bridges between fibrils suggest that the network compensates for osmotic swelling in proteoglycans. In turn, that further enhances the cartilage stiffness [12, 13].

### 1.1.3 Lubricin

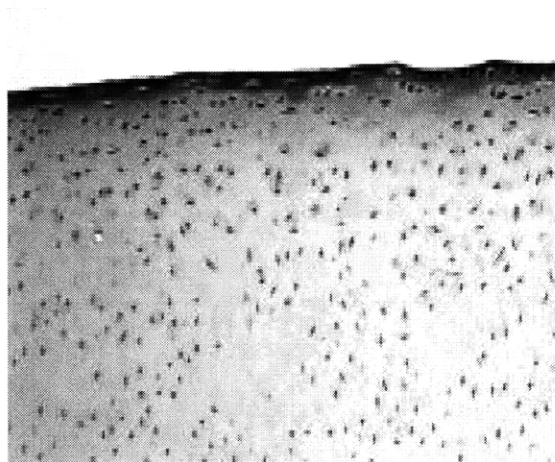


**Figure 1.6.** Lubricin distribution in articular cartilage using G35 antilubricin stain [14]

As mentioned before, one essential feature of articular cartilage is the ability to transfer load during motion across the frictionless surface. A major contributor to the interfacial lubrication between the joints is lubricin, an O-linked glycoprotein derived from the gene proteoglycan 4 (PRG4) of both synoviocytes on the lining of the joint capsules and the chondrocytes in the superficial layer of the cartilage (Figure 1.6) [15-17]. Much of the answer to how lubricin functions lies in its amino acid sequence, (Figure 1.7). Lubricin has two domains in the sequence, somatomedin B (SMB) and hemopexin-like domains (PEX), which resemble that of vitronectin, an adhesive glycoprotein found in blood plasma and extracellular matrix [18]. Furthermore, the saturated negatively charged O-linked glycosylation in the middle mucin-like domain enhances the boundary lubrication of the cartilage surface due to the strong repulsive hydration forces [15, 19, 20].

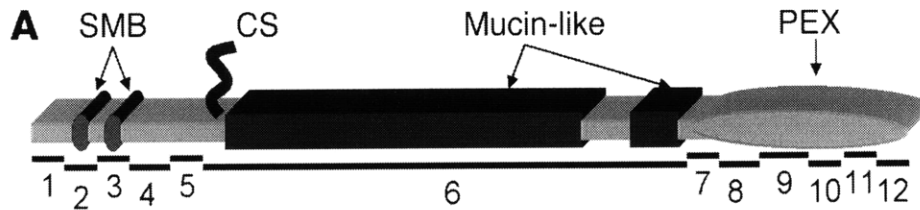


**Figure 1.7** Lubricin structure and PRG4 gene targeting in mice [21].

Not only does lubricin provide smooth articulation in joints, it is essential to preventing cell overgrowth, abnormal protein deposition on articular cartilage surface, and synovium cells from being hyperplastic, all of which can lead to joint failure [21].

## 1.2 Mechanical Regulation of the Structure

The development of the ECM is related to how the chondrocytes continually synthesize, assemble, and turn over matrix proteins inside the cartilage in response to the mechanical environment. Soluble proteins including growth factors and cytokines play important roles in modulating chondrocyte biosynthesis and differentiation [22]. Chondrocyte biosynthetic activities can also be regulated by their surrounding mechanical environment due to external loading conditions. Concomitant mechanical and physiochemical forces and flows have been shown to stimulate chondrocyte biosynthesis in the matrix and to regulate the cellular activities that maintain cartilage homeostasis [23]. However, there is yet no complete characterization of the signaling pathway by which mechanotransduction regulates cellular processes *in vivo*. Therefore, cellular biosynthesis and health rely greatly on mechanotransduction (the translation of mechanical signals to biochemical signals) to regulate the tissue's matrix composition and its related physical properties (e.g. ion concentration, osmotic pressure, and electrokinetic properties) [24, 25].

The constant compressive and shear mechanical loading of cartilage can deform the ECM, which directly perturbs the biochemical environment and induces a complex series of cellular responses. Furthermore, the resulting changes in the matrix affect the mechanical properties of the cartilage.

The equilibrium compressive modulus of cartilage tissue is approximately 500-800 kPa [26], while the dynamic compressive modulus has been shown to be around 13-37 MPa when 0.5-2.5% strain amplitude is applied at 1 Hz, similar to walking frequency [27-29]. Furthermore,

previous research has indicated that applying dynamic compressive loading to cartilage explants enables a coupling between dynamic fluid flow and slight matrix deformation within the tissue [28]. Hence, mechanical deformation promotes the exchange of soluble factors between the cartilage and the surrounding synovial fluid. The combination of mechanical signals, enhanced transport can increase the biosynthetic activity of cells localized near the peripheral region of cylindrical bovine cartilage explants [25, 29]. In fact, oscillatory compressive strain between 1-5% at 0.01-1 Hz can increase the sulfate and proline incorporation, indicative of GAG and protein synthesis, respectively, by 20-40% after just 24 hours of loading [27].

Dynamic tissue shear loading decouples mechanical deformation from fluid flow because shear force produces little amount of volumetric deformation. Previous findings show that application of dynamic tissue shear loading can increase protein and proteoglycan synthesis by ~50% and ~25%, respectively, in cartilage explants at frequencies between 0.01 and 1.0 Hz and shear strain amplitude of 3% [30].

On a similar note, previous research has been conducted to study how mechanical loading may modulate the frictional behavior of the cartilage surface and synthesis of the lubricin. Dynamic compression and dynamic shear have been well documented to enhance matrix biosynthesis, while static compression inhibits synthesis [27, 30-33]. However, both dynamic and static compressions affect chondrocyte lubricin secretion as well as the friction coefficient during the loading period, while dynamic shear augmented the release by 3-4 fold [34-36]. *In vitro* dynamic compression, frequencies of 0.05, 0.5, and 1Hz produced oscillating friction coefficients of 0.092 and 0.382, while the value for static compression was 0.153. One explanation is that the interstitial fluid pressure increases as the load transfers from solid to fluid phase, and the transient frictional coefficient is thereby reduced [37]. Yet, when the pressure tends to zero after the static loading, the friction coefficient of the cartilage increases to a level too high for lubrication [35]. At the crest of dynamic loading cycle when the applied force ( $W$ ) is at its minimum, the fluid load support is negative ( $W^P$ ). Thus, the resulting suction leads to a high solid-to-solid friction force ( $W^{SS}$ ) according to the boundary friction model (Eq. 1) which quantifies the solid and fluid load sharing at the cartilage interface [37].

$$W^{SS} = W - (1-\phi)W^P \quad (1)$$

The fraction of the total contact area where solid-to-solid contact occurs,  $\phi$ , is set to 0.1 for the experiment.

Together, these studies illuminate the frictional behavior of cartilage during normal exercise or daily activity. More importantly, they pave the way to further investigate what happens at the cartilage interface during abnormal or injurious load.

### 1.3 Significance of Lubricin to Mechanical Loading of Cartilage

The importance of lubricin to the articular surface mechanics was demonstrated by contrasting the low CoF of normal SF with the high CoF of SF that lacked lubricin in PRG4 knockout mice and Camptodactyly-Arthropathy-Coxa vara-Pericarditis (CACP) patients [21, 38]. Furthermore, previous works have shown that the increase in CoF after lubricin extraction can be recovered after replenishing the articular surface with synovial fluid or recombinant full-length lubricin [14].

Although lubricin secretion was low during compression, there was a heightened lubricin synthesis beyond 200  $\mu\text{m}$  depth for all compacted samples compared to controls [34]. Likewise, dynamic shear loading induced a significant increase in lubricin expression at the 200-400  $\mu\text{m}$  below the articular surface compared to control and statically loaded samples [36]. Interestingly, lubricin release during 24-hr recovery returned to control value for the 100kPa static compression and elevated to 46% over control for 300kPa dynamic compression. Then, in the next 2-3 days, lubricin secretion fell back to 50% of the respective increased amount for both loading conditions [34]. In contrast, not only did shear force greatly amplify lubricin expression during loading, it sustained that level for the 72-hr post loading recovery time [36].

### 1.4 Impact of Injury

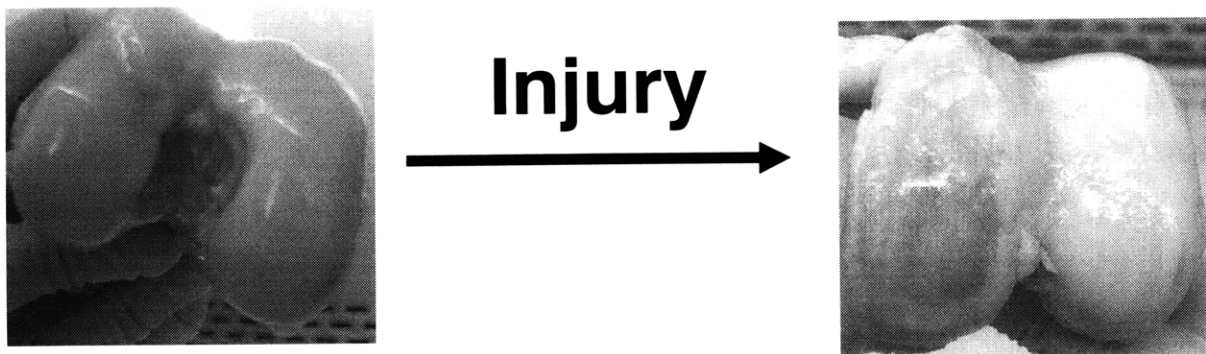


**Figure 1.8.** Possible progression from healthy human cartilage to OA ridden cartilage through injury

Despite its strength, cartilage has limited regenerative capabilities once injured or degraded due to its aneural, avascular, and alymphatic nature. Mechanical trauma to the cartilage, although a discrete event, can lead to degeneration of the articular cartilage and surrounding joint known as osteoarthritis (OA) (Figure 1.8). The likelihood of that happening depends on age, obesity, joint instability, and other health issues. Nevertheless, the progression towards OA consists of interactions between the consequent biomechanical and inflammatory factors [39]. However, the signaling pathways which culminate in OA have yet to be mapped. Thus, understanding the short and long term posttraumatic response in cartilage gene expression and chondrocyte biosynthesis, along with its coupled reaction to drug treatment will help bridge that gap.

The initial phase that marks the path to OA is an increase in concentration of proinflammatory cytokines such as interleukin 1 (IL-1) and tumor necrosis factor (TNF- $\alpha$ ) in cartilage and synovial fluid [40, 41]. Generally, the catabolic effects of these cytokines involve inhibiting proteoglycan and collagen production, while stimulating enzymes and factors responsible for matrix degradation. In fact, some cytokines, such as IL-6 and IL-17, interact synergistically to initiate the independent pathogenic events of cartilage breakdown and inflammation in OA [42, 43]. Therefore, therapeutic treatment for the disease at a certain point along the pathogenic cascade does not necessarily account for both fronts of the problem.

#### **1.4.1 *In vivo* Injury Models and Lubricin**

Joint trauma increase the risk of developing secondary OA in later life due to the interaction between mechanical injury and induced inflammatory factors. SF from rabbits with induced ACL injury have demonstrated increased friction coefficient and type II collagen concentration after three weeks. This observation has also been noted in human patients with knee joint synovitis and RA [44]. In addition, SF aspirated from human knees 32-364 days after ACL injury exhibits lower lubricin concentration and full length lubricin compared to control and ones with severe meniscus damage [45]. This relationship was confirmed in a guinea pig model where SF taken 9 months after ACL injury has significantly reduced lubricin concentration and heightened CoF compared to normal [46]. An induced arthritis model using BSA and Freund's complete adjuvant demonstrated the proteolytic degradation of lubricin due to the resulting increase in cathepsin B expression. Not only was O-linked section of the lubricin fully degraded after 12 hours in 0.5 units/ml cathepsin B as shown by the friction coefficient increase, arthritis

also caused significant increase in cathepsin B and IL-1 $\beta$  expressions [47]. These studies reinforce the link between injury and arthritis as well as their common negative impact on the SF lubricating ability.

### **1.4.2 *In vitro* Injury Model**

The *in vitro* injury model established in this lab simulates a high impact injury by applying a single, high strain rate injurious compression to a cartilage explant. An important focus in this research is simulating, *in vitro*, the different peak stresses, peak strains, and strain rates experienced by the injured cartilage. Then, based on a sequence of biochemical tests, an assessment can be made regarding the threshold loading conditions where the matrix and cell begin to significantly deform. Previous findings demonstrate that neither final strain up to 65% nor peak stress up to 14 MPa results in profound damage provided that the strain rate is kept around 1% s<sup>-1</sup> or lower [48-50]. The nature of the injury also determines the cartilage degeneration. If the injury is a single high impact loading, without damage to the matrix, then there might be minimal risk of future degeneration [51, 52]. However, because the joint loading conditions may be altered after trauma, the effect of continued mechanical load thereafter remains to be a question.

Previous works demonstrated that this injury protocol causes escalation in MMP-3, TGF- $\beta$ , and ADAMTS-5 expressions, as well as GAG loss, and biosynthesis rate and cell viability reduction in middle zone cartilage [49, 50, 53, 54].

## **1.5 Objectives**

The objectives of this study are to investigate the effect of injurious deformation on articular cartilage surface.

Chapter 2 will discern the effect of injury on surface properties through by measuring the friction coefficient and surface roughness. The topography of the articular surface after various mechanical treatments will also be shown through surface roughness height profiles and environmental scanning electron microscope.

Chapter 3 will characterize the effect of injury on lubricin synthesis from the cartilage through lubricin gene expression, lubricin secretion, and lubricin retained on the cartilage surface.



Furthermore, this study will include the relation between lubricin and friction coefficient of the articular cartilage surface.

Chapter 4 will explore how the TGF- $\beta$  pathway may be a possible mechanism in modulating the effect of injury on lubricin synthesis through gene expression, protein secretion using ELISA.

Chapter 5 will describe the microscope stage mechanical actuator design for the purpose of observing the real-time intracellular response of superficial zone chondrocytes to injury.

Appendix A will include the published paper that was shown in the January, 2009 issue of *Arthritis and Rheumatism*.

Appendix B will include the other gene expressions investigated in the TGF- $\beta$  pathway study in Chapter 4.

Appendix C will include the derivation for the hydraulic permeability.

Appendix D will include the circuit design schematic in the mechanical actuator 1.0.

Appendix E will include the illustration of the mechanical actuator 2.0 platform.

Appendix F will will layout the blueprint of selected key parts of mechanical actuator 2.0.

## 1.6 Bibliography

1. Skalak, R. and S. Chien, eds. *Handbook of Bioengineering*. 1987.
2. Ateshian, G.A. and V.C. Mow, *Friction, lubrication, and wear of articular cartilage and diarthrodial joints*. 3rd ed. Basic Orthopaedic Biomechanics and Mechanobiology, ed. V.C. Mow and R. Huskes. 2005, Philadelphia: Lippincott, Williams & Wilkins. 447-494.
3. Ateshian, G.A., et al., *An asymptotic solution for the contact of two biphasic cartilage layers*. J Biomech, 1994. **27**(11): p. 1347-60.
4. Mow, V.C., G.A. Ateshian, and R.L. Spilker, *Biomechanics of diarthrodial joints: a review of twenty years of progress*. J Biomech Eng, 1993. **115**(4B): p. 460-7.
5. Eckstein, F., M. Hudelmaier, and R. Putz, *The effects of exercise on human articular cartilage*. J Anat, 2006. **208**(4): p. 491-512.
6. Maroudas, A., *Physico-chemical Properties of Articular Cartilage*, in *Adult Articular Cartilage*, M.A.R. Freeman, Editor. 1979: Pitman, England. p. 215-290.
7. Ng, L., et al., *Individual cartilage aggrecan macromolecules and their constituent glycosaminoglycans visualized via atomic force microscopy*. J Struct Biol, 2003. **143**(3): p. 242-57.
8. Buschmann, M.D., et al., *Mechanical compression modulates matrix biosynthesis in chondrocyte/agarose culture*. J Cell Sci, 1995. **108** ( Pt 4): p. 1497-508.
9. Urban, J.P., et al., *Swelling pressures of proteoglycans at the concentrations found in cartilaginous tissues*. Biorheology, 1979. **16**(6): p. 447-64.
10. Eyre, D.R. and J.J. Wu, *Collagen structure and cartilage matrix integrity*. J Rheumatol Suppl, 1995. **43**: p. 82-5.
11. .
12. Eyre, D., *Collagen of articular cartilage*. Arthritis Res, 2002. **4**(1): p. 30-5.
13. Cremer, M.A., E.F. Rosloniec, and A.H. Kang, *The cartilage collagens: a review of their structure, organization, and role in the pathogenesis of experimental arthritis in animals and in human rheumatic disease*. J Mol Med, 1998. **76**(3-4): p. 275-88.
14. Jones, A.R., et al., *Binding and localization of recombinant lubricin to articular cartilage surfaces*. J Orthop Res, 2007. **25**(3): p. 283-92.
15. Swann, D.A., et al., *The molecular structure and lubricating activity of lubricin isolated from bovine and human synovial fluids*. Biochem J, 1985. **225**(1): p. 195-201.
16. Schumacher, B.L., et al., *A novel proteoglycan synthesized and secreted by chondrocytes of the superficial zone of articular cartilage*. Arch Biochem Biophys, 1994. **311**(1): p. 144-52.
17. Schumacher, B.L., et al., *Immunodetection and partial cDNA sequence of the proteoglycan, superficial zone protein, synthesized by cells lining synovial joints*. J Orthop Res, 1999. **17**(1): p. 110-20.
18. Schwartz, I., D. Seger, and S. Shaltiel, *Vitronectin*. Int J Biochem Cell Biol, 1999. **31**(5): p. 539-44.
19. Jay, G.D., D.A. Harris, and C.J. Cha, *Boundary lubrication by lubricin is mediated by O-linked beta(1-3)Gal-GalNAc oligosaccharides*. Glycoconj J, 2001. **18**(10): p. 807-15.

20. Jay, G.D., B.P. Lane, and L. Sokoloff, *Characterization of a bovine synovial fluid lubricating factor. III. The interaction with hyaluronic acid*. *Connect Tissue Res*, 1992. **28**(4): p. 245-55.
21. Rhee, D.K., et al., *The secreted glycoprotein lubricin protects cartilage surfaces and inhibits synovial cell overgrowth*. *J Clin Invest*, 2005. **115**(3): p. 622-31.
22. Hering, T.M., *Regulation of chondrocyte gene expression*. *Front Biosci*, 1999. **4**: p. D743-61.
23. Grodzinsky, A.J., et al., *Cartilage tissue remodeling in response to mechanical forces*. *Annu Rev Biomed Eng*, 2000. **2**: p. 691-713.
24. Gray, M.L., et al., *Mechanical and physiochemical determinants of the chondrocyte biosynthetic response*. *J Orthop Res*, 1988. **6**(6): p. 777-92.
25. Kim, Y.J., et al., *Mechanical regulation of cartilage biosynthetic behavior: physical stimuli*. *Arch Biochem Biophys*, 1994. **311**(1): p. 1-12.
26. Armstrong, C.G. and V.C. Mow, *Variations in the intrinsic mechanical properties of human articular cartilage with age, degeneration, and water content*. *J Bone Joint Surg Am*, 1982. **64**(1): p. 88-94.
27. Sah, R.L., et al., *Biosynthetic response of cartilage explants to dynamic compression*. *J Orthop Res*, 1989. **7**(5): p. 619-36.
28. Kim, Y.J., L.J. Bonassar, and A.J. Grodzinsky, *The role of cartilage streaming potential, fluid flow and pressure in the stimulation of chondrocyte biosynthesis during dynamic compression*. *J Biomech*, 1995. **28**(9): p. 1055-66.
29. Buschmann, M.D., et al., *Stimulation of aggrecan synthesis in cartilage explants by cyclic loading is localized to regions of high interstitial fluid flow*. *Arch Biochem Biophys*, 1999. **366**(1): p. 1-7.
30. Jin, M., et al., *Tissue shear deformation stimulates proteoglycan and protein biosynthesis in bovine cartilage explants*. *Arch Biochem Biophys*, 2001. **395**(1): p. 41-8.
31. Ragan, P.M., et al., *Down-regulation of chondrocyte aggrecan and type-II collagen gene expression correlates with increases in static compression magnitude and duration*. *J Orthop Res*, 1999. **17**(6): p. 836-42.
32. Fitzgerald, J.B., et al., *Mechanical compression of cartilage explants induces multiple time-dependent gene expression patterns and involves intracellular calcium and cyclic AMP*. *J Biol Chem*, 2004. **279**(19): p. 19502-11.
33. Jones, I.L., A. Klamfeldt, and T. Sandstrom, *The effect of continuous mechanical pressure upon the turnover of articular cartilage proteoglycans in vitro*. *Clin Orthop Relat Res*, 1982(165): p. 283-9.
34. Nugent, G.E., et al., *Static and dynamic compression regulate cartilage metabolism of PRoteoGlycan 4 (PRG4)*. *Biorheology*, 2006. **43**(3-4): p. 191-200.
35. Krishnan, R., E.N. Mariner, and G.A. Ateshian, *Effect of dynamic loading on the frictional response of bovine articular cartilage*. *J Biomech*, 2005. **38**(8): p. 1665-73.
36. Nugent, G.E., et al., *Dynamic shear stimulation of bovine cartilage biosynthesis of proteoglycan 4*. *Arthritis Rheum*, 2006. **54**(6): p. 1888-96.
37. Ateshian, G.A., H. Wang, and W.M. Lai, *The role of interstitial fluid pressurization and surface porosities on the boundary friction of articular cartilage*. *Journal of Tribology*, 1998. **120**: p. 241-251.
38. Jay, G.D., et al., *Association between friction and wear in diarthrodial joints lacking lubricin*. *Arthritis Rheum*, 2007. **56**(11): p. 3662-9.

39. Guilak, F., et al., *The role of biomechanics and inflammation in cartilage injury and repair*. Clin Orthop Relat Res, 2004(423): p. 17-26.
40. Pickvance, E.A., T.R. Oegema, Jr., and R.C. Thompson, Jr., *Immunolocalization of selected cytokines and proteases in canine articular cartilage after transarticular loading*. J Orthop Res, 1993. **11**(3): p. 313-23.
41. Lukoschek, M., et al., *Comparison of joint degeneration models. Surgical instability and repetitive impulsive loading*. Acta Orthop Scand, 1986. **57**(4): p. 349-53.
42. Rowan, A.D., et al., *Synergistic effects of glycoprotein 130 binding cytokines in combination with interleukin-1 on cartilage collagen breakdown*. Arthritis Rheum, 2001. **44**(7): p. 1620-32.
43. LeGrand, A., et al., *Interleukin-1, tumor necrosis factor alpha, and interleukin-17 synergistically up-regulate nitric oxide and prostaglandin E2 production in explants of human osteoarthritic knee menisci*. Arthritis Rheum, 2001. **44**(9): p. 2078-83.
44. Elsaid, K.A., et al., *Association of articular cartilage degradation and loss of boundary-lubricating ability of synovial fluid following injury and inflammatory arthritis*. Arthritis Rheum, 2005. **52**(6): p. 1746-55.
45. Elsaid, K.A., et al. *Synovial Fluid Lubricin Concentrations are Decreased Following Anterior Cruciate Ligament Injury in Humans and are Associated with Increased Cartilage Damage*. in *Annual Meeting of the Orthopaedic Research Society*. 2007. San Diego.
46. Teeple, E., et al., *Coefficients of friction, lubricin, and cartilage damage in the anterior cruciate ligament-deficient guinea pig knee*. J Orthop Res, 2008. **26**(2): p. 231-7.
47. Jay, G.D., et al., *The role of lubricin in the mechanical behavior of synovial fluid*. Proc Natl Acad Sci U S A, 2007. **104**(15): p. 6194-9.
48. Quinn, T.M., et al., *Matrix and cell injury due to sub-impact loading of adult bovine articular cartilage explants: effects of strain rate and peak stress*. J Orthop Res, 2001. **19**(2): p. 242-9.
49. Kurz, B., et al., *Biosynthetic response and mechanical properties of articular cartilage after injurious compression*. J Orthop Res, 2001. **19**(6): p. 1140-6.
50. Loening, A.M., et al., *Injurious mechanical compression of bovine articular cartilage induces chondrocyte apoptosis*. Arch Biochem Biophys, 2000. **381**(2): p. 205-12.
51. Oegema, T.R., Jr., J.L. Lewis, and R.C. Thompson, Jr., *Role of acute trauma in development of osteoarthritis*. Agents Actions, 1993. **40**(3-4): p. 220-3.
52. Donohue, J.M., et al., *The effects of indirect blunt trauma on adult canine articular cartilage*. J Bone Joint Surg Am, 1983. **65**(7): p. 948-57.
53. Grad, S., et al., *Surface motion upregulates superficial zone protein and hyaluronan production in chondrocyte-seeded three-dimensional scaffolds*. Tissue Eng, 2005. **11**(1-2): p. 249-56.
54. Lee, J.H., et al., *Mechanical injury of cartilage explants causes specific time-dependent changes in chondrocyte gene expression*. Arthritis Rheum, 2005. **52**(8): p. 2386-95.

## 2 Effect of Injury on Cartilage Surface Properties

### 2.1 Introduction

Since OA initiates at the articular cartilage surface, the purpose of this study is to quantify the effect of injury on the surface mechanical properties of the cartilage using an *in vitro* model. When determining the equilibrium friction coefficient ( $\mu_{eq}$ ), lateral motion is superimposed on a nontrivial normal load to simulate boundary mode lubrication of diarthrodial cartilage during motion. Cartilage surface topography is then visualized after being subjected to one or both of these mechanical stimuli using 3-D optical profilometry and environmental scanning electron microscopy (ESEM). Since lubricin is responsible for the smoothness of cartilage, the effectiveness of this glycoprotein in recovering the surface property of injured cartilage surface will be examined through friction coefficient measurement.

The next two sections will describe the mechanics of the injury model and boundary mode lubrication and their physiological relevance.

#### 2.1.1 Description of the *in vitro* injury model

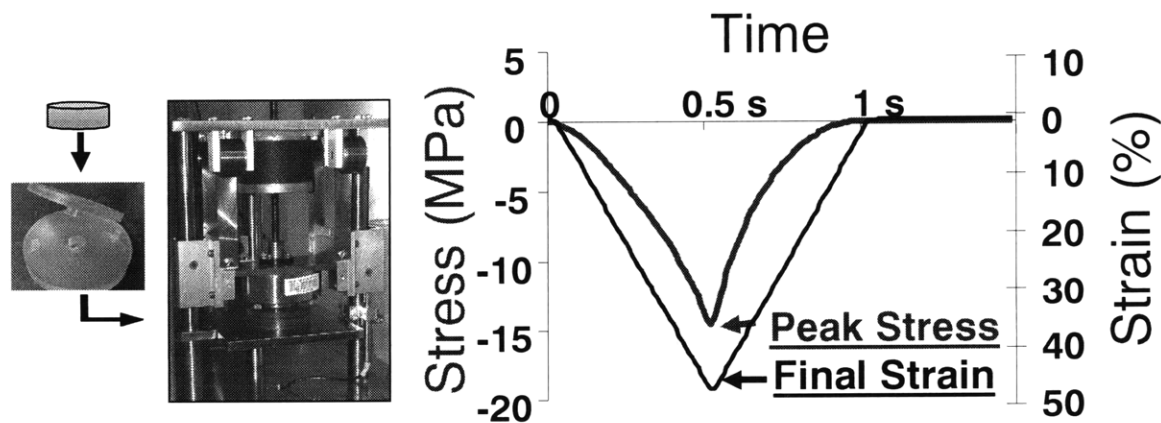


**Figure 2.1** In house injurious loading apparatus [1] along with the loading protocol waveforms

A customized loading chamber with the single cartilage disk placed inside is entered into the in house injurious loading apparatus (Figure 2.1). The apparatus determines the thickness with a linear variable differential transformer (LVDT) at a tare load of -50g before applying compression and recording the load. By controlling the strain and the ramp time, the apparatus

can modulate the strain rate applied to the disk. The v-shaped compressive protocol used for injury is intended to simulate a single, high stress impact to the knee.

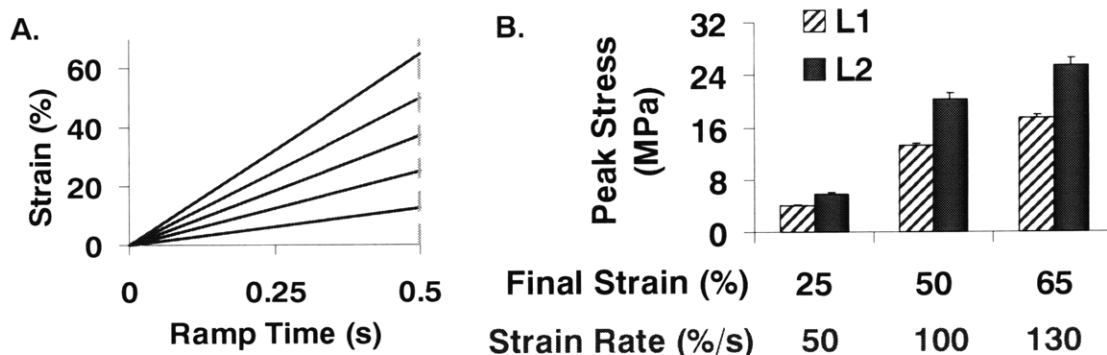


**Figure 2.2** A) Increasing strain while keeping ramp time constant B) directly influences strain rate and the peak stress within cartilage

Figure 2.2 illustrates the effect of increasing strain rate on the peak stress of two consecutive layers of cartilage by raising the strain while keep the ramp constant. L1 indicates the top layer of the cartilage including the articular surface and L2 being the subsequent layer in the middle zone region. This increasing trend in peak stress with increasing strain rate is consistent with previous literature on L2 cartilage [2]. Furthermore, L2 cartilage reaches a higher peak stress compared to the superficial layer at each of the strain tested. The depth dependence of the peak stress is reasonable since even when cartilage is under 10% compression, the measured modulus,  $H_{AD}$ , closest to the cartilage surface is the lowest and increases with depth (Figure 2.3C, ▲). As expected, the local strain,  $E_{zz}$ , (Figure 2.3B) is the lowest near the surface and declines with depth [3].

Since cartilage is a poroelastic material as shown, the peak stress varies proportionally with strain rate. For the standard injury protocol, the parameters selected are 50% strain at 100%/s. The criteria for selecting those parameters are to obtain the peak stress around 15-20 MPa, the upper range of stress values that human cartilage undergo on a daily basis [4].

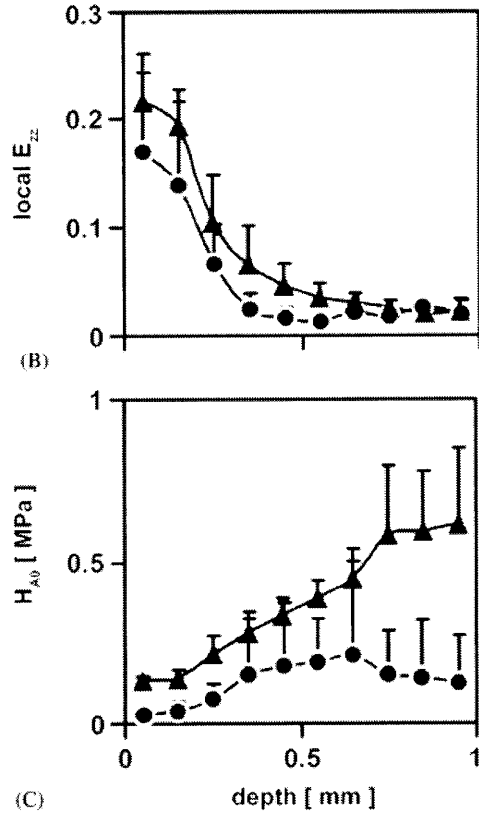


**Figure 2.3.** B) The local strain ( $E_{zz}$ ) at 10% compression, and C) confined compressive modulus ( $H_{AD}$ ) as a function of depth from the articular surface (n=4). (Only observe the newborn calf data marked by  $\blacktriangle$ ) [3]

## 2.1.2 Boundary Mode Lubrication

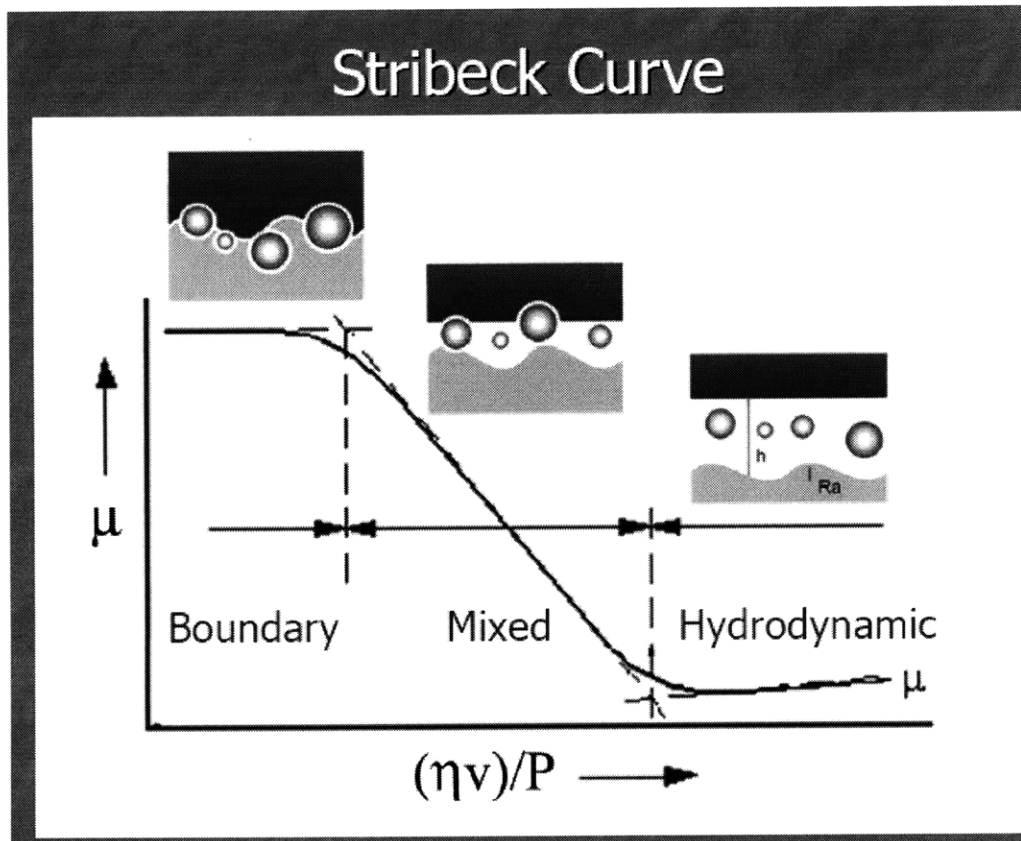


**Figure 2.4** The Stribeck Curve: showing how relationship between friction coefficient ( $\mu$ ), viscosity ( $\eta$ ), speed ( $v$ ), and  $P$  (normal load) varies in the three modes of lubrication. (Dr. J. Gleghorn)

With synovial fluid as the lubricant, frictionless articulation of the diarthrodial cartilage range from hydrodynamic to boundary mode. According to the Stribeck curve (Figure 2.4), boundary lubrication is the region of lubrication when the friction coefficient is the highest. That occurs at low entraining speed ( $v$ ) and high normal load ( $P$ ) where opposing surface asperities dominate the friction coefficient [5]. The reason for focusing on boundary mode lubrication is because most of the wear between the joints occurs during articulation under high compressive load. Over time, that causes cartilage degeneration, and eventually can lead to OA.

To determine the boundary mode region, the entraining speed was swept from 0.25 mm/sec to 5 mm/sec, and normal load range was swept from 10% to 50%. The pair of parameters which yielded a constant friction coefficient was selected.



## 2.2 Methods

### 2.2.1 Harvesting Cartilage Explants

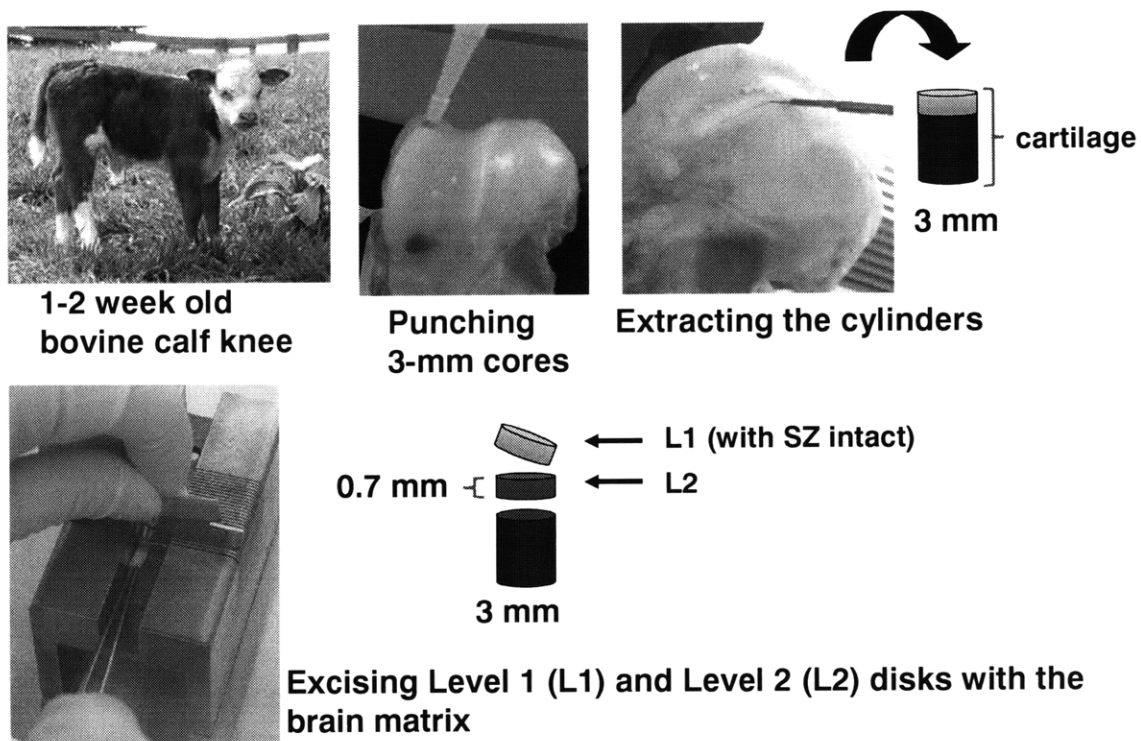


Figure 2.5. Harvesting procedure to extract L1 and L2 cartilage disks

Ø 3mm cartilage cylinders were cored from the femoropatellar groove of 1-2 week old calves using dermal punch and subsequently removed using a surgical blade. Using a brain matrix (TM-1000, ASI Instruments, Warren, MI), 700~800  $\mu\text{m}$  thick discs of the top layer (L1) including intact superficial zone, and the subsequent layer (L2) were sliced from the cylinders (Figure 2.5). These samples were pre-cultured in medium containing low glucose DMEM, 0.1 mM non-essential amino acid (NEAA), 10 mM HEPES buffered solution, 100 U/ml penicillin, 100  $\mu\text{g}/\text{ml}$  streptomycin, 0.4 mM proline, supplemented with 1% ITS (10  $\mu\text{g}/\text{ml}$  insulin, 5.5  $\mu\text{g}/\text{ml}$  transferrin, and 5 ng/ml sodium selenite) at 37°C in an atmosphere of 5%  $\text{CO}_2$ .

### 2.2.2 Injurious compression

Following 48 hours of pre-culture, injurious compression was performed utilizing a custom-designed incubator-housed loading apparatus where single cartilage discs underwent radially unconfined compression in a polysulfone chamber well [1]. The mechanical injury protocol

consisted of a single ramp compression (strain=50%; v=100%/s) where explants were compressed to 50% of the thickness in 0.5 seconds, followed by immediate release at the same rate [2].

### 2.2.3 Dynamic Shear

After injury loading or free swell, discs from the same layer (n=6) were placed evenly in a 12-well custom-made polysulfone chamber filled with PBS, which is mounted inside a custom incubator-housed apparatus [1]. 3% dynamic tissue shear strain, superimposed on 15% normal strain, was placed on the chamber relative to stationary platens for 1 hour to produce simple shear loading. Minimal slippage between the cartilage and platen was ensured since the THD determined from the shear loading waveforms fell less than 10% (data not shown).

This shear-loading regimen was chosen since it has been demonstrated to stimulate biosynthesis in normal cartilage [6]. Also, it enables a comparison between the effects that tissue shear loading and lateral motion from the friction test would produce on surface roughness.

### 2.2.4 Friction Test

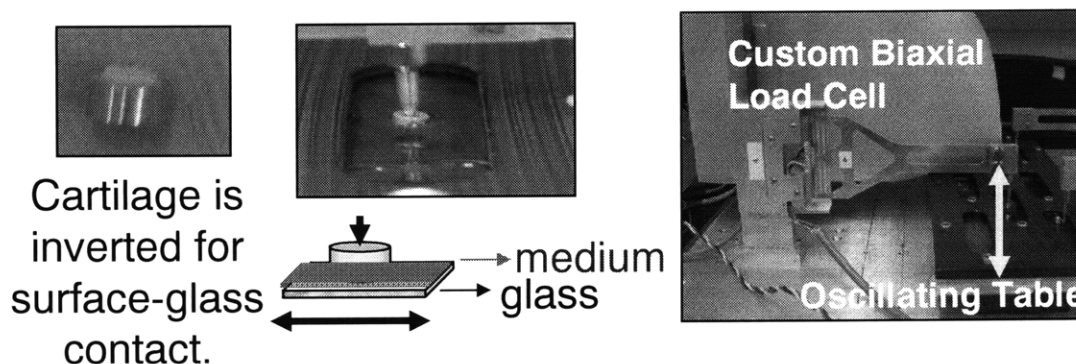
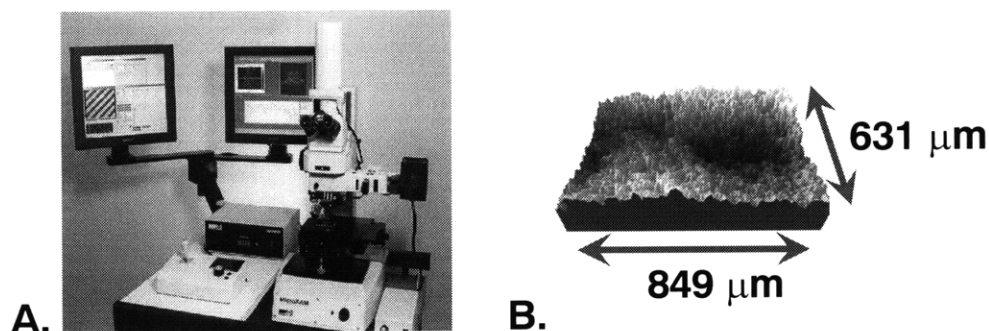


Figure 2.6 Custom built friction coefficient test apparatus [7]

Following injury loading or free swell, discs were flash frozen in liquid nitrogen, maintained at -80°C, and thawed at room temperature before friction testing. Equilibrium friction coefficients ( $\mu_{eq}$ ) were obtained for both layers in boundary lubrication mode (30% normal strain, v = 0.33 mm/s) using PBS as a lubricant, in a custom linear cartilage-on-glass system over 1 hour [8]. The friction testing apparatus consisted of a glass counterface/lubricant bath that linearly oscillates under the cartilage sample. A servo motor, and a custom biaxial load cell drove the system by applying a normal strain to the tissue and measuring the normal and frictional shear

loads on the sample [9]. L1 and L2 explants were tested with the articular surface and the top surface against the glass, respectively. The temporal friction coefficient ( $\mu(t)$ ) was recorded and data is presented as the equilibrium friction coefficient ( $\mu_{eq}$ ) calculated from a poroelastic relaxation model fit to the  $\mu(t)$  data. (Dr. Jason P. Gleghorn, Natalie, Galley, Cornell University)

### 2.2.5 Surface Roughness



**Figure 2.7** A) 3-D optical profilometer B) Area of the height profile that is scanned on the cartilage disk

Discs were flash frozen and stored at  $-80^{\circ}\text{C}$  similar to the ones for friction testing. Prior to surface profiling, samples were thawed at room temperature in PBS and placed underneath the objective of 3D non-contact optical profiler tabletop system (MicroXAM, ADE) with the top surface up. The sample platform was leveled to ensure a horizontal surface during scanning. Average surface roughness and 3-D image were taken at 10X optical magnification over an  $849 \times 631 \text{ m}$  area. These measurements were repeated at 3 different areas of each sample. (Natalie Galley, Cornell University)

### 2.2.6 Equilibrium Modulus

One hour was used to evaluate the equilibrium unconfined compressive modulus of cartilage. Injured samples were equilibrated in PBS for 1 hour prior to modulus measurement in the Dynastat. Four sequential ramp-and-hold compressions at 5, 10, 15, and 20% strain were applied on each sample. The equilibrium stresses were determined from fitting the corresponding stress relaxation data to a five-element exponential decaying model using Matlab. In turn, the modulus was extracted from the slope of the linear stress-strain relationship.

### 2.2.7 Environmental Scanning Electron Microscope (ESEM) Images

The cartilage disks were fixed after friction test and/or surface roughness imaging. Then, they were rinsed with PBS prior to imaging in wet mode. The vacuum was turned on and water vapor was let into the sample chamber to prevent dehydration of tissue. Images were taken using Quanta 600 for the SEM.(FEI, Inc.). (Natalie Galley, Cornell University)

### 2.2.8 Statistics

All data were analyzed using 2-way ANOVA followed by Tukey post-hoc pairwise comparisons.

## 2.3 Results

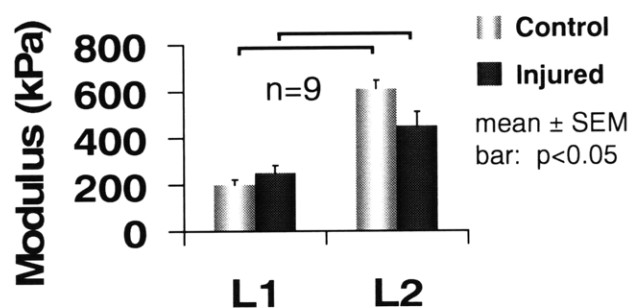
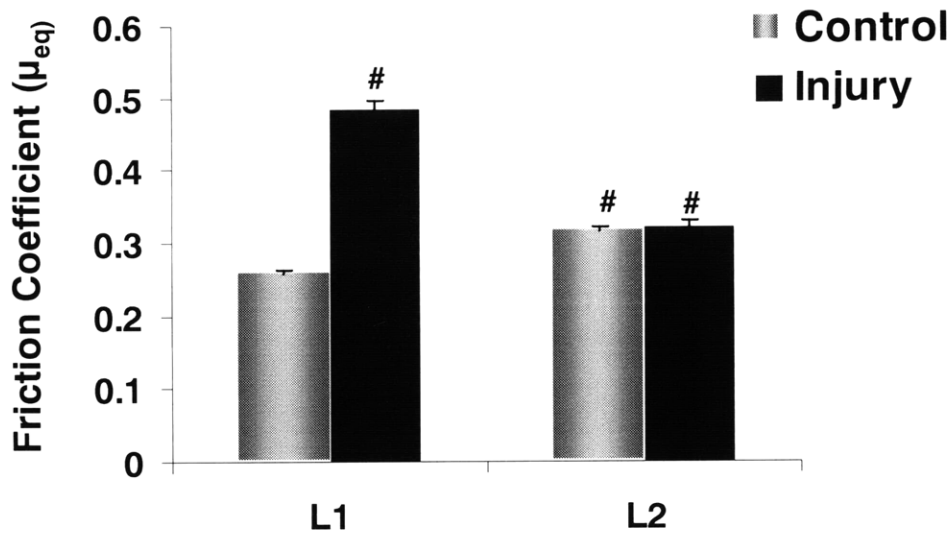


Figure 2.8. Equilibrium modulus of L1 and L2 cartilage disks.

Equilibrium modulus (Figure 2.8) ( $p < 0.0001$ ), as well as the peak stress during injury ( $p < 0.05$ ) (Figure 2.2B), were higher in L2 vs. L1 samples regardless of mechanical treatment. Injury had an overall effect (ANOVA,  $p = 0.05$ ) on the equilibrium modulus with a slight difference between L2 control and injury moduli ( $p = 0.059$ ).



**Figure 2.9.** Equilibrium friction coefficient of L1 and L2 normal and injured cartilage disks (n=6). #  $\rightarrow$  p<0.05 compared to L1 control.

L1 injured discs had the highest  $\mu_{eq}$  (p<0.001) relative to other conditions, shown in Figure 2.9. L2 control and injured disks demonstrated a higher  $\mu_{eq}$  (p<0.05) than L1 control samples, but injury did not significantly alter  $\mu_{eq}$  for L2 tissues (Figure 2.9).

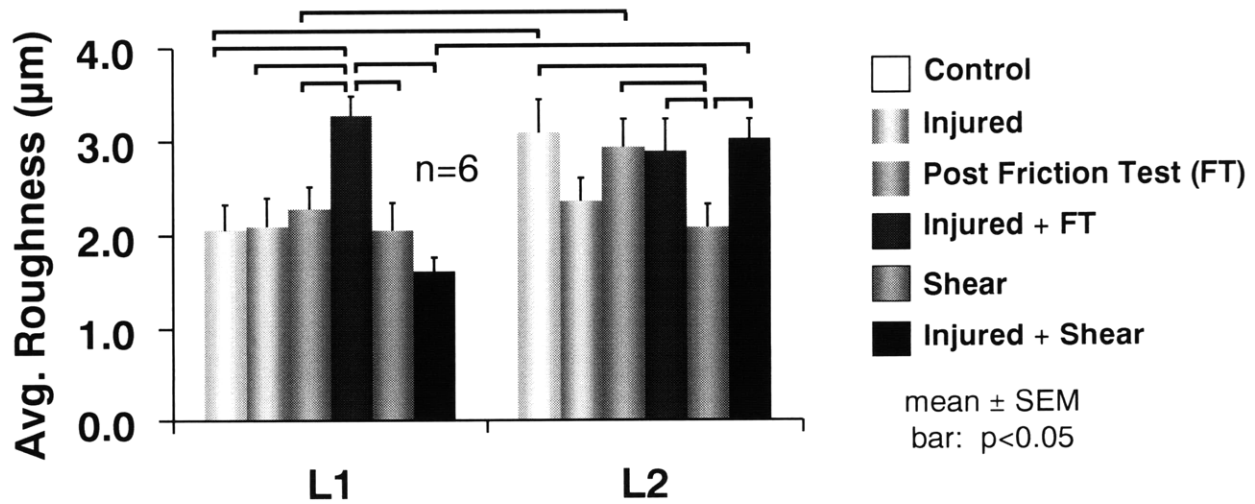


**Figure 2.10** Average surface roughness after various mechanical treatments.

Likewise, none of the mechanical treatments altered L2 cartilage surface roughness. Only injured L1 samples that had been subjected to lateral surface motion superimposed on a normal compressive load showed increased surface roughness (p<0.031) compared to other L1 samples (Figure 2.10). The L1 injured + FT samples had similar surface roughness compared to all L2

cartilage samples. Tissue shear loading along seemed to have a small, but significant effect on L2 normal cartilage, but not L1 cartilage samples.

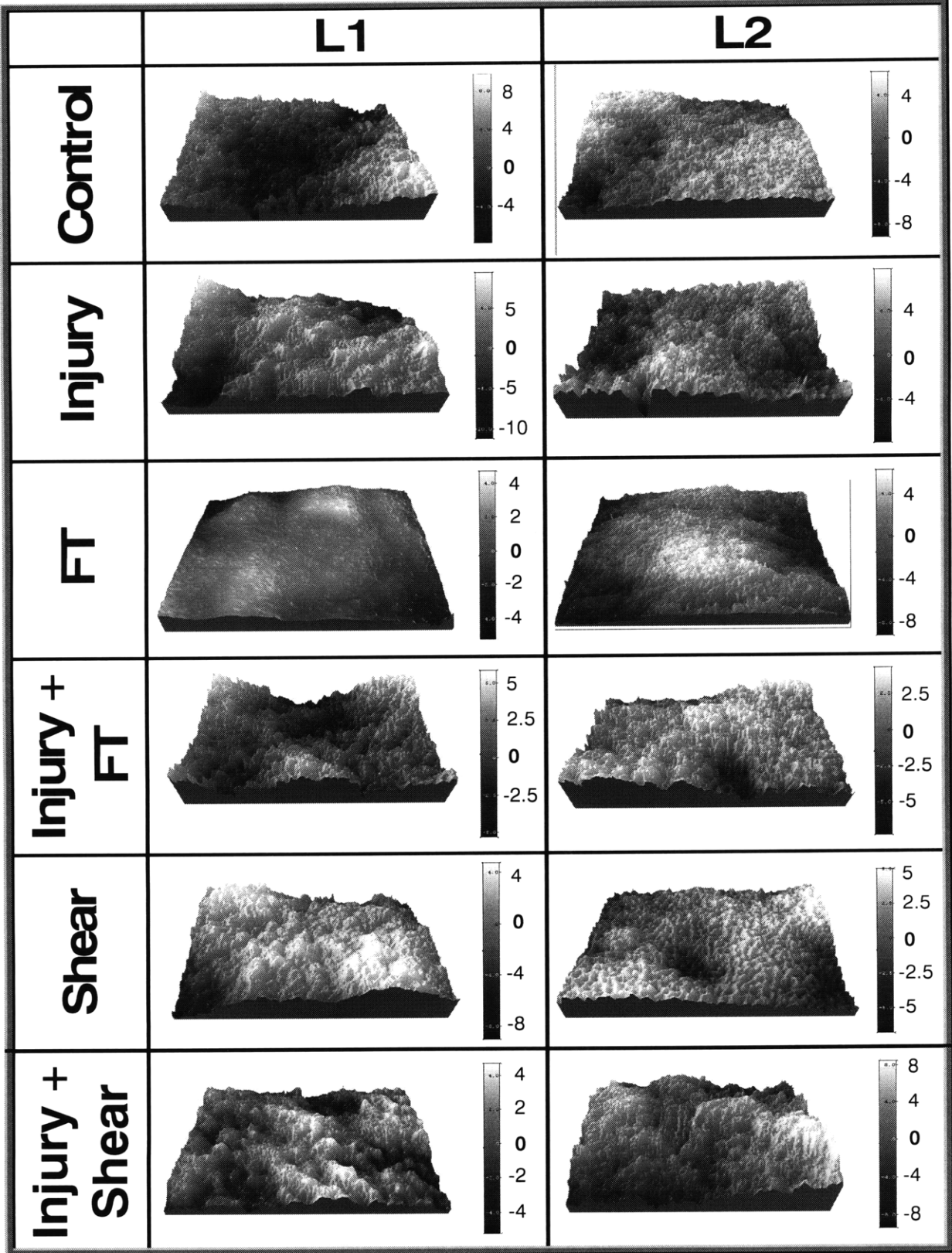
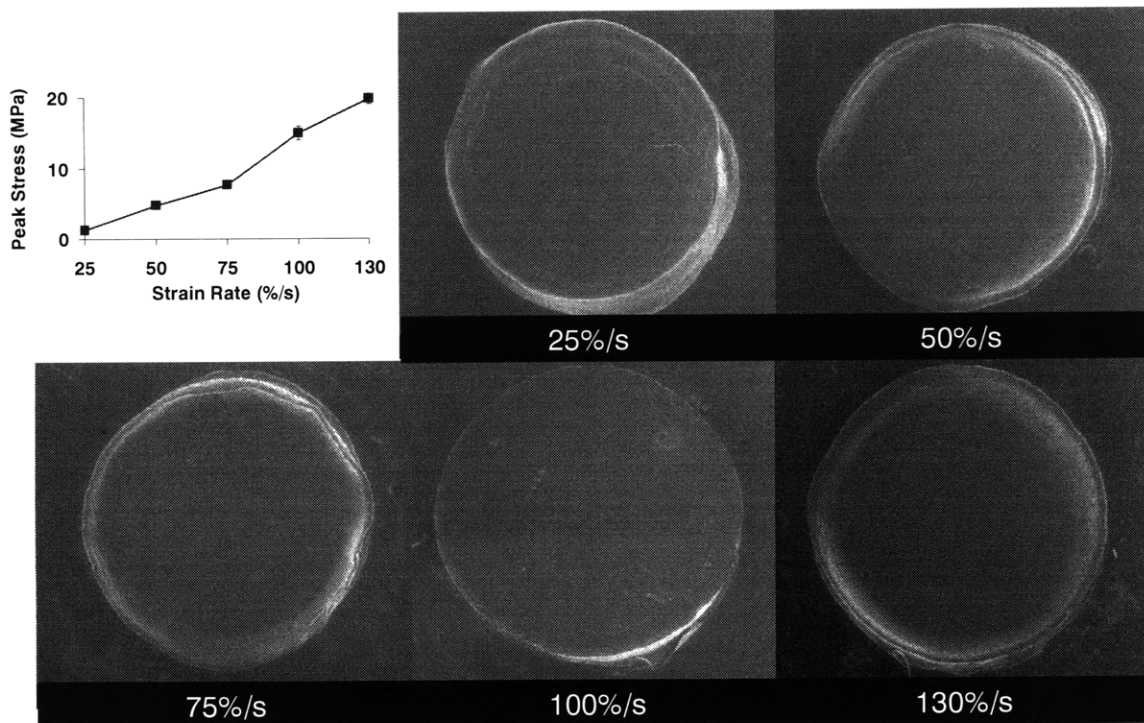


Figure 2.11 The height profiles of the 3D profilometer scans for surface roughness.

Profilometer images reinforce the fact that the friction test caused additional fibrillation, thus increasing surface roughness, on the L1 injured surfaces. The L2 cartilage surfaces remained rough regardless of mechanical treatment perhaps because they started off with a cut surface whereas the L1 started with an intact articular surface (Figure 2.11).

In order to obtain a more global view of the cartilage surface after mechanical injury, ESEM images were taken of L1 cartilage samples that were injured at different strain rates.



**Figure 2.12. L1 cartilage surface that were injured at various strain rates.**



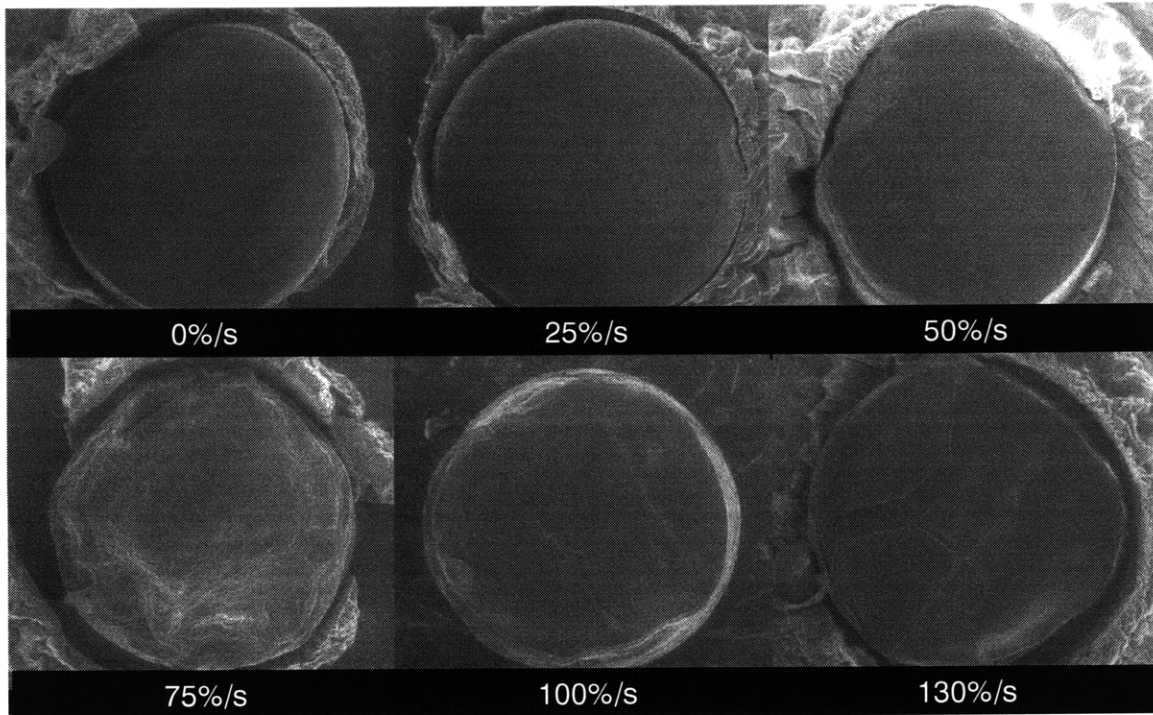


**Figure 2.13.** L1 cartilage disks that were injured and friction tested, thus subjected to additional lateral motion superimposed on normal load.

The cartilage disks with intact surface, L1, showed that injury alone (Figure 2.12) did not cause significant damage to the surface even with increasing strain rate. However, when additional lateral motion at a nontrivial compressive load was placed onto the injured disc, there was increasing visible damage as the strain rate elevated (Figure 2.13).

## 2.4 Discussion

This study demonstrates that *in vitro* mechanical injury has profound consequences on the mechanical properties of cartilage and that these effects have distinct depth-dependence. Such mechanical inhomogeneity has often been observed in adult cartilage. In addition, our finding that the unconfined compression modulus of uninjured L2 is 3 times stiffer than uninjured L1 confirms an earlier study on newborn bovine cartilage [3]. Mechanical injury had little effect on the equilibrium modulus of L1, but decreased the modulus of L2 (Figure 2.8), consistent with previous literature [2]. In contrast, L1  $\mu_{eq}$  drastically increased due to injury, while no effect on L2  $\mu_{eq}$  was observed (Figure 2.9). The combination of mechanical injury and lateral motion induced structural changes in L1 tissue, but L2 tissue was apparently not susceptible to such changes (Figure 2.11). The lack of an apparent injurious effect may be due to

the pre-existing damage imposed on L2 from cutting, while the L1 surface remained intact. Simple dynamic shear strain was not sufficient to perturb the L1 injured tissue surface in a manner similar to the friction test. Still, there was a depth-dependence in surface roughness due to shear, as demonstrated in an earlier work [7]. The high friction coefficient for L1 injured samples and their increased surface roughness following the friction test imply that intense lateral motion superimposed on a normal strain applied to an injured intact surface may exacerbate fibrillation. These observations are consistent with the global view of the cartilage surface images taken using ESEM. At the given range of strain rates tested, injury alone did not appear to cause profoundly visible surface damage. However, the damage due to higher strain rates gradually became more apparent as oscillating lateral motion superimposed on a normal strain is applied for one hour. The apparent necessity of multiple types of mechanical events to induce surface damage may be important in understanding the process of tissue damage and degradation in arthritis and may lead to the development of more relevant *in vitro* models of cartilage injury.

## 2.5 Bibliography

1. Frank, E.H., et al., *A versatile shear and compression apparatus for mechanical stimulation of tissue culture explants*. J Biomech, 2000. 33(11): p. 1523-7.
2. Kurz, B., et al., *Biosynthetic response and mechanical properties of articular cartilage after injurious compression*. J Orthop Res, 2001. 19(6): p. 1140-6.
3. Klein, T.J., et al., *Depth-dependent biomechanical and biochemical properties of fetal, newborn, and tissue-engineered articular cartilage*. J Biomech, 2007. 40(1): p. 182-90.
4. Hodge, W.A., et al., *Contact pressures in the human hip joint measured in vivo*. Proc Natl Acad Sci U S A, 1986. 83(9): p. 2879-83.
5. Lu, X., M.M. Khonsari, and E.R.M. Gelinck, *The Stribeck Curve: Experimental Results and Theoretical Prediction*. 2006.
6. Jin, M., et al., *Tissue shear deformation stimulates proteoglycan and protein biosynthesis in bovine cartilage explants*. Arch Biochem Biophys, 2001. 395(1): p. 41-8.
7. Gleghorn, J.P., et al., *Boundary mode frictional properties of engineered cartilaginous tissues*. Eur Cell Mater, 2007. 14: p. 20-8; discussion 28-9.
8. Jones, A.R., et al., *Modulation of lubricin biosynthesis and tissue surface properties following cartilage mechanical injury*. Arthritis Rheum, 2009. 60(1): p. 133-42.
9. Jones, A.R., et al., *Binding and localization of recombinant lubricin to articular cartilage surfaces*. J Orthop Res, 2007. 25(3): p. 283-92.
10. Schumacher, B.L., et al., *Immunodetection and partial cDNA sequence of the proteoglycan, superficial zone protein, synthesized by cells lining synovial joints*. J Orthop Res, 1999. 17(1): p. 110-20.
11. Schumacher, B.L., et al., *A novel proteoglycan synthesized and secreted by chondrocytes of the superficial zone of articular cartilage*. Arch Biochem Biophys, 1994. 311(1): p. 144-52.
12. Swann, D.A., et al., *The molecular structure and lubricating activity of lubricin isolated from bovine and human synovial fluids*. Biochem J, 1985. 225(1): p. 195-201.

13. Jay, G.D., B.P. Lane, and L. Sokoloff, *Characterization of a bovine synovial fluid lubricating factor. III. The interaction with hyaluronic acid*. *Connect Tissue Res*, 1992. 28(4): p. 245-55.
14. Jay, G.D., D.A. Harris, and C.J. Cha, *Boundary lubrication by lubricin is mediated by O-linked beta(1-3)Gal-GalNAc oligosaccharides*. *Glycoconj J*, 2001. 18(10): p. 807-15.
15. Fitzgerald, J.B., M. Jin, and A.J. Grodzinsky, *Shear and compression differentially regulate clusters of functionally related temporal transcription patterns in cartilage tissue*. *J Biol Chem*, 2006. 281(34): p. 24095-103.
16. Sah, R.L., et al., *Biosynthetic response of cartilage explants to dynamic compression*. *J Orthop Res*, 1989. 7(5): p. 619-36.
17. Grad, S., et al., *Surface motion upregulates superficial zone protein and hyaluronan production in chondrocyte-seeded three-dimensional scaffolds*. *Tissue Eng*, 2005. 11(1-2): p. 249-56.
18. Nugent, G.E., et al., *Static and dynamic compression regulate cartilage metabolism of PRoteoGlycan 4 (PRG4)*. *Biorheology*, 2006. 43(3-4): p. 191-200.
19. Nugent, G.E., et al., *Dynamic shear stimulation of bovine cartilage biosynthesis of proteoglycan 4*. *Arthritis Rheum*, 2006. 54(6): p. 1888-96.

## **3 Effect of Injury on Lubricin Synthesis from Cartilage**

### **3.1 Introduction**

Recent experiments have specifically demonstrated that dynamic shear and compressive loading increase PRG4 secretion and expression by many folds compared to static compression and even free swell controls [1-3]. These studies suggest by moderating the lubricin production, mechanical stimulation plays a role in preserving the articular surface smoothness with a low CoF. Lack of lubricin on the cartilage surface increases the friction coefficient of normal uninjured cartilage. However, only the presence of lubricin on the surface and in the lubricant was able to reduce the friction coefficient of injured cartilage. The objective of this study is to characterize the effect of injury on the lubricin gene expression and protein synthesis.

Mechanical injury increases the friction coefficient of cartilage with endogenous lubricin and additional lateral motion on injured articular surface increases its roughness. Lubricin has been widely researched as primary determinant of lubrication in SF. Lubricin and superficial zone protein (SZP) are homologous glycoproteins derived from the gene proteoglycan 4 (PRG4) of synoviocytes and superficial chondrocytes, respectively [4-6]. Their saturated negatively charged O-linked glycosylation in the middle mucin-like domain enhances boundary lubrication of the cartilage surface due to the strong repulsive hydration forces [6, 7]. In fact, removing the O-linked  $\beta(1-3)$  Gal-GalNAc oligosaccharides in SF lubricin by 54% can reduce the lubricating ability by 80% [8]. As a result, the purpose of this next study is to see how lubricin on the cartilage surface and/or in the synovial fluid impact the surface properties of injured L1 cartilage.

## 3.2 Methods

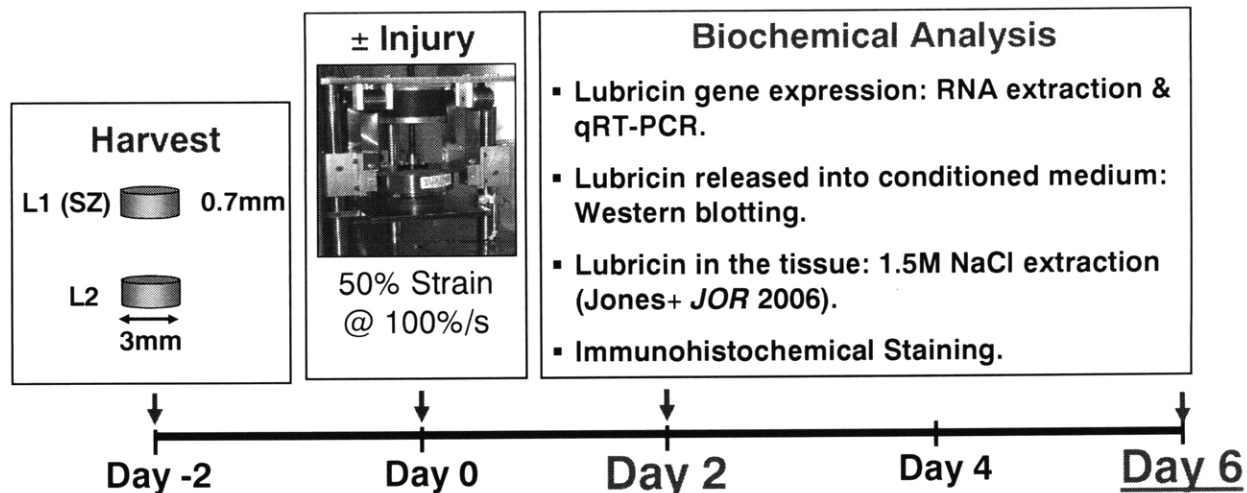


Figure 3.1. Timeline of the steps taken in analyzing the gene expression and protein synthesis

### 3.2.1 Harvest and Injurious Compression

Cartilage disks from 1-2 week old bovine calves (Research 87) were extracted and excised using the same procedure described in Chapter 2. After 2 days of equilibration in 1% ITS supplemented cultural medium, equal groups of 8 cartilage disks are either placed in free swelling condition or subjected to injurious compression (50% strain at 100%/s strain rate). The treated disks were placed in new medium that is refreshed every other day. On day 2 and 6 after injury when the experiment is terminated, lubricin gene expression, protein released into the medium and retained on the cartilage surface, and synthesis through immunohistochemical staining were assessed (Figure 3.1).

### 3.2.2 Lubricin Gene Expression

3 animals were used for lubricin gene expression. On day 2 and 6 after injury, the discs were flash frozen in liquid nitrogen prior to storing in -80 °C. 8 uninjured or injured disks from the 3 animals were pooled for RNA extraction followed by absorbance measurements in 260 and 280  $\mu\text{m}$  to assess the RNA concentration and purity. Next, RNA samples were reverse transcribed into cDNA for RT-PCR in a 1-step process (Applied Biosystems). The bovine lubricin primer/probe sequences used were 5'-GAGCAGACCTGAATCCGTGTATT for forward primer, 5'-GGTGGGTTCTGTTTGTAAGTGTA for reverse primer, and 5'-CTGAACGCTGCCACCTCTCTTGAAA for the probe (5'FAM, 3'TAMRA) [1]. The

housekeeping gene used for normalizing the lubricin gene expression was GAPDH. Housekeeping genes are genes that are constitutively expressed to maintain the cell sustenance. As a result, they are often used as the internal reference in quantifying the relative amplification of another gene. The sequences used for GAPDH were 5'- AAGCTCGTCATCAATGGAAAGG for the forward primer, 5'-GCATCACCCCACTTGATGTTG for the reverse primer, and 5'-TCACCATCTTCCAGGAGCGAGATCC for the probe (5'FAM, 3'TAMRA) [9]. Details of the RT-PCR procedure conducted at Wyeth Research by Dr. Aled Jones are in Appendix A.

### 3.2.3 Lubricin Protein Secretion

The spent cultural medium during the 48 hours prior to the termination of the experiment was collected and assessed for protein secretion using Western Blotting (Appendix A).

### 3.2.4 Lubricin Retained on the Cartilage Surface

Lubricin is extracted from the cartilage disks using the salt extraction method previously established with minimal damage to aggrecan and collagen content [10]. Groups of 8 discs that were uninjured and injured were placed in 1 ml of 1.5 M NaCl at 4°C for an hour before storing the salt solution containing the extracted lubricin in -20°C. The protein amount was then qualified using Western Blotting (Appendix A).

### 3.2.5 Lubricin Protein Synthesis

The uninjured and injured disks for immunohistochemistry (IHC) analysis were fixed and stored in 70% ethanol. (Appendix A)

### 3.2.6 Friction Test Paradigm

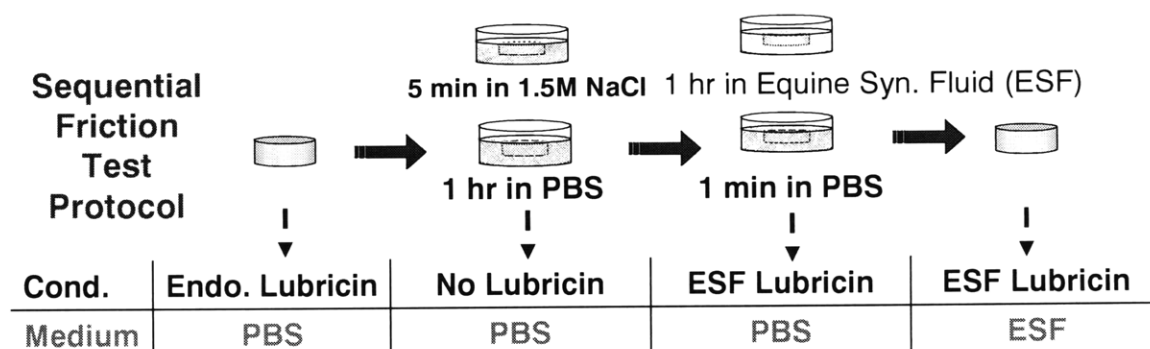
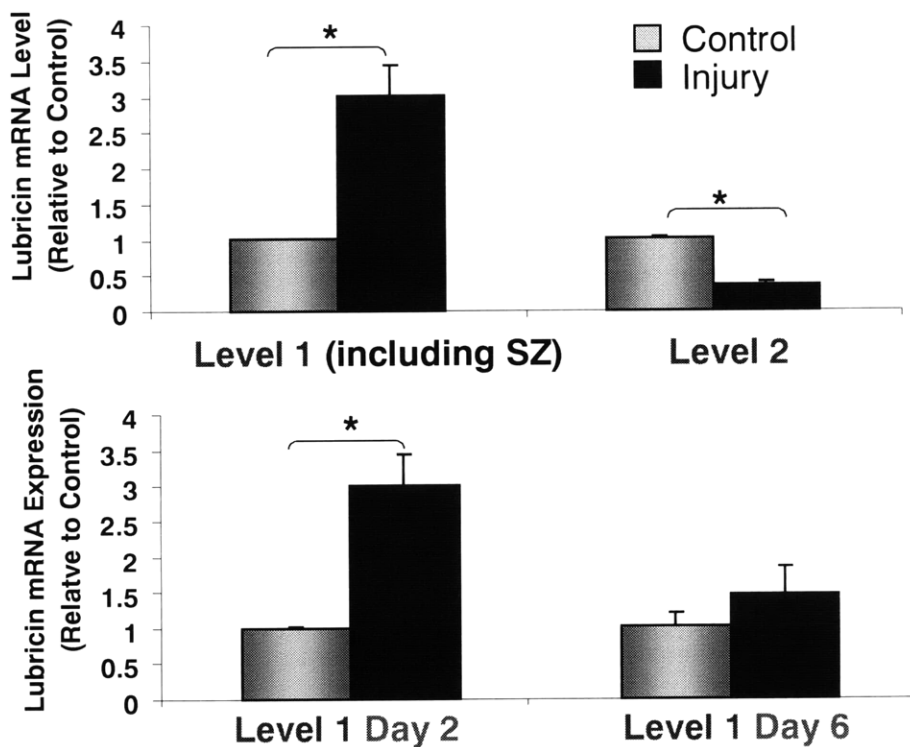


Figure 3.2. The paradigm for testing the effect of lubricin on friction coefficient.

Friction coefficient was initially measured on injured and normal cartilage in the presence of endogenous lubricin. Endogenous lubricin was extracted using 1.5 M NaCl, a concentration shown to strip the natural lubricin without too much damage to the surface [10]. Friction coefficient measurement was taken after 1 hour of PBS equilibration to see the effect of lubricin on normal and injured cartilage. The cartilage was then soaked in equine synovial fluid (ESF) briefly to see if exogenous lubricin can be localize at the cartilage surface and function like the endogenous lubricin as measured by friction coefficient. The importance of the exchange between the lubricin on the cartilage surface and lubricin in the bath was tested by immersing the disk with the exogenous lubricin immersed in ESF [11]. Additional details can be found in Appendix A.

### 3.3 Results



**Figure 3.3.** Lubricin gene expression of L1 and L2 cartilage days after injury (n=3 animals; mean±SEM; \*→p<0.05)

Injury heightened the lubricin gene expression in L1 cartilage, but declined the expression in L2 cartilage 2 days after injury. When comparing L1 cartilage 2 days and 6 days after injury, the increase in lubricin expression 2 days after injury diminishes by day 6. Together,



these results show that there is a depth and temporal dependence in lubricin gene expression (Figure 3.3).

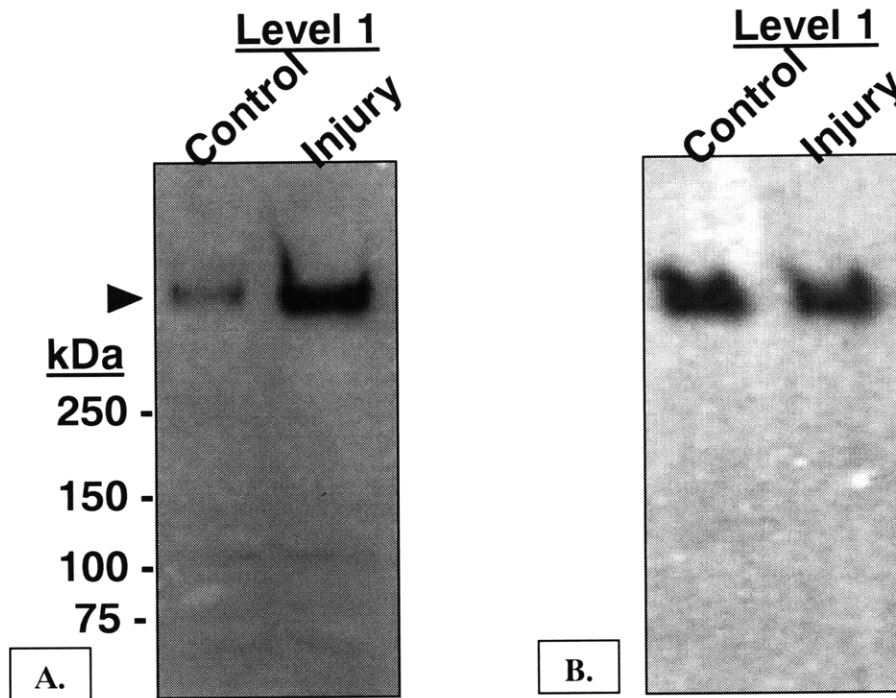


**Figure 3.4.** Western blot of **A)** lubricin protein secretion into the medium and **B)** lubricin extracted from L1 cartilage 2 days after injury

Injury also seems to increase the lubricin protein secretion (Figure 3.4A) into medium for L1 cartilage, but not for L2 cartilage (Appendix A). However, the amount of lubricin extracted from L1 cartilage appears to be comparable between injured and normal L1 cartilage (Figure 3.4B). If the amount of lubricin secreted (Figure 3.4A) is combined with amount extracted (Figure 3.4B), then the total amount of lubricin in the L1 injured cartilage looks greater than that in L1 normal cartilage. This trend tracks with the lubricin gene expression finding (Figure 3.3).

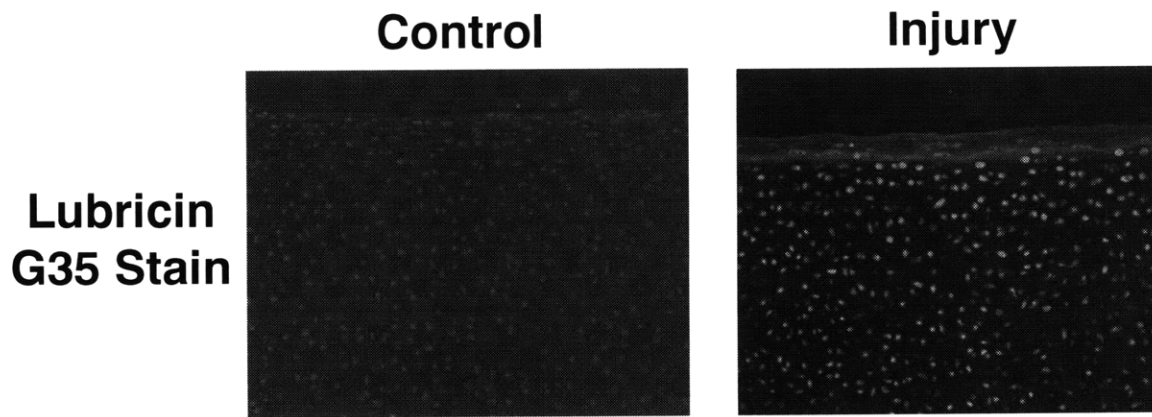


**Figure 3.5.** Immunohistochemical stain of lubricin in L1 normal and injured cartilage 2 days after injury using G35 antilubricin stain

Furthermore, injured L1 cartilage displays a brighter stain compared to normal L1 cartilage indicating higher lubricin synthesis (Figure 3.5).

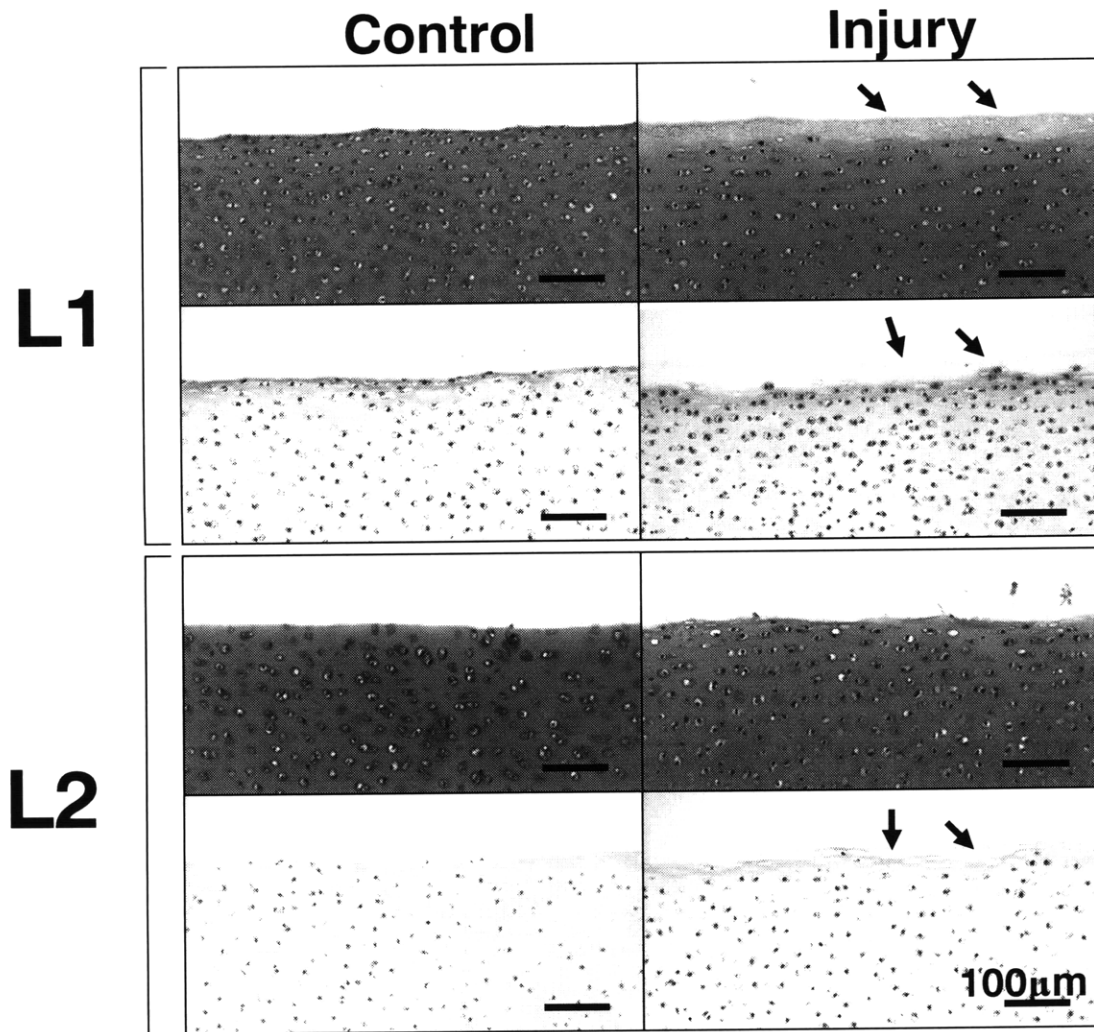


**Figure 3.6.** GAG stained with Safranin O (shown in 1<sup>st</sup> and 3<sup>rd</sup> rows) and collagen stained with Trichrome (shown in 2<sup>nd</sup> and 4<sup>th</sup> rows) of L1 and L2 normal and injured cartilage

Comparing the injured case to the noninjured case for L1 cartilage, there is an apparent depletion in GAG and collagen content near the surface (Figure 3.6). However, injury does not seem to cause as profound a loss in GAG and collagen near the L2 cartilage surface as it did to L1 cartilage surface.

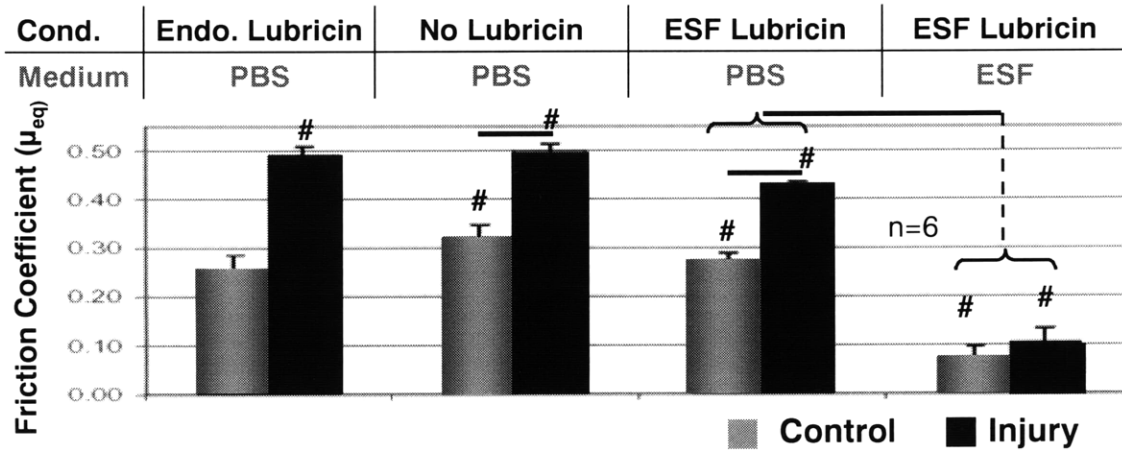


**Figure 3.7.** Effect of endogenous and exogenous lubricin on the friction coefficient of normal and injured L1 cartilage

Stripping the cartilage of lubricin affected only the friction coefficient of L1 normal cartilage. When exogenous lubricin was localized on its surface, the friction coefficient did not decrease. Both endogenous and exogenous lubricin did not affect the increased friction coefficient of injured L1 cartilage. However, when the bath changed from PBS to ESF during the friction test, the friction coefficients for both uninjured and injured cartilage were significantly reduced. Another consequence of applying lateral motion using a lubricin rich bath environment is that the friction coefficient of injured cartilage will be comparable to the one of its uninjured counterpart. (Figure 3.7).

### 3.4 Discussion

Previous research have shown a single injurious compression can induce ~20 MPa in bovine middle zone cartilage, a peak stress value comparable to what human joints experience in daily life [12]. Such high peak stress leads to apoptosis, GAG loss, gene expression, as well as decreased dynamic and equilibrium compressive and shear stiffness [13-15]. Our results demonstrate that cartilage with the superficial zone intact is more susceptible to GAG and collagen depletion after injury compared to the middle zone. This difference can be attributed to the fact that compressive modulus as well as shear modulus increase with depth from the surface [16, 17]. It is therefore expected that a weak superficial layer with low GAG and collagen content near the surface would experience more tissue damage due to injury [16]. Furthermore, the histology shows injury did not cause profound structural fibrillation at the surface, consistent

with our finding in Chapter 2 that the average roughness was not increased as a direct consequence of injury.

Since injury leads to higher risk of OA which initiates at the surface and lubricin is a glycoprotein which concentrates at the superficial layer, our study is the premier demonstration of how mechanical injurious compression affects lubricin gene expression and protein synthesis. Given that lubricin gene expression is increased 2 days after injury, but returns to control level at 6 days post injury, it suggests lubricin gene expression in L1 cartilage responds to mechanical injury in a temporal manner. The fact that injury also increased the combined lubricin protein expression for L1 cartilage after 2 days reinforces our finding in the corresponding gene expression profile. The depth dependence in the response of lubricin gene expression to injury is expected since lubricin is mainly localized near the superficial layer [5].

According to the immunohistochemical (IHC) staining, injured cartilage seems to have more lubricin synthesis near the surface compared to uninjured cartilage. Yet, the lubricin extracted from the injured and uninjured surface as shown in the Western blot were comparable. A possible justification is that the salt extraction shows the lubricin content from the entire 700  $\mu\text{m}$  of the cartilage disk, while the IHC staining highlights the lubricin near the surface.

The presence of endogenous lubricin significantly affects the surface properties of uninjured cartilage. When endogenous lubricin is stripped, exogenous lubricin which localized at the surface slightly mitigate the elevated friction coefficient of the uninjured cartilage. Furthermore, increased friction coefficient of injured surface is not responsive to either endogenous or exogenous lubricin when the medium is PBS. However, ESF allows equal smooth lateral motion on injured cartilage surface as on uninjured, normal surface. In fact, friction coefficient of articular cartilage surface under boundary lubrication decreases with increasing concentration of synovial fluid [18]. Our finding suggests that as long as synovial fluid is rich in lubricin and other lubricating molecules, injured articular cartilage can maintain smooth joint motion just like a healthy normal cartilage would regardless whether there is endogenous lubricin present at the articular surface. One study that reinforces the protective aspect of exogenous demonstrated regular injection of recombinant lubricin for four weeks how OA in cartilage using a rat model was prevented after induced injury by (Figure 3.8, [19]).

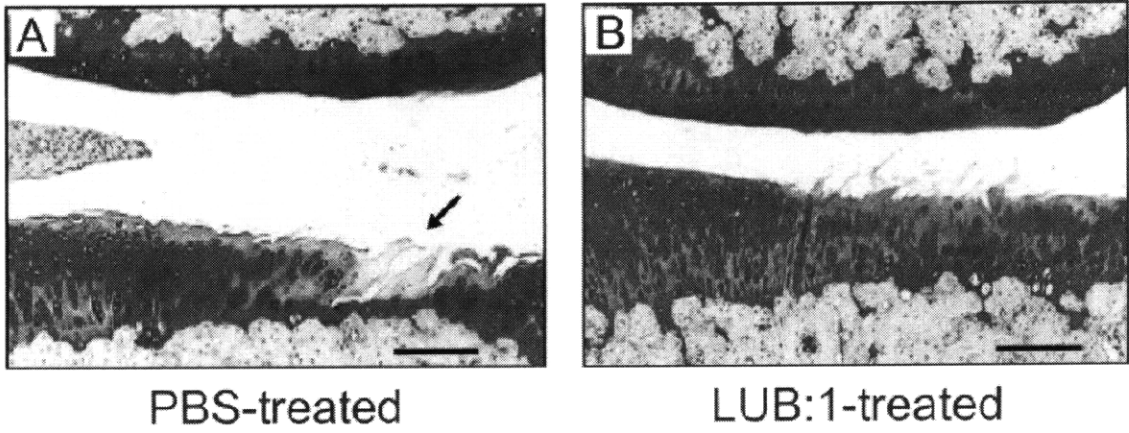


**Figure 3.8.** Rat OA joint after treated with PBS or recombinant Lubricin for 4 weeks [19]. Additional analysis and discussion are provided in Appendix A.

### 3.5 Bibliography

1. Grad, S., et al., *Surface motion upregulates superficial zone protein and hyaluronan production in chondrocyte-seeded three-dimensional scaffolds*. Tissue Eng, 2005. **11**(1-2): p. 249-56.
2. Nugent, G.E., et al., *Static and dynamic compression regulate cartilage metabolism of PRoteoGlycan 4 (PRG4)*. Biorheology, 2006. **43**(3-4): p. 191-200.
3. Nugent, G.E., et al., *Dynamic shear stimulation of bovine cartilage biosynthesis of proteoglycan 4*. Arthritis Rheum, 2006. **54**(6): p. 1888-96.
4. Schumacher, B.L., et al., *Immunodetection and partial cDNA sequence of the proteoglycan, superficial zone protein, synthesized by cells lining synovial joints*. J Orthop Res, 1999. **17**(1): p. 110-20.
5. Schumacher, B.L., et al., *A novel proteoglycan synthesized and secreted by chondrocytes of the superficial zone of articular cartilage*. Arch Biochem Biophys, 1994. **311**(1): p. 144-52.
6. Swann, D.A., et al., *The molecular structure and lubricating activity of lubricin isolated from bovine and human synovial fluids*. Biochem J, 1985. **225**(1): p. 195-201.
7. Jay, G.D., B.P. Lane, and L. Sokoloff, *Characterization of a bovine synovial fluid lubricating factor. III. The interaction with hyaluronic acid*. Connect Tissue Res, 1992. **28**(4): p. 245-55.
8. Jay, G.D., D.A. Harris, and C.J. Cha, *Boundary lubrication by lubricin is mediated by O-linked beta(1-3)Gal-GalNAc oligosaccharides*. Glycoconj J, 2001. **18**(10): p. 807-15.
9. Wong, M., M. Siegrist, and K. Goodwin, *Cyclic tensile strain and cyclic hydrostatic pressure differentially regulate expression of hypertrophic markers in primary chondrocytes*. Bone, 2003. **33**(4): p. 685-93.
10. Jones, A.R., et al., *Binding and localization of recombinant lubricin to articular cartilage surfaces*. J Orthop Res, 2007. **25**(3): p. 283-92.
11. Gleghorn, J.P., et al., *Boundary mode frictional properties of engineered cartilaginous tissues*. Eur Cell Mater, 2007. **14**: p. 20-8; discussion 28-9.
12. Hodge, W.A., et al., *Contact pressures in the human hip joint measured in vivo*. Proc Natl Acad Sci U S A, 1986. **83**(9): p. 2879-83.
13. Lee, J.H., et al., *Mechanical injury of cartilage explants causes specific time-dependent changes in chondrocyte gene expression*. Arthritis Rheum, 2005. **52**(8): p. 2386-95.
14. Loening, A.M., et al., *Injurious mechanical compression of bovine articular cartilage induces chondrocyte apoptosis*. Arch Biochem Biophys, 2000. **381**(2): p. 205-12.
15. Kurz, B., et al., *Biosynthetic response and mechanical properties of articular cartilage after injurious compression*. J Orthop Res, 2001. **19**(6): p. 1140-6.
16. Klein, T.J., et al., *Depth-dependent biomechanical and biochemical properties of fetal, newborn, and tissue-engineered articular cartilage*. J Biomech, 2007. **40**(1): p. 182-90.
17. Buckley, M.R., et al., *Mapping the depth dependence of shear properties in articular cartilage*. J Biomech, 2008. **41**(11): p. 2430-7.
18. Schmidt, T.A., et al., *Boundary lubrication of articular cartilage: role of synovial fluid constituents*. Arthritis Rheum, 2007. **56**(3): p. 882-91.
19. Flannery, C.R., et al., *Prevention of cartilage degeneration in a rat model of osteoarthritis by intraarticular treatment with recombinant lubricin*. Arthritis Rheum, 2009. **60**(3): p. 840-7.

## **4 Induction of lubricin expression by mechanical injury through the TGF- $\beta$ signaling pathway**

### **4.1 Introduction**

In Chapter 3, we established that injurious mechanical compression caused a notable increase in lubricin gene expression and biosynthesis in the cartilage superficial layer 2 days after injury as well as a distinguishable loss of lubricin protein to the culture medium. Mechanical injury also caused a significant increase in TGF- $\beta$  (transforming growth factor- $\beta$ ) gene expression during the initial 24-hours post-injury period in middle zone cartilage [1]. In separate studies, exogenous TGF- $\beta$  was shown to upregulate lubricin expression and biosynthesis in cartilage explants [2], and blocking the TGF- $\beta$  pathway reduced the increase in lubricin expression caused by non-injurious dynamic shear loading [3]. These reports, which suggest a relation between TGF- $\beta$  signaling and mechanotransduction, motivate the objective of this study to test the hypothesis that blocking the TGF- $\beta$  pathway suppresses the increase in lubricin gene expression and protein secretion caused by injurious compression of cartilage. Meanwhile, this study will first verify that mechanical injury also upregulates TGF- $\beta$  gene in superficial layer of cartilage as well as protein expression for confirmation. Since the modulus for cartilage superficial layer is lower than the middle zone [4], a range of strain and strain rates will be applied to test the effect of injury on TGF- $\beta$ .

The following sections will entail descriptions of the canonical TGF- $\beta$  signaling pathway, and the TGF- $\beta$  blocker selected for this experiment.

#### **4.1.1 Canonical TGF- $\beta$ Signaling Pathway**

TGF- $\beta$  is a secreted growth factor that is a part of the TGF- $\beta$  superfamily of pleiotropic cytokines that are involved in cell growth, differentiation, migration, cell survival, and adhesion [5]. The members of this superfamily fall into two major branches: TGF- $\beta$ /Activin/Nodal and BMP/GDF (Bone Morphogenetic Protein/Growth and Differentiation Factor) [6]. TGF- $\beta$ 1 is a potent regulator in the matrix synthesis and plays a role in wound healing [7, 8].



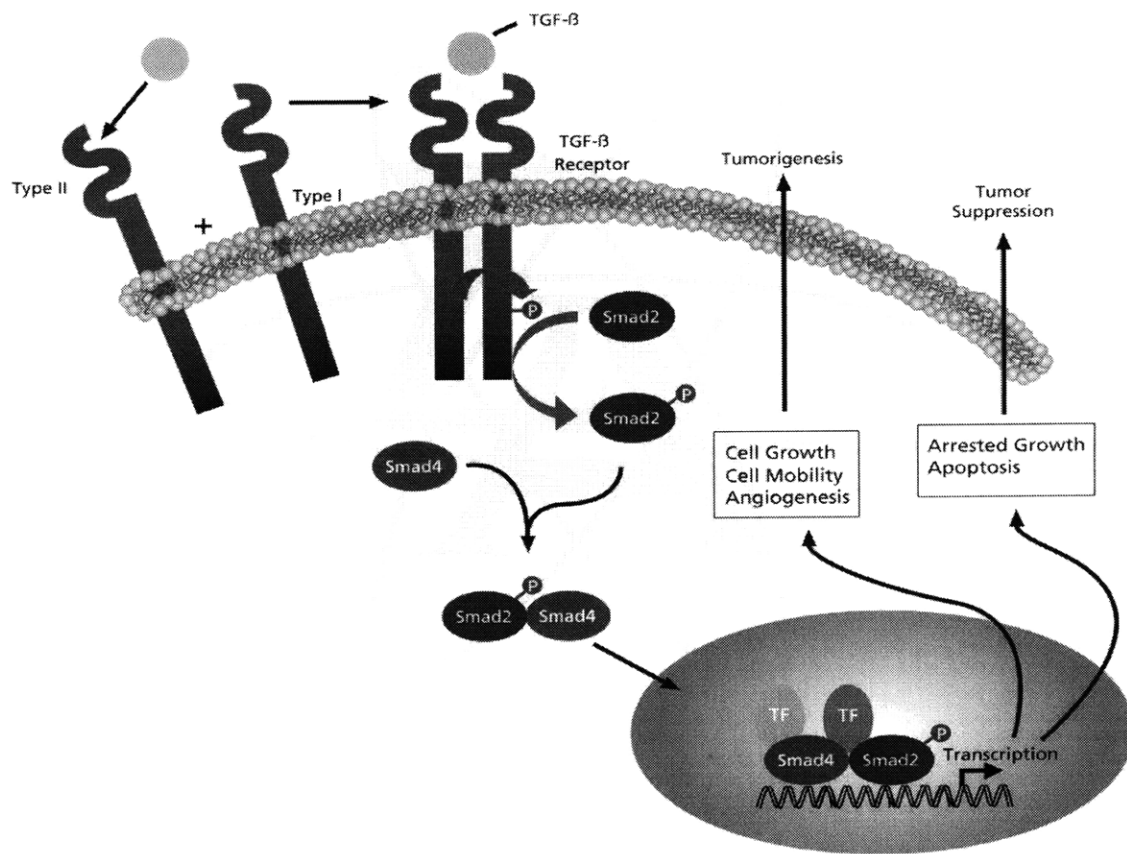


**Figure 4.1** The canonical TGF-β signaling pathway through SMAD 2/3 phosphorylation [9]

The canonical TGF-β signaling (Figure 4.1) begins with TGF-β first binding to Type II receptor, phosphorylates the serine residue of Type I receptor, and then forms a complex with those two transmembrane serine/threonine kinases receptors. Then, the Type I receptor phosphorylates the serine residue of the receptor-SMAD (SMAD 2/3) after SARA, an anchoring protein, recruits it. The activated SMAD 2/3 travels to the cytoplasm, phosphorylates and forms a complex with co-SMAD, SMAD4. The SMAD 2/3 + SMAD4 complex then goes into the nucleus to moderate transcription [6, 10].

It is important to note that TGF-β signaling is very complex. It also occur through many non-SMAD pathways including MAP kinase pathway, Rho-like GTPase signaling pathway, and AKT pathway [11]. In addition, there is much signaling cross-talk that can take place between the TGF-β/BMP pathway and other signaling pathways just mentioned [12]. Nevertheless, the importance of the SMAD 2/3 pathway lies in the fact that SMAD proteins are the only

substrates which has demonstrated to directly influence the target gene responses to the TGF- $\beta$  family [5].

#### 4.1.2 TGF- $\beta$ Blocker Selection

The TGF- $\beta$  blocker chosen is a small molecule, SB431542, (Figure 4.2) which blocks the Type I receptor and prevents the phosphorylation of SMAD 2 proteins [13].

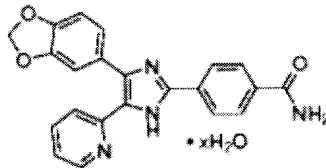


**Figure 4.2** Chemical structure of SB431542, small molecule which blocks the Type I receptor of TGF- $\beta$  [14] This blocker has been documented in previous works to [3, 15], and has been shown to have the half maximum inhibiting potency ( $I_{50}$ ) against Type I receptor of TGF- $\beta$  (ALK5) branch and not the Type I receptor of the Activin (ALK4) branch.  $I_{50}$  is the concentration of the inhibitor at which half of the signaling is blocked. Because the kinase region of the two Type I receptors are so similar, it is important to make sure there is much lower concentration threshold the blocker needs to overcome before effectively blocking ALK5 [13]. Another reason that this blocker is selected is because ALK5 is critical to TGF- $\beta$  signaling since Type II receptor only phosphorylates ALK5, but plays no role in downstream signaling [16, 17]. By blocking ALK5, the most direct impact that TGF- $\beta$  would have its target genes would be gone.

## 4.2 Methods

### 4.2.1 Tissue Harvest

Ø 3-mm cylinders were harvested from patellofemoral grooves of 1-2 wk old 700- $\mu$ m thick disks including the intact superficial layer were transversely sliced from each bovine cylinder with a brain matrix.

### 4.2.2 Strain Dependence of TGF- $\beta$ Gene and Protein Expression

Four groups of 8 cartilage disks from each animal (n=4 animals) were equilibrated for 48 hours in ITS% supplemented cultural medium. Then, the four groups were subjected to 0, 25, 50, and 65% strain in 0.5 s respectively and released immediately. The average measured peak

stress were 0, 4, 13, 18 MPa respectively. TGF- $\beta$ 1 gene expression and protein secretion were assessed after culturing the disks in fresh ITS% supplemented cultural medium for 48 hours. The TGF- $\beta$ 1 ELISA was done on the collected medium using the human TGF- $\beta$ 1 immunoassay (R&D Systems).

### 4.2.3 Effect of SB431542 on Lubricin Gene and Protein Expression of Injured Tissue

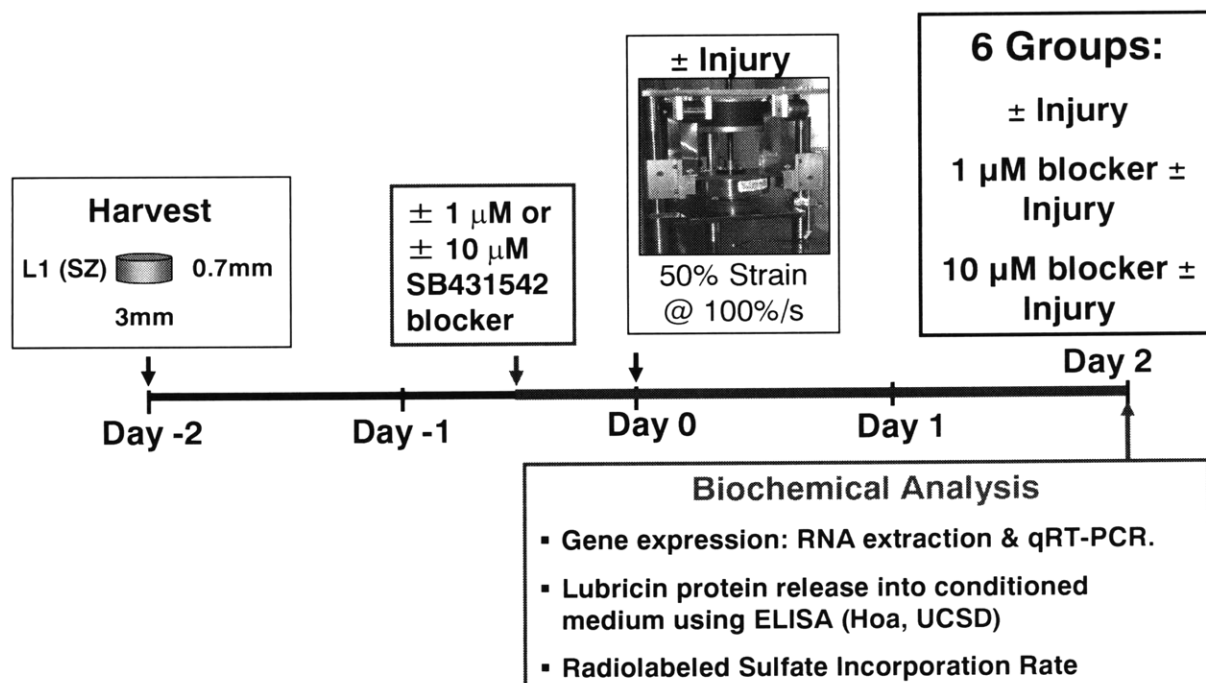


**Figure 4.3** The experiment scheme to test the effect of the blocker on injured

Cartilage disks (n=4 animals) were incubated in 1% ITS supplemented culture medium for 36 hours. Disks were used in six experimental groups, pre-incubated in 2 ml of medium for 12 hours in the presence of 1  $\mu\text{M}$  (2 groups) or 10  $\mu\text{M}$  (2 groups) of SB431542, a small molecule inhibitor of the TGF- $\beta$  type-I receptor, or no treatment (2 groups). Explants from one set of the 3 medium conditions were subjected individually to injurious compression of 50% strain at 100%/s strain rate while the other disks remained in free swelling conditions (CTL). Cartilage disks were then transferred to new ITS% supplemented cultural medium with or without the same blocker concentrations for 48 hours or being flash frozen for analysis of gene expression. The medium

during the 2 days of post-injury incubation was collected for each condition to assay for PRG4 protein release by ELISA using 3-A-4 monoclonal antibody [18].

#### **4.2.4 Sulfate Incorporation Rate Analysis**

Cartilage disks (n=7 disks / condition from 1 animal, same 6 conditions) were analyzed to assess the effects of the blocker on aggrecan biosynthesis by measuring  $S^{35}$  sulfate incorporation rate 2 days post-injury for 24 hrs.

#### **4.2.5 RNA Isolation and qRT-PCR**

RNA was extracted from 8 pooled disks by pulverizing and homogenizing them in TRIzol reagent (Invitrogen, San Diego, USA). Then, RNA was separated and isolated by using Phase Gels tubes (Eppendorf, Hamburg, Germany) and the RNAeasy Mini Kit (Qiagen, Chatsworth, CA). Once concentration and purity of RNA was determined at 260 and 180 nm, 1  $\mu$ g of RNA was reverse transcribed into cDNA, and analyzed by qRT-PCR using Primer Express Software (Applied Biosystems). The primer gene expression was determined using the standard curve generated from the amplification curves of each primer, and is reported as relative copy number normalized to expression of 18S and then to free swelling control values. The lubricin primers are AGGAATGCACTGTGGAGCTT for forward sequence, and GCCATAATCGGAACAGCACT for reverse sequence. The TGF- $\beta$  primers are CACGTGGAGCTGTACCAGAA for the forward sequence and ACGTCAAAGGACAGCCACTC for the reverse sequence (Figure 4.3).

#### **4.2.6 Statistical Analysis**

All data in the ELISA and gene expression were log transformed before analyzing for statistics using a linear mixed model followed by a post-hoc Tukey's test. Fixed variables are injury and 1  $\mu$ M blocker as well as injury and 10  $\mu$ M blocker. The random effect is animal. Each factors had 2 levels. Two-way ANOVA was used to analyze sulfate incorporation data. Post-hoc Tukey tests followed the respective statistical analyses for pairwise comparisons.

### 4.3 Results

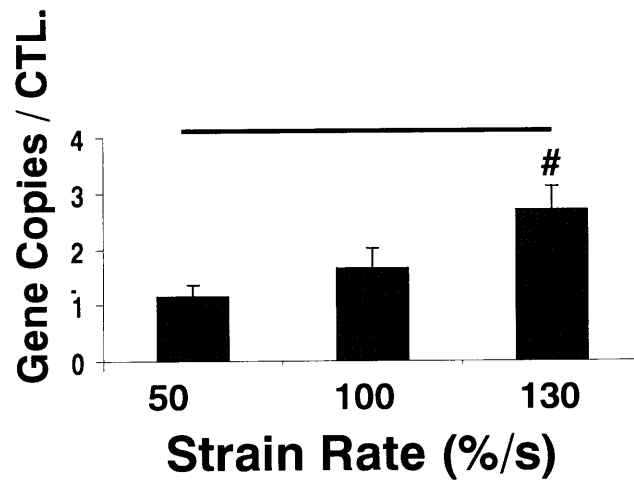


Figure 4.4 Effect of strain rate on TGF- $\beta$  gene expression

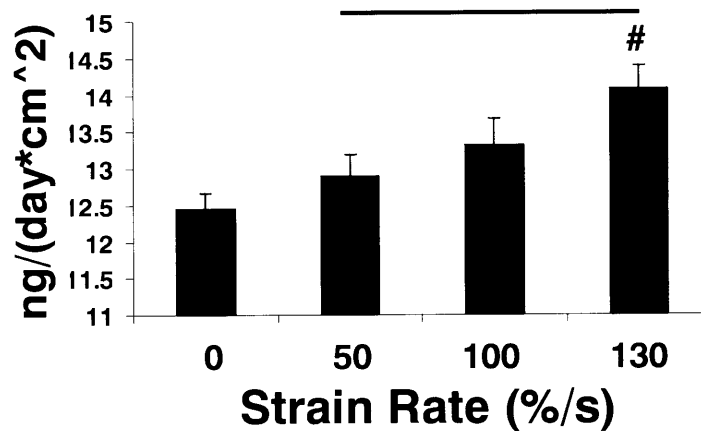


Figure 4.5 Effect of strain rate on TGF- $\beta$  protein release

Indeed, injury increased gene expression and protein secretion of TGF- $\beta$  after 2 days in cartilage with intact superficial zone in a strain-dose-dependent manner ( $p < 0.05$ , Figure 4.4, Figure 4.5). This finding is novel because this is the first time TGF- $\beta$  protein secretion has been reported in response to injury and also in a strain rate dose-dependent manner near the superficial zone. Meanwhile, the housekeeping gene, 18S, has shown to remain stable throughout the various strain rates (Figure 4.6).

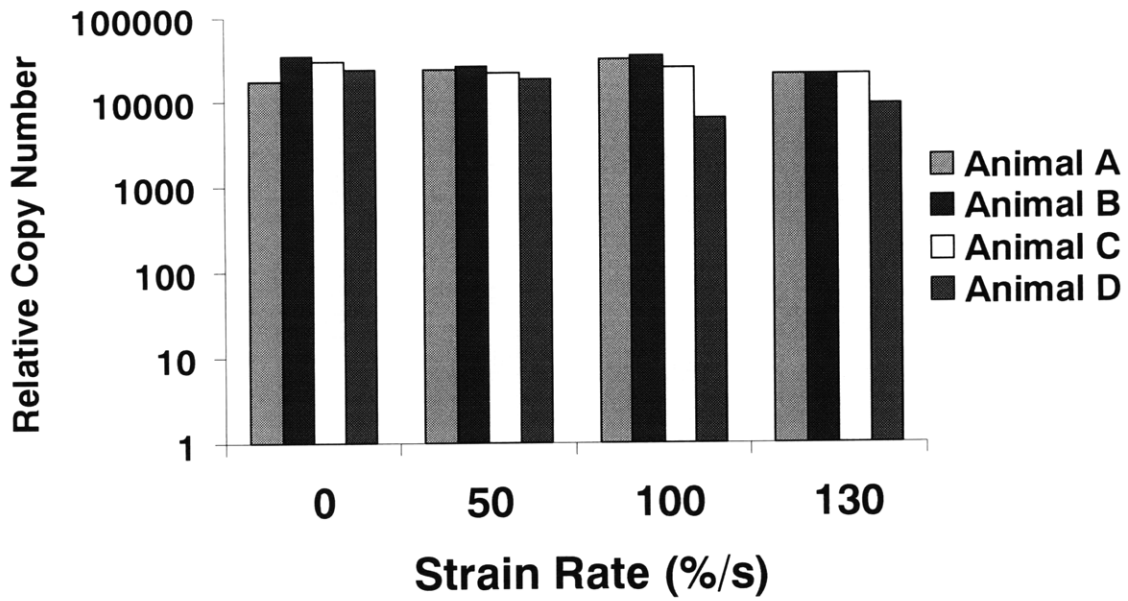


Figure 4.6 Relative Copy Number of 18S gene expression

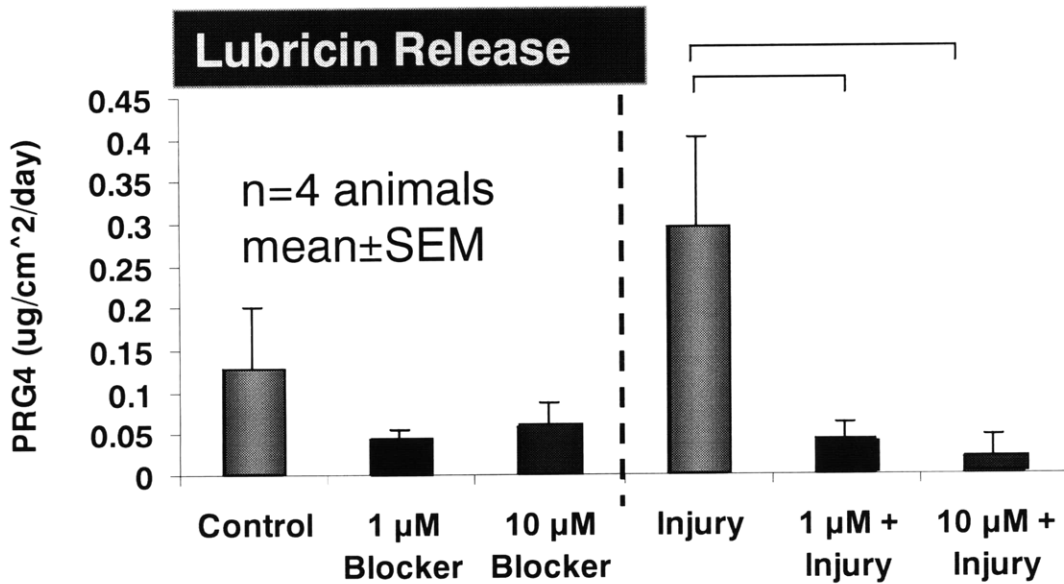


Figure 4.7 The Effect of blocker on the lubricin protein release from L1 injured versus noninjured cartilage

Compared to uninjured control disks, treatment with the TGF- $\beta$  blocker resulted in a trend towards decreased lubricin secretion and gene expression by 48 hours (Figure 4.7, Figure 4.8). Injurious compression resulted in peak stress values of 14~16 MPa that were similar under all treatment conditions (i.e.,  $\pm$ blocker) for disks from all animals ( $p > 0.05$ ) (data not shown).

Compared to injury alone, secretion of lubricin by injured cartilage disks was significantly decreased after being treated with either concentrations of TGF- $\beta$  blocker (Figure 4.7). However, lubricin gene expression (Figure 4.8) was significantly reduced only in the presence of 10  $\mu$ M blocker.

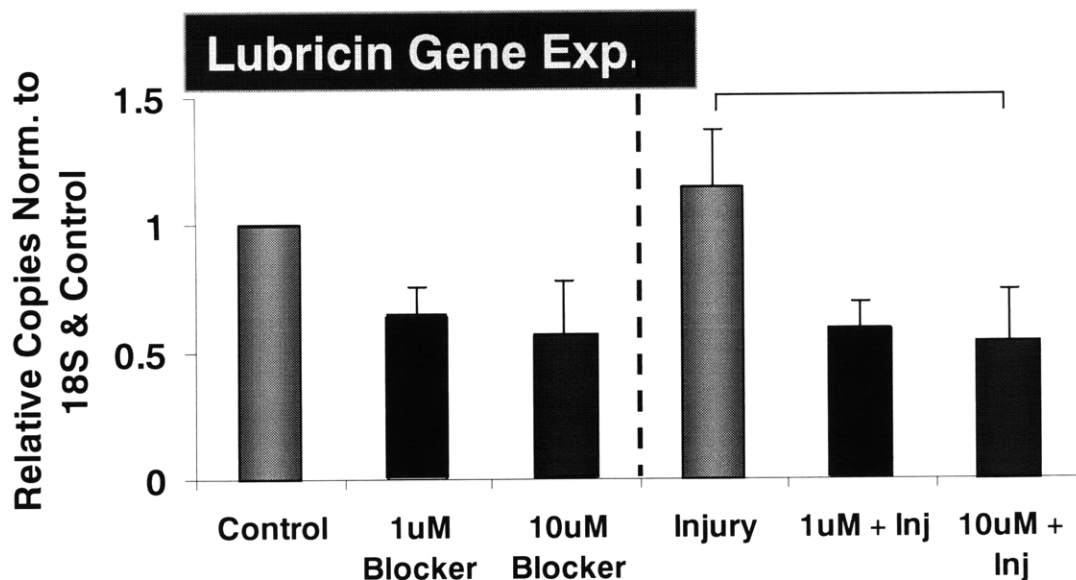


Figure 4.8 The Effect of TGF- $\beta$  blocker on lubricin gene expression in L1 injured or noninjured cartilage.

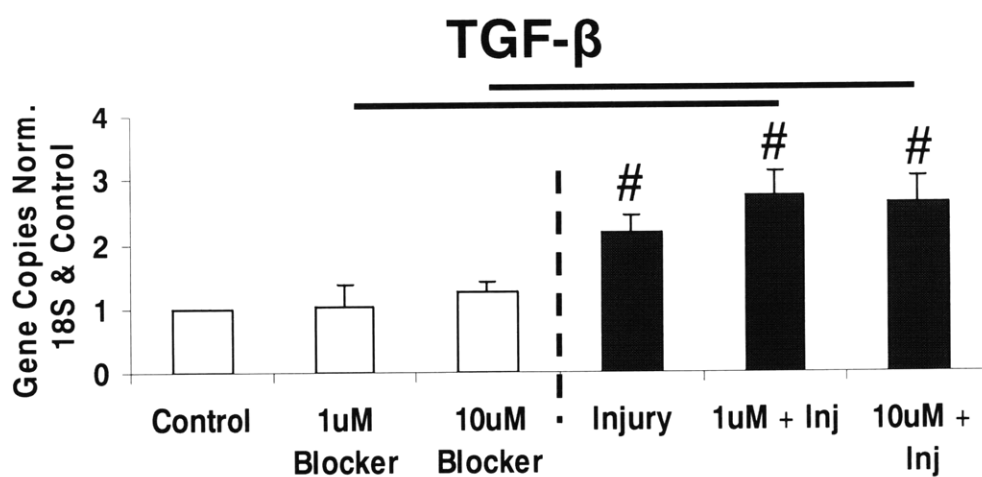


Figure 4.9 The Effect of TGF- $\beta$  blocker on TGF- $\beta$  gene expression in L1 injured or noninjured cartilage

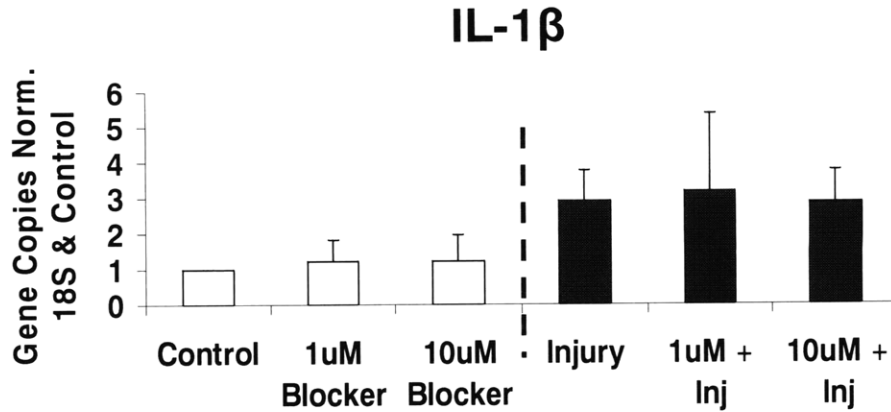


Figure 4.10 The effect of TGF- $\beta$  blocker on IL-1 $\beta$  gene expression in L1 injured or noninjured cartilage

TGF- $\beta$  gene expression (Figure 4.9) did not change due to either concentrations of the blocker, but did respond positively to injury. Similarly, IL-1  $\beta$ , a cytokine which negatively impacts lubricin protein release was unaffected by the blocker (Figure 4.10).

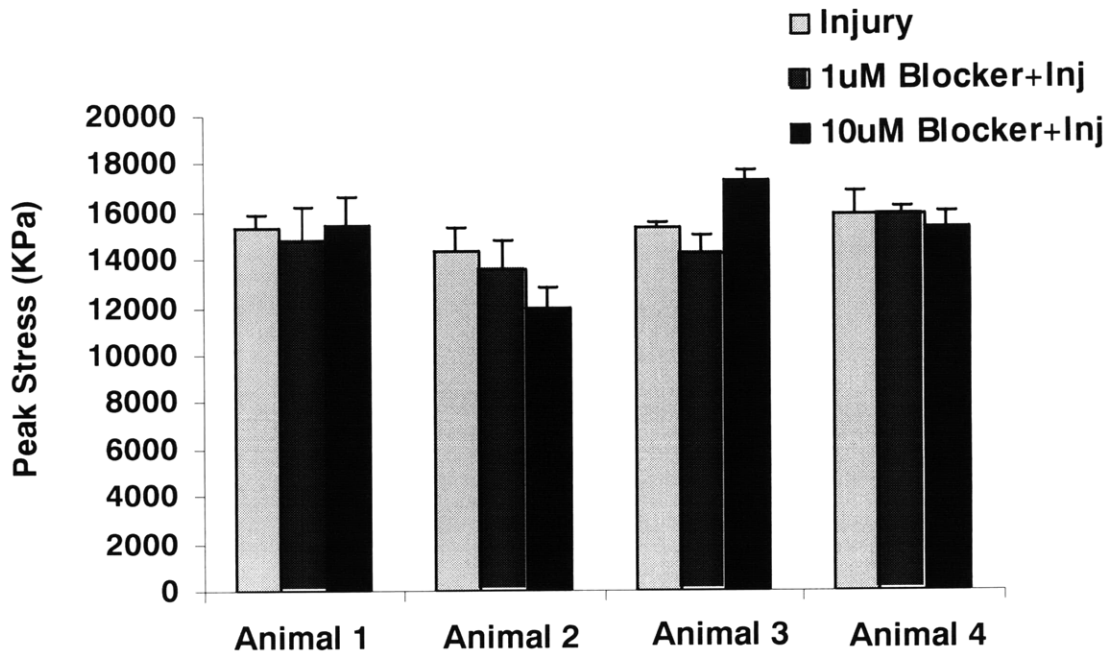


Figure 4.11. Peak stress among all the injury conditions across the 4 animals.

The peak stress did not change ( $p > 0.05$ ) with blocker concentration. Disks cultured in the presence of the TGF- $\beta$  blocker showed a significant dose-dependent decrease in sulfate



incorporation compared to untreated control disks (Figure 4.12). Injury alone also caused a significant decrease in proteoglycan biosynthesis compared to untreated controls. However, proteoglycan biosynthesis in injured disks was not significantly affected by the presence of the TGF- $\beta$  blocker.

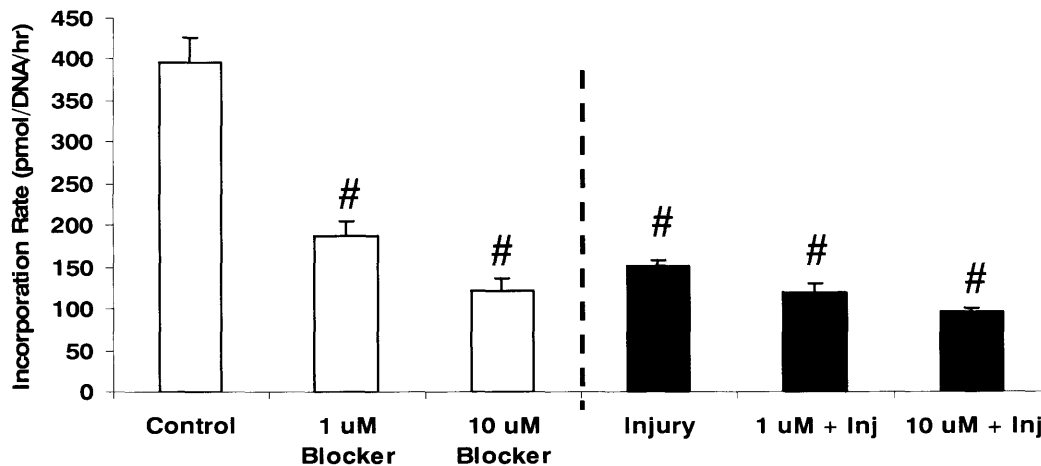


Figure 4.12 Effect of blocker on sulfate incorporation rate

#### 4.4 Discussion

Our results support the hypothesis that the TGF- $\beta$  type I receptor (ALK5), in the pathway following SMAD 2/3 phosphorylation, is involved in lubricin secretion and gene expression in injured cartilage containing the intact superficial zone. The importance of ALK5 in TGF- $\beta$  signaling is further explored in the murin embryonic fibroblast where the cells without ALK5 are unaffected by TGF- $\beta$  signaling [17]. As expected, blocking ALK5 with a higher concentration of SB431542 was apparently more effective in reducing both lubricin gene expression and protein secretion [15]. In addition, this study showed that TGF- $\beta$  gene and protein expression increased in cartilage containing intact superficial zone with increasing injurious compressive strain. Since one of TGF- $\beta$ 's functions is wound healing, it seems probable TGF- $\beta$  is having an anabolic response to injury in a strain dependent manner [6].

Since aggrecan is a target of TGF- $\beta$  signaling, the reduction in sulfate incorporation rate after blocking the signal is expected. However, the decrease in sulfate incorporation following injury, also noted in middle zone bovine calf cartilage following injury [19], was unaffected by the TGF- $\beta$  blocker. Our results, together with the findings that TGF- $\beta$  and injury both upregulate lubricin [2, 20], demonstrate that the TGF- $\beta$  pathway may be an important mechanism in

modulating the effects of injury on lubricin. Additional genes are listed in Appendix C. The main point is to illustrate that the blocker did not significantly change the expressions of many of the other genes.

## 4.5 Bibliography

1. Lee, J.H., et al., *Mechanical injury of cartilage explants causes specific time-dependent changes in chondrocyte gene expression*. Arthritis Rheum, 2005. **52**(8): p. 2386-95.
2. Jones, A.R. and C.R. Flannery, *Bioregulation of lubricin expression by growth factors and cytokines*. Eur Cell Mater, 2007. **13**: p. 40-5; discussion 45.
3. Neu, C.P., et al., *Mechanotransduction of bovine articular cartilage superficial zone protein by transforming growth factor beta signaling*. Arthritis Rheum, 2007. **56**(11): p. 3706-14.
4. Klein, T.J., et al., *Depth-dependent biomechanical and biochemical properties of fetal, newborn, and tissue-engineered articular cartilage*. J Biomech, 2007. **40**(1): p. 182-90.
5. Massague, J. and Y.G. Chen, *Controlling TGF-beta signaling*. Genes Dev, 2000. **14**(6): p. 627-44.
6. Verrecchia, F. and A. Mauviel, *Transforming growth factor-beta signaling through the Smad pathway: role in extracellular matrix gene expression and regulation*. J Invest Dermatol, 2002. **118**(2): p. 211-5.
7. Nakamura, T., et al., *Production of extracellular matrix by glomerular epithelial cells is regulated by transforming growth factor-beta 1*. Kidney Int, 1992. **41**(5): p. 1213-21.
8. Ziyadeh, F.N., et al., *Stimulation of collagen gene expression and protein synthesis in murine mesangial cells by high glucose is mediated by autocrine activation of transforming growth factor-beta*. J Clin Invest, 1994. **93**(2): p. 536-42.
9. **Volume**,
10. Massague, J., *How cells read TGF-beta signals*. Nat Rev Mol Cell Biol, 2000. **1**(3): p. 169-78.
11. Zhang, Y.E., *Non-Smad pathways in TGF-beta signaling*. Cell Res, 2009. **19**(1): p. 128-39.
12. Guo, X. and X.F. Wang, *Signaling cross-talk between TGF-beta/BMP and other pathways*. Cell Res, 2009. **19**(1): p. 71-88.
13. Inman, G.J., et al., *SB-431542 is a potent and specific inhibitor of transforming growth factor-beta superfamily type I activin receptor-like kinase (ALK) receptors ALK4, ALK5, and ALK7*. Mol Pharmacol, 2002. **62**(1): p. 65-74.
14. .
15. Niikura, T. and A.H. Reddi, *Differential regulation of lubricin/superficial zone protein by transforming growth factor beta/bone morphogenetic protein superfamily members in articular chondrocytes and synoviocytes*. Arthritis Rheum, 2007. **56**(7): p. 2312-21.
16. Frazier, K., et al., *Inhibition of ALK5 signaling induces physeal dysplasia in rats*. Toxicol Pathol, 2007. **35**(2): p. 284-95.
17. Karlsson, G., et al., *Gene expression profiling demonstrates that TGF-beta1 signals exclusively through receptor complexes involving Alk5 and identifies targets of TGF-beta signaling*. Physiol Genomics, 2005. **21**(3): p. 396-403.
18. Schmidt, T.A., et al., *Synthesis of proteoglycan 4 by chondrocyte subpopulations in cartilage explants, monolayer cultures, and resurfaced cartilage cultures*. Arthritis Rheum, 2004. **50**(9): p. 2849-57.
19. Kurz, B., et al., *Biosynthetic response and mechanical properties of articular cartilage after injurious compression*. J Orthop Res, 2001. **19**(6): p. 1140-6.
20. Jones, A.R., et al., *Modulation of lubricin biosynthesis and tissue surface properties following cartilage mechanical injury*. Arthritis Rheum, 2009. **60**(1): p. 133-42.



## 5 Microscope Stage Actuator Design for Observing Intracellular Transient Behavior of Chondrocytes under Injury

### 5.1 Introduction

Novel live cell dyes and advanced fluorescent confocal microscopy systems have enabled extensive probing of chondrocyte morphology and understanding of its intracellular dynamics. The chondrocyte cytoskeleton is an integration of actin microfilaments, microtubules, and intermediate filaments. Since mature articular chondrocytes no longer proliferate, these proteins play a major role in cell-matrix interaction, cell signaling, and transport functions. These functions are regulated in part by the increased tubule concentration in the chondrocytes from the weightbearing areas of cartilage [1]. Cytoskeletal density varies with depth from the superficial to the deep zone. Denser cytoskeleton may be localized in area of greater deformation they offer greater resistance to shear stress compared to intermediate fibrils and microtubules [2].

The mechanical behavior of cartilage has been well represented using the viscoelastic and the poroelastic models. The linear solid 3-element viscoelastic model works well in predicting time dependent mechanics of any single-phase interactions within the matrix. However, Maurice Biot's linear poroelastic equations also accounts for the mechanical loss coupled between the solid and fluid phase during cartilage deformation. In addition, the poroelastic model takes into consideration both temporal and spatial dynamics during deformation.

Chondrocyte mechanics have been examined extensively using micropipette aspiration, AFM nanoindentation, and other cytoindentation techniques [3]. In one approach, chondrocyte stress-relaxation time constant ( $\tau_e$ ) and equilibrium modulus were derived by fitting experimental data to the standard linear solid viscoelastic model consisting of a dashpot and spring in parallel with a spring [3-5]. The  $\tau_e$  attained from indenting single chondrocyte using AFM and the one estimated from indenting the agarose gel seeded with chondrocytes were both approximately 4 seconds. However, the  $\tau_e$  derived from the data fitting did not include the instantaneous stress relaxation transient, which may be the time frame where many important cellular events take place [4, 6].

Since the cytoskeletal organization regulate chondrocyte stiffness, one can imagine that other immediate intracellular aftermath post loading also attribute significantly to cell mechanics

and mechanotransduction [7]. Thus far, the confocal imaging studies performed on cells included quantifying the Poisson ratio, the volume, and surface area are affected by deforming a cell seeded gel construct or in explants. Those that have probed into the intracellular domain generally involved observing the organelle morphological changes after the cell has reached a relaxed state [8-15]. In addition, other intracellular images involves qualitatively assessing features in fixed samples [16, 17]. In both cases, the mechanism that ultimately alters cellular biosynthesis was not captured.

Since the interaction of cytosol and organelles dictates the functionality of the cell, the spatial component of poroelastic model may provide insight into what governs the cell's initial response to high peak stress and high strain rate during injury. Thus, this study will focus on real time live imaging during deformation so that it will acquire the instantaneous poroelastic stress-relaxation time while drawing from the model developed by Charras.

In the poroelastic model developed by Charras, the cell is treated as a fluid and solid mosaic medium with negligible inertial effects. This poroelastic model in one dimension consists of modified versions of the stress-strain relationship, Darcy's law, and the continuity equation shown respectively in Eqs 1, 2, and 3. The  $H$  is the drained bulk modulus;  $u$  equals the solid displacement;  $\phi$  represents the bulk porosity;  $p$  is the fluid pressure;  $\phi$  is the local porosity;  $v$  is the fluid velocity; and  $k$  is the hydraulic permeability. Also, Eq. 3 satisfies the continuity

law in one dimension,  $\frac{\partial}{\partial x} \left( \frac{\partial u}{\partial t} + U \right) = 0$ , if  $U_o = 0$  in  $\frac{\partial u}{\partial t} + U + U_o = 0$  because  $U = \phi \left( v - \frac{\partial u}{\partial t} \right)$ .

$$\sigma = H \frac{\partial u}{\partial x} - \phi p \quad (1)$$

$$\phi \left( v - \frac{\partial u}{\partial t} \right) = -k \frac{\partial p}{\partial x} \quad (2)$$

$$-\frac{\partial u}{\partial t} = \phi \left( v - \frac{\partial u}{\partial t} \right) \quad (3)$$

Once the three equations are incorporated into  $\frac{\partial \sigma}{\partial x} + f = 0$ , where  $f$  is the external body force on the cell, the diffusion equation of the solid matrix can be depicted as shown in Eq. 4.

$$\frac{Hk}{\phi} \frac{\partial^2 u}{\partial x^2} + \frac{k}{\phi} f = \frac{\partial u}{\partial t} \quad (4)$$

Treating the chondrocyte as a poroelastic media, the relaxation time constant is given in Eq. 5 where L is the characteristic length (diameter) of the cell.

$$\tau = \frac{L^2}{Kk} \quad (5)$$

L and H have empirically been determined to be ~10  $\mu\text{m}$  and ~1 kPa respectively for chondrocyte, but the value of k varies by orders of magnitude depending on the model used and the cellular parameters selected (see Appendix C). As a result, the theoretical expected values for the poroelastic time constant also differ by three orders of magnitude.

## 5.2 Actuator Design 1.0

The goal of the study is to empirically determine the poroelastic relaxation time constant of the cell when the cartilage is under mechanical loading. Thus, the experimental concept involves acquiring live cell confocal images in real time as the actuator deforms the cartilage tissue. As illustrated in (Figure 5.1), the solenoid, controlled by the circuit box, will actuate the stainless steel applicator to deform the cartilage in the x direction against the porous metal. Simultaneously, the confocal system will record the intracellular deformation and relaxation at the boundary between the cartilage and porous material.

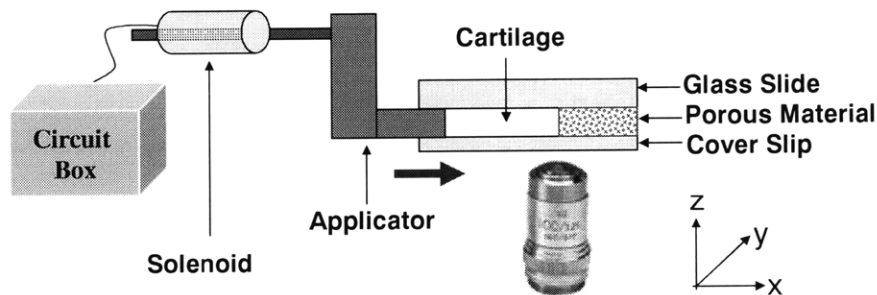


**Figure 5.1.** Experimental concept of the real-time observation of cellular deformation as the cartilage is compressed by the applicator (shown by the blue arrow).

### 5.2.1 Mechanical Stage Design

In order to conduct the experiment on the microscope (Zeiss Axiovert 200), the first step is to design a custom mechanical stage that will hold the sample and the solenoid. The 1/2”

diameter x 1" long push tubular solenoid was obtained from Saia-Burgess, while the porous stainless steel with a porosity of 20  $\mu\text{m}$  is provided by Porous Technologies Inc. and trimmed to 12.8 x 25 x 1 mm by the MIT Central Machine Shop. Meanwhile, the stainless steel pieces, indicated in Fig. 5, are designed and outsourced using the emachineshop schematic software.

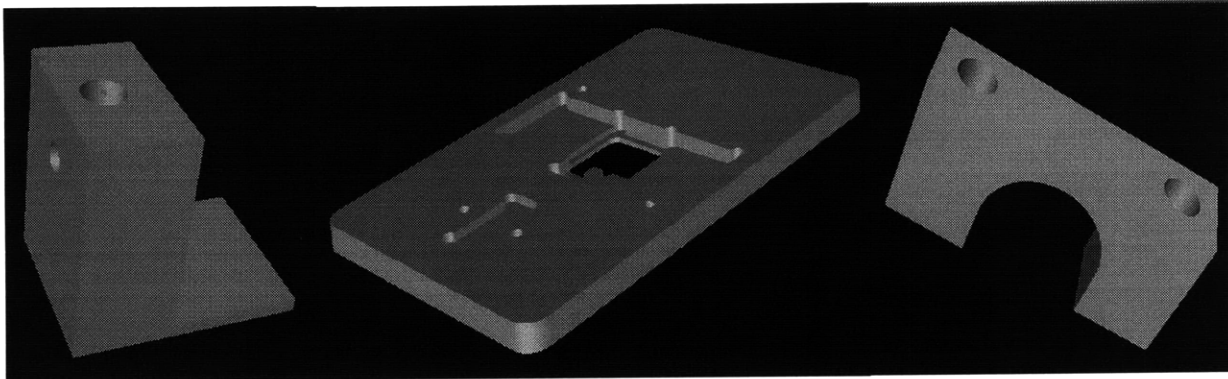


**Figure 5.2.** 3-D models of the applicator, the stage, and the bridge that secures the solenoid (left to right).

Together, the whole assembly looks like the following:

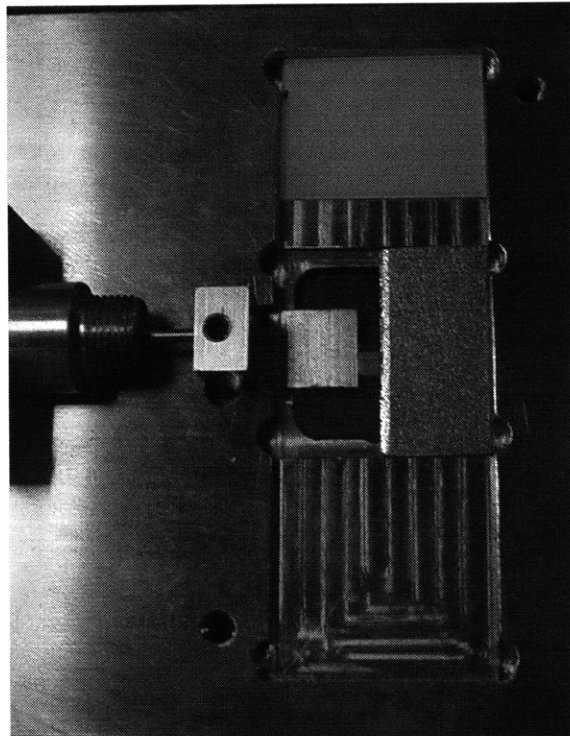


**Figure 5.3.** Setup of mechanical system which reflects the concept illustrated in the. **Figure 5.1**

### 5.2.2 Electrical Circuit Design

In order to amplify and control the voltage output to the solenoid, a circuit was built with an embedded monostable to deliver 30V to the solenoid for two seconds before lowering to 10V, as shown in (Figure 5.4). The two seconds were chosen to prevent overheating in the solenoid when applying a maximum force of 3N to the cartilage. A schematic of the circuit is presented in Appendix D.

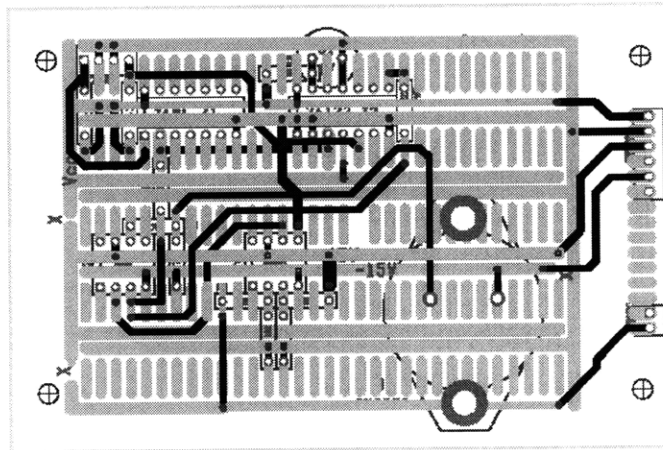


**Figure 5.4.** The electronics embedded in the circuit box.

### 5.3 Actuator Design 2.0: Upgrade

Currently, the solenoid delivers a small instantaneous force of 3 N to the tissue that induces minute deformation. Additionally, if the fluid does not escape in time, the limited deformation to the tissue translates to undetectable deformation to the cell. Therefore, the upgrade will replace the solenoid with a DuraPlus linear actuator with a micro-stepper driver to modulate the strain rate and increase the tissue deformation. Also, the geometry of applicator and the platen will be porous in half cylindrical shapes. Similarly, the tissue sample will also be a half cylinder with a high aspect ratio between the length and the width. Furthermore, its two faces will be confined between the porous materials while its plane of symmetry is laying on the glass cover slide and the lateral edge is left unconfined. In addition, past research has shown that there is minimal fluid flow for both confined and unconfined compression if the diameter to thickness ratio is large. In turn, the matrix moduli measured for both cases are similar. The poroelastic aggregate modulus ( $H_A$ ) and hydraulic permeability ( $k$ ) were determined to be 0.56



MPa and  $1.6 \times 10^{-15} \text{ m}^4 \text{ N}^{-1} \text{ s}$  for confined compression and 0.5~0.7 MPa and  $0.63 \times 10^{-15} \text{ m}^4 \text{ N}^{-1} \text{ s}$  for unconfined compression [19, 20]. As a result, this experimental configuration will enable most of the fluid to be exuded into the porous materials and allow more uniaxial solid matrix deformation.

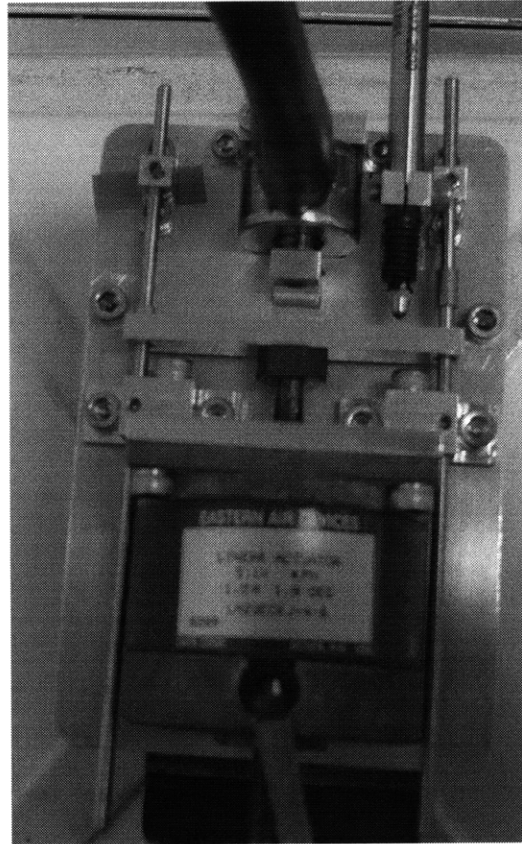


**Figure 5.5.** Mechanical actuator device designed using Solidworks (top view)

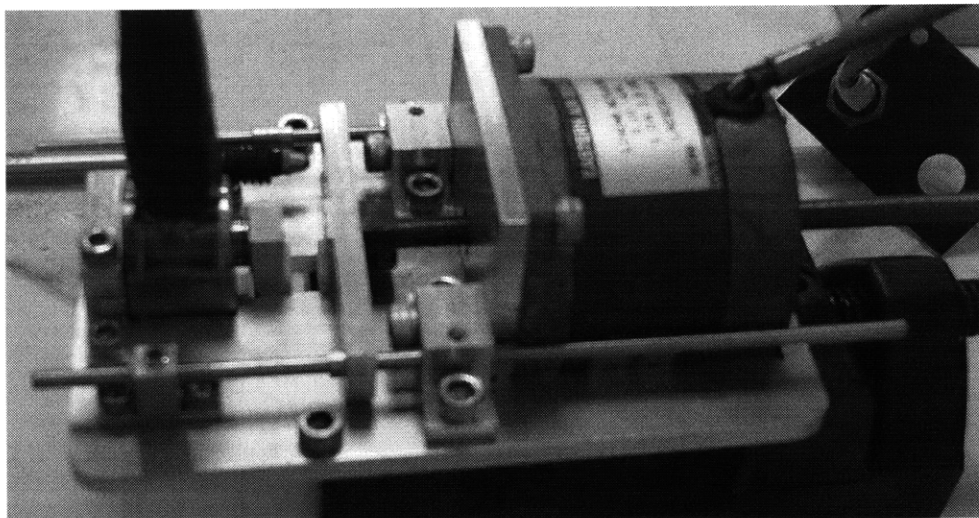


**Figure 5.6** Side view of mechanical actuator (side view)

## **5.4 Experimental Setup**

### **5.4.1 Harvest**

First, 6-mm cores are extracted from both sides of the femoral groove. Then, the first 1-mm slice is taken from each core to obtain a 3 x 3 x 1 mm cube. Meanwhile, each sample is incubated in 0.5 ml of 1% ITS supplemented culture medium for 1-2 days of equilibration before staining for imaging.

Once the mechanical setup is upgraded, the samples will be 8-mm diameter x 1-mm thick cartilage discs cut in half.

### **5.4.2 Dye Application**

Since the repertoire of dyes for living tissue/cell is limited, the two dyes were chosen such that they only act as a marker in the cell without interfering with the intracellular functions. The MitoTracker Red CMXRos ( $C_{32}H_{32}Cl_2N_2O$ ) from Molecular Probes is a fixable dye that tracks the active mitochondria at absorption and emission wavelengths of 579 and 599 nm. The advantage of this probe is that it contains a mildly thiol-reactive chloromethyl moiety that retains the dye in the mitochondria even after fixation (Molecular Probes). More importantly, because this dye anchors to a specific organelle, the discrete concentration can be better visualized.

The CellTracker Green CMFDA (5-chloromethylfluorescent diacetate), which absorbs and emits at 492 and 517 respectively, belongs to a series of fluorescent probes that are passed down to daughter cells. Essentially, once the colorless, nonfluorescent, uncharged dye permeates through the membrane, the cytosolic esterases cleave the acetates, thereby releasing the fluorescent probe and resulting in a charged form that is cell impermeable (Molecular Probes).

The general protocol consists of immersing each 3x3x1 mm sample in 0.5-ml of dye diluted in high glucose DMEM solution for 1 hour in 37 °C and wash for 1 hour in DMEM only. The MitoTracker concentration is about 2  $\mu$ M while the CMFDA concentration is 5 $\mu$ M.

### **5.4.3 Image Acquisition**

Imaging acquisition will be done using the Nipkow Dual-Spinning Disk Confocal System (Zeiss Axiovert 200M, PerkinElmer Ultraview) from the Whitehead-MIT Bioimaging Center, as

illustrated in Figure 5.7. In order to achieve the temporal resolution on the order of 0.1 s, the spatial resolution will be slightly compromised by setting a 2x2 binning and an exposure time of 45ms. The objective used will be Zeiss 100x/1.45 oil immersion objective.

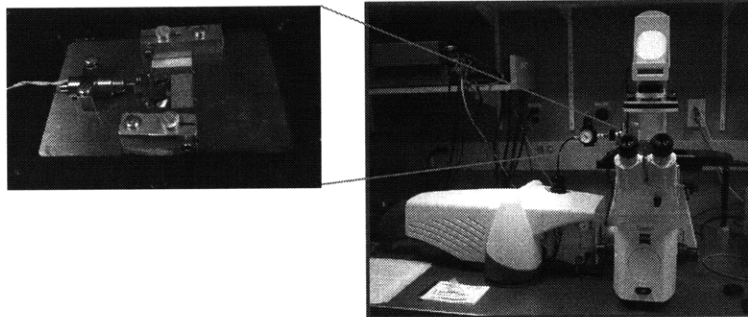


**Figure 5.7.** Diagram of the custom stage and the confocal microscope system

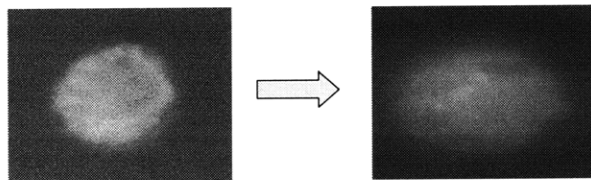


**Figure 5.8.** Pictorial concept of intracellular structures progressing from the deformed state (left) to the relaxed state (right) as indicated by the distribution of the MitoTracker dye

After setup, the 1344 x 1024 pixels CCD camera (Hamamatsu Orca-ER) will capture the 10-second 2D time lapse at ~16 f/s including the two seconds of induced tissue/cell deformation as well as the cellular relaxation thereafter.

## 5.5 Bibliography

1. Eggli, P.S., E.B. Hunziker, and R.K. Schenk, *Quantitation of structural features characterizing weight- and less-weight-bearing regions in articular cartilage: a stereological analysis of medial femoral condyles in young adult rabbits*. *Anat Rec*, 1988. **222**(3): p. 217-27.
2. Langelier, E., et al., *The chondrocyte cytoskeleton in mature articular cartilage: structure and distribution of actin, tubulin, and vimentin filaments*. *J Histochem Cytochem*, 2000. **48**(10): p. 1307-20.
3. Trickey, W.R., G.M. Lee, and F. Guilak, *Viscoelastic properties of chondrocytes from normal and osteoarthritic human cartilage*. *J Orthop Res*, 2000. **18**(6): p. 891-8.
4. Darling, E.M., S. Zauscher, and F. Guilak, *Viscoelastic properties of zonal articular chondrocytes measured by atomic force microscopy*. *Osteoarthritis Cartilage*, 2006. **14**(6): p. 571-9.
5. Ng, L., et al., *Nanomechanical properties of individual chondrocytes and their developing growth factor-stimulated pericellular matrix*. *J Biomech*, 2006.
6. Shieh, A.C., E.J. Koay, and K.A. Athanasiou, *Strain-dependent recovery behavior of single chondrocytes*. *Biomech Model Mechanobiol*, 2006. **5**(2-3): p. 172-9.
7. Trickey, W.R., T.P. Vail, and F. Guilak, *The role of the cytoskeleton in the viscoelastic properties of human articular chondrocytes*. *J Orthop Res*, 2004. **22**(1): p. 131-9.
8. Guilak, F., A. Ratcliffe, and V.C. Mow, *Chondrocyte deformation and local tissue strain in articular cartilage: a confocal microscopy study*. *J Orthop Res*, 1995. **13**(3): p. 410-21.
9. Sawae, Y., et al., *Confocal analysis of local and cellular strains in chondrocyte-agarose constructs subjected to mechanical shear*. *Ann Biomed Eng*, 2004. **32**(6): p. 860-70.
10. Knight, M.M., et al., *Cell and nucleus deformation in compressed chondrocyte-alginate constructs: temporal changes and calculation of cell modulus*. *Biochim Biophys Acta*, 2002. **1570**(1): p. 1-8.
11. Lee, D.A., et al., *Chondrocyte deformation within compressed agarose constructs at the cellular and sub-cellular levels*. *J Biomech*, 2000. **33**(1): p. 81-95.
12. Knight, M.M., et al., *Chondrocyte deformation induces mitochondrial distortion and heterogeneous intracellular strain fields*. *Biomech Model Mechanobiol*, 2006. **5**(2-3): p. 180-91.
13. Freeman, P.M., et al., *Chondrocyte cells respond mechanically to compressive loads*. *J Orthop Res*, 1994. **12**(3): p. 311-20.
14. Errington, R.J., et al., *Four-dimensional imaging of living chondrocytes in cartilage using confocal microscopy: a pragmatic approach*. *Am J Physiol*, 1997. **272**(3 Pt 1): p. C1040-51.
15. Szafranski, J.D., et al., *Chondrocyte mechanotransduction: effects of compression on deformation of intracellular organelles and relevance to cellular biosynthesis*. *Osteoarthritis Cartilage*, 2004. **12**(12): p. 937-46.
16. Idowu, B.D., et al., *Confocal analysis of cytoskeletal organisation within isolated chondrocyte sub-populations cultured in agarose*. *Histochem J*, 2000. **32**(3): p. 165-74.

17. Knight, M.M., et al., *Mechanical compression and hydrostatic pressure induce reversible changes in actin cytoskeletal organisation in chondrocytes in agarose*. J Biomech, 2006. **39**(8): p. 1547-51.
18. Charras, G.T., et al., *Non-equilibration of hydrostatic pressure in blebbing cells*. Nature, 2005. **435**(7040): p. 365-9.
19. Buschmann, M.D., et al., *Confined compression of articular cartilage: linearity in ramp and sinusoidal tests and the importance of interdigitation and incomplete confinement*. J Biomech, 1998. **31**(2): p. 171-8.
20. Fortin, M., et al., *Unconfined compression of articular cartilage: nonlinear behavior and comparison with a fibril-reinforced biphasic model*. J Biomech Eng, 2000. **122**(2): p. 189-95.

## 6 Conclusion

Mechanical injury induces very different responses from cartilage near the articular surface versus cartilage in the middle zone. It has been shown that injury alone at high strain and strain rates can cause apoptosis, GAG loss, and other biochemical damage. However, this study has shown for the first time that additional dynamic shear motion superimposed on a static normal strain lead to grave surface fibrillation and roughening on an injured cartilage with intact superficial layer. Meanwhile, it has no effect on injured middle zone cartilage.

Lubricin expression on the cartilage surface is regulated by mechanical injury in a depth dependent and temporal manner. Mechanical injury increases lubricin gene expression and loss to media 2 days after injury. However, the lubricin gene expression near superficial zone cartilage returns to control after 6 days. It is possible that the remaining healthy cells respond anabolically to synthesize more lubricin, but over time, the catabolic effects become more dominant. Nevertheless, if the synovial fluid has sufficiently high concentration of lubricin, it can help replenish and provide smooth articulation of the joints regardless whether the cartilage surface has been previously injured.

Mechanical injury can increase TGF- $\beta$  gene expression in middle zone cartilage within 24 hours post injury. This study has confirmed that trend in superficial layer cartilage as well. Furthermore, results from this study indicate that TGF- $\beta$  gene and protein expression near the superficial cartilage increases in a strain dose dependent manner. Previous reports show that exogenous TGF- $\beta$  increases lubricin gene and protein expression. Furthermore, other investigators demonstrated that blocking the canonical TGF- $\beta$  signaling pathway diminishes the increased lubricin protein expression induced by dynamic shear motion. In addition, this study showed that by blocking the TGF- $\beta$  signaling pathway using a TGF- $\beta$  type I receptor, it also reduces the increased lubricin gene and protein expression caused by mechanical injury. This study further supports the fact that TGF- $\beta$  signaling pathway influences the modulation of lubricin caused by injury.

## **A. *Arthritis and Rheumatism* Journal Publication**

### **Modulation of Lubricin Biosynthesis and Tissue Surface Properties Following Cartilage Mechanical Injury**

Aled R.C. Jones<sup>1</sup>, Shuodan Chen<sup>2</sup>, Diana H. Chai<sup>2</sup>, Anna L. Stevens<sup>2</sup>, Jason P. Gleghorn<sup>3</sup>,  
Lawrence J. Bonassar<sup>3</sup>, Alan J. Grodzinsky<sup>2</sup> and Carl R. Flannery<sup>1</sup>

**Published January, 2009**

<sup>1</sup>Aled R.C. Jones, PhD, Carl R. Flannery, PhD: Wyeth Research, Cambridge, MA

<sup>2</sup>Shuodan Chen, MS, Diana Chai, BS, Anna L. Stevens, PhD, Alan J. Grodzinsky, ScD:  
Massachusetts Institute of Technology, Cambridge, MA

<sup>3</sup>Jason P. Gleghorn, BS, Lawrence J. Bonassar, PhD: Department of Biomedical Engineering,  
Cornell University, Ithaca, NY

Address correspondence to:

Carl R. Flannery, PhD, Wyeth Research, 200 CambridgePark Drive, Cambridge, MA 02140,  
USA. Email: [cflannery@wyeth.com](mailto:cflannery@wyeth.com); Tel: 617-665-5341; Fax: 617-665-5386





## ABSTRACT

**Objective.** To evaluate the effects of injurious compression on the biosynthesis of lubricin at different depths within articular cartilage, and to examine alterations in structure and function of the articular surface following mechanical injury.

**Methods.** Bovine cartilage explants were subdivided into level 1, with intact articular surface, and level 2, containing middle and deep zone cartilage. Following mechanical injury, lubricin messenger RNA (mRNA) levels were monitored by quantitative RT-PCR, and soluble or cartilage-associated lubricin protein was analyzed by Western blotting and immunohistochemistry. Cartilage morphology was assessed by histological staining, and tissue functionality was assessed by friction testing.

**Results.** At two days post-injury, lubricin mRNA expression was upregulated approximately 3-fold for level 1 explants, and was downregulated for level 2 explants. Lubricin expression in level 1 cartilage returned to control levels after 6 days in culture. Similarly, lubricin protein synthesis and secretion increased in response to injury for level 1 explants and decreased for level 2 cartilage. Histological staining revealed changes in the articular surface of level 1 explants following injury, with respect to glycosaminoglycan and collagen content. Injured level 1 explants displayed an increased coefficient of friction relative to controls.

**Conclusions.** Increased lubricin biosynthesis appears to be an early transient response of surface-layer cartilage to injurious compression. However, distinct morphological changes occur with injury that appear to compromise the frictional properties of the tissue.

## INTRODUCTION

Osteoarthritis (OA) is characterized by the degeneration of articular cartilage, leading to matrix fibrillation, fissuring and the development of lesions. In the final stages of the disease, erosion of cartilage leads to painful bone-on-bone contact. The etiology of OA is complex and involves multiple biochemical, biomechanical and genetic factors in addition to ageing (1-3). Cartilage injury in young individuals is a prominent predisposing factor leading to increased risk

for the subsequent development of OA (4, 5), and as such represents a discrete pathological event. Damage to the meniscus or ligaments sustained during a traumatic joint injury causes instability, subjecting articular cartilage to abnormal biomechanical forces and resulting in the release of inflammatory mediators (6). Several animal models of OA are thus based on the observation that joint instability, i.e. via anterior cruciate ligament transaction or perturbation of the meniscus (7), results in the rapid onset of articular cartilage degeneration with an OA-like phenotype. The initial events following joint injury are thought to be crucial, as surgical interventions to restore joint stability do not seem to reduce the risk of developing post-traumatic OA (8).

The link between traumatic joint injury and OA may therefore provide unique insights into the pathophysiology of the disease, and has been explored using *in vitro* application of injurious compression (9). These models allow investigators to circumvent the loading variability inherent *in vivo* by applying defined mechanical forces to articular cartilage and observing the subsequent effects. Such models have utilized, for example, a single compression of human or bovine cartilage up to 65% strain (10-17) or cyclic loading of various amplitudes (18, 19). Injurious compression of cartilage *in vitro* has been shown to effect a number of biochemical and biophysical changes, including GAG loss (10, 13, 15, 19), collagen denaturation (16, 18, 19), increased water content (13, 16, 20, 21) and decreased stiffness (13, 21). Cell death by apoptosis and necrosis also occurs in response to mechanical compression (11, 16, 18, 21, 22). In addition, mechanically injured cartilage displays increased expression of extracellular matrix- (ECM) degrading enzymes such as matrix metalloproteinase-3 (MMP-3) and ADAMTS-5 (aggrecanase-2) (23).

Healthy articular cartilage maintains a smooth, well-lubricated surface that endows the tissue with an extremely low coefficient of friction (24). These properties are due, at least in part, to the presence of lubricin, a multidomain glycoprotein that is a product of the proteoglycan 4 (PRG4) gene (HGNC:9364). Lubricin is homologous to molecules also referred to as superficial zone protein (SZP), megakaryocyte stimulating factor (MSF) precursor, camptodactylarthopathy-coxa vara-pericarditis (CACP) protein, ‘downstream of the liposarcoma-associated fusion oncoprotein’ 54 (DOL54) and PRG4 (25-30), and is a component of synovial fluid that is expressed and secreted by superficial zone chondrocytes and synoviocytes. Lubricin has been localized to the surface of multiple synovial tissues including

cartilage, meniscus, ligament and tendon (30-34), whereupon it acts as a boundary lubricant and as a deterrent against abnormal protein deposition and/or cellular adhesion (35, 36). In addition, lubricin contributes to the load-dissipating elasticity of synovial fluid (37). Lubricin monomers are comprised of a central mucin-like domain substituted with O-linked  $\beta$ -(1-3)-Gal-GalNAc oligosaccharides partially capped with NeuAc, which are believed to facilitate boundary lubrication (38), with flanking terminal globular domains which may play a role in aggregation and matrix binding (25, 39). The importance of lubricin in synovial joint metabolism is emphasized through the phenotyping of CACP syndrome in humans, in which genetic mutations elicit a lack of lubricin expression. Patients with CACP syndrome exhibit non-inflammatory synovial hyperplasia, fibrosis and premature joint failure (29), and these features are also apparent in lubricin knockout mice (36). Downregulation of lubricin expression is also reported in some animal models of arthritis (40, 41).

Several studies have investigated the effects of biochemical regulators (cytokines and growth factors) on lubricin expression (25, 42-44), and recent research has also examined some of the effects of biomechanical stimuli (45-49). To date, the effect of a single injurious compression of lubricin expression and secretion by articular cartilage has not been studied. Therefore, a primary objective of the current study was to determine the effects of cartilage mechanical injury on lubricin expression and secretion at different depths within articular cartilage explants utilizing a well-established *in vitro* model. A secondary objective of the study was to characterize the general functional and morphological alterations of an intact articular surface in response to injurious compression. We observed changes in lubricin biosynthesis and alterations in surface morphology and functionality after injury, both of which may be indicative of a specific response of the superficial zone of articular cartilage to injurious compression. These results provide information concerning the immediate response of the articular surface to cartilage injury *in vitro*, and provide a basis for future studies into the effect of cartilage injury *in vivo*, with a view towards developing potential therapies.

## **MATERIALS AND METHODS**

**Isolation of calf articular cartilage explants.** Bovine articular cartilage disks were harvested from the femoropatellar groove of 1-2 week old calves similar to previously established methods (23). Briefly, cartilage cylinders (3 mm diameter) were cored using a dermal punch, followed by removal of subchondral bone with a blade. Cylinders were then sequentially

sliced into two transverse sections with a depth of ~0.5 – 0.7 mm using a brain matrix (TM-1000, ASI Instruments, Warren, MI). The uppermost section, containing the intact articular surface, was termed ‘level 1’, and the next section containing the distal zone of cartilage below level 1 was termed ‘level 2’ (Figure 1). Following tissue harvest, disks were precultured for 48 hours at 37°C in an atmosphere of 5% CO<sub>2</sub> in culture media comprised of low glucose DMEM, 0.1 mM non-essential amino acid (NEAA), 10 mM HEPES buffered solution, 100 U/ml penicillin, 100 µg/ml streptomycin, 0.4 mM proline, supplemented with 1% ITS (10 µg/ml insulin, 5.5 µg/ml transferrin, and 5 ng/ml sodium selenite).

**Injurious compression.** Following equilibration of the cartilage explants during a 48 hour pre-culture period, injurious compression was performed utilizing a custom-designed incubator-housed loading apparatus (50) shown in Figure 1. Cartilage explants were placed individually in a well at the center of a polysulfone chamber, which allows for radially unconfined compression. The thickness of cartilage explants at zero-strain was measured to correct for tissue swelling in the 48 hour equilibration period. The mechanical injury protocol consisted of a single ramp compression to 50% of the original cartilage thickness at a velocity of 100%/second, followed by immediate removal of compression at the same rate. Thus, explants were compressed to half their original height over the period of 0.5 seconds, after which time compression was removed over the following 0.5 seconds. Measurements of peak stress values during the loading protocol showed higher values for level 2 explants (22.151 MPa, n = 19 explants from 1 animal) than for level 1 (15.066 MPa, n = 20 explants from 1 animal) indicating that compressive modulus increases with cartilage depth, in concordance with other studies (51). ‘Free-swelling’ control explants were placed into the chamber but were not compressed. Injured explants and free-swelling controls were placed in fresh serum-free medium, and cultures were terminated after 2, 4 and 6 days.

**RNA extraction and quantitative RT-PCR.** After culture, conditioned media was collected and cartilage explants were flash-frozen in liquid nitrogen prior to storage at -80°C. Explants (2-3 per purification) were freeze-milled and resuspended in Tri-reagent (Sigma, St. Louis, MO). After separation of protein and nucleic acid by the addition of chloroform, RNA was purified using RNeasy spin kits, including an on-column DNase I digestion step (Qiagen, Valencia, CA). Absorbance values were taken at 260 nm and 280 nm to establish RNA concentration and purity. Quantitative real-time RT-PCR for bovine lubricin was performed as

described previously (42). Briefly, assays were performed using one-step quantitative RT-PCR reagents (Applied Biosystems, Foster City, CA) and primer/probe sets (5'-FAM/3'-TAMRA, Integrated DNA Technologies, Coralville, IA) specific to the exon 9/10 boundary of bovine lubricin (45) and for the housekeeping gene GAPDH. Lubricin mRNA levels were normalized to GAPDH and expressed relative to control (uninjured) levels ( $\Delta\Delta C_T$  method, Applied Biosystems).

**Biochemical analyses and Western blotting.** Western blotting for lubricin was performed essentially as described (39). Conditioned media from level 1 explants was mixed with 4X SDS-PAGE sample buffer and 10% (v/v)  $\beta$ -mercaptoethanol prior to separation on 4-12% Tris-glycine SDS-PAGE gels (Invitrogen, Carlsbad, CA). Conditioned media from level 2 explants was concentrated 10-fold on 100 kDa cutoff spin columns (Millipore, Billerica, MA) prior to analysis. Explants (n = 8) were also extracted in 1.5 M NaCl as described previously (39). Gels were transferred to Protran BA85 nitrocellulose membranes (Whatman, Florham Park, NJ), blocked with 5% (w/v) bovine serum albumin (BSA) in Tris-buffered saline (TBS, pH 7.4) and analyzed by Western blotting with monoclonal antibody 6-A-1 (25, 32), raised against native bovine lubricin (generously provided by Dr. C.E. Hughes and Prof. B. Caterson, Cardiff University). After an overnight incubation with antibody 6-A-1, membranes were washed and incubated with rabbit anti-mouse HRP conjugate (Pierce, Rockland, IL) diluted in 1% (w/v) BSA in TBS for 1 hour, followed by multiple washes in TBS. Reactive bands were detected with enhanced chemiluminescence (ECL) reagents (GE Healthcare, Piscataway, NJ) and BioMax Light autoradiography film (Kodak Molecular Imaging, New Haven, CT).

**Histological analyses.** After culture, cartilage explants were fixed with 4% (w/v) paraformaldehyde for 24 hours then transferred to 70% ethanol. Following dehydration, tissue was embedded in paraffin, and 8  $\mu$ m sections were cut and placed onto microscope slides (Superfrost Plus, VWR, West Chester, PA). After rehydration with xylene and graded ethanols, sections were stained using standard histological techniques for proteoglycan (Safranin O-fast green) and collagen (trichrome) or analyzed by immunohistochemical detection with rabbit anti-lubricin antibody G35 (immunizing peptide: CGEGYSRDAT) or non-specific rabbit IgG as described previously (39).

**Friction testing.** Cartilage explants (n = 6 per treatment group) were flash frozen in liquid nitrogen after the culture period and stored at -80°C prior to friction testing. Briefly, a custom

linear cartilage-on-glass friction testing apparatus was utilized to measure the friction coefficient ( $\mu$ ) in the boundary lubrication mode using PBS as a bathing solution. The friction testing apparatus consisted of a glass counterface/lubricant bath that linearly oscillates under the cartilage sample driven by a servo motor, and a custom biaxial load cell which applies a normal strain to the tissue and measures the normal and frictional shear loads on the sample (52). Level 1 explants were tested with the articular surface against the glass counterface, level 2 explants were tested with the upper surface (distal to the former site of subchondral bone attachment) against the glass counterface. Friction tests were performed on level 1 and level 2 injured samples and unloaded controls before and after extraction with 1.5 M NaCl, with cartilage slices equilibrated in PBS for 1 hour after extraction prior to friction testing. Subsequent tests were performed with level 1 explants after a 1 hour soak in equine synovial fluid (ESF) with PBS as the lubricant, followed by a final test with ESF as the lubricant. Samples were tested with an applied normal strain of 30%, and an entraining velocity of 0.33 mm/s resulting in boundary mode lubrication as confirmed by previous studies (53). The temporal friction coefficient ( $\mu(t)$ ) was recorded and data is presented as the equilibrium friction coefficient ( $\mu_{eq}$ ) calculated from a poroelastic relaxation model fit to the  $\mu(t)$  data. Statistical analyses of differences between groups were performed using Tukey's post hoc test.

## RESULTS

**Effects of injurious compression on levels of soluble and cartilage-associated lubricin.** Mechanical injury of cartilage explants resulted in opposing effects on lubricin biosynthesis in level 1 and level 2 explants. For level 1 cartilage, increased secretion of lubricin protein into the conditioned media was observed in response to injury (Fig. 2A). In contrast, injurious compression of level 2 cartilage resulted in a reduction in the amount of lubricin present in media samples. Extraction of bovine cartilage with 1.5 M NaCl has previously been shown to remove cartilage-associated lubricin (39) and a similar extraction procedure was used for explants from these studies. Similar amounts of lubricin were extracted from injured level 1 explants and free-swelling controls (Fig. 2B). No detectable lubricin was extracted from control or injured explants from level 2.

**Effects of injurious compression on lubricin mRNA expression.** For level 1 cartilage, elevated expression of lubricin mRNA was observed after 48 hours in culture post-injury (Fig. 3A). In contrast, injurious compression of level 2 cartilage caused a reduction in lubricin mRNA

levels, in agreement with the lowered amounts of lubricin present in conditioned media samples (Fig. 2A). In a separate experiment, the response of lubricin mRNA levels to injury in level 1 explants was investigated further by extending the post-injury culture period to 6 days (Fig. 3B). Lubricin mRNA levels again increased in response to injury on day 2, but by day 6 mRNA expression was not significantly different between injured cartilage and free-swelling controls, suggesting that lubricin mRNA upregulation is a temporary response to injurious compression in explants containing an intact articular surface.

#### **Histological and immunohistochemical analyses of injured versus control explants.**

The uppermost layer of injured level 1 cartilage exhibited marked cellular depletion, and displayed an amorphous/‘swollen’ surface architecture with diminished glycosaminoglycan (Fig. 4a, b) and collagen (Fig. 4c, d) content. For level 2 explants, injured tissue displayed some loss in glycosaminoglycan (Fig. 4e, f) and collagen (Fig. 4g, h) content, but the effect was not as prominent as for level 1 explants, demonstrating a specific response of superficial zone-containing explants to injury. Immunohistochemistry for lubricin (Fig. 5) confirmed enhanced cellular biosynthesis of lubricin in injured level 1 tissue.

**Effect of injurious compression on cartilage frictional properties.** To evaluate the functional effects of the changes in lubricin biosynthesis and cartilage morphology described above, cartilage explants from level 1 and level 2 were cultured for 48 hours after injury, and subjected to biomechanical testing to analyze the frictional characteristics of the tissue (Fig. 6). The observed friction coefficient of untreated articular cartilage (Level 1, control) was  $\sim 0.25$ , similar in range to the kinetic friction coefficient observed in other studies using bovine cartilage and PBS as a bathing solution (54). Injured explants from level 1 displayed a significantly higher level of friction ( $\mu_{eq}$ ) than free-swelling controls (Fig. 6A). Friction testing after extraction of control level 1 explants with 1.5 M NaCl to remove endogenous lubricin revealed an increase in friction. However, the extraction procedure did not increase the  $\mu_{eq}$  value of level 1 injured explants, indicating that the extensive morphological changes in the superficial zone, such as observed in figure 4, contribute significantly to the loss of lubrication. Control cartilage from level 2 exhibited a higher average  $\mu_{eq}$  value compared with control cartilage from level 1, and injury did not significantly change the frictional characteristics of level 2 cartilage. Notably, the baseline  $\mu_{eq}$  value of unextracted control level 2 cartilage was similar to 1.5 M NaCl-extracted control level 1 cartilage. Salt extraction had no effect on the  $\mu_{eq}$  values of control or injured

cartilage from level 2. Level 1 control and injured explants were tested after a 1 hour soak in equine synovial fluid (ESF) with PBS as the lubricant solution (Fig. 6B), which reduced the observed  $\mu_{\text{eq}}$  values for both groups, although the  $\mu_{\text{eq}}$  for injured cartilage was still significantly higher than for control cartilage. Finally, level 1 control and injured explants were tested with ESF in the lubricant bath. Observed  $\mu_{\text{eq}}$  values for both groups were substantially reduced (Fig. 6B), highlighting the role of synovial fluid constituents in the boundary lubrication of articular cartilage as described by other researchers (55, 56). However, even with synovial fluid as the lubricant, injured cartilage displayed a higher coefficient of friction than free-swelling controls.

## **DISCUSSION**

Previous investigations into the effects of a single injurious compression on bovine cartilage explants have demonstrated upregulated catabolic gene expression in addition to decreased chondrocyte viability, decreased ECM biosynthesis and changes in biomechanical properties (10, 13, 23). In many such studies, the surface (approximately 200  $\mu\text{m}$ ) layer of cartilage had been removed, whereas in the current experiments the superficial zone was retained on the level 1 explants. Elevated lubricin protein levels in conditioned media were observed for cultured level 1 explants in response to injury (Fig. 2), and a corresponding upregulation of lubricin mRNA synthesis occurred after 48 hours in culture post-injury (Fig. 3A). After 6 days in culture, levels of lubricin mRNA for injured level 1 specimens decreased and approached control levels (Fig. 3B). For level 2 cartilage, lubricin synthesis by control samples was substantially lower than for level 1 controls (data not shown), and was further diminished following injury (Fig. 2A).

The levels of extracted lubricin for both injured and control cartilage were similar after 2 and 6 days (Fig. 2 and data not shown), although enhanced lubricin expression below the articular surface of injured level 1 explants (Fig. 5) indicates that the lubricin extracted from such samples may not all be surface-localized. No lubricin was detected in extracts of level 2 cartilage, in agreement with other studies that document lubricin expression and localization specifically within the superficial zone of articular cartilage (30). The morphology of the articular surface was markedly altered in injured cartilage from level 1, and this was less apparent in injured explants from level 2 (Fig. 4). This may be indicative of a distinct biosynthetic response to injurious compression by chondrocytes present in the superficial zone of level 1, which does not occur in cells from the deeper zone(s) of articular cartilage.



Injured explants from level 1 displayed an increased coefficient of friction ( $\mu_{eq}$ ) upon biomechanical testing (Fig. 6), suggesting that the structural changes observed (Fig. 4) contribute significantly to a loss of this tissue function. Extraction of lubricin from control level 1 explants with 1.5M NaCl resulted in an increase in friction, whereas the friction coefficient of extracted, injured level 1 explants was not significantly altered. It may be noted, however, that while this extraction protocol results in the effective removal of lubricin (Figure 2), other components of the 1.5M NaCl extract (39) might also contribute to the tribological properties of the articular surface. Control explants from level 2 displayed a higher frictional coefficient than those from level 1, with values similar to those obtained for extracted level 1 cartilage. Furthermore, the frictional properties of level 2 explants were not significantly affected by injurious compression or extraction with 1.5 M NaCl. The coefficient of friction decreased for both control and injured level 1 cartilage tested after soaking in ESF and also with ESF in the lubricant bath. The results indicate that the surface lubricating properties of injured cartilage may be rescued by adequate levels of synovial fluid lubricants, including lubricin. It will be of interest to determine whether the structural and functional changes to the injured superficial zone are reversible events, such that the tissue can function in a manner similar to that of uninjured cartilage after longer periods in culture, and/or in response to particular biochemical/biomechanical stimuli, or upon treatment with applicable biolubricants. For example, dynamic shear and compressive forces are known to increase lubricin expression in a bovine explant culture system (47, 48), and surface motion has a positive effect on lubricin synthesis in tissue-engineered cartilage constructs (45) and in a novel whole-joint bioreactor simulating continuous passive motion (49). It will be informative to assess the influence of these biomechanical stimuli on both lubricin expression and general tissue morphology within injured articular cartilage. Also of interest is the nature of the structural changes of the superficial zone in response to injury, and obtaining accurate profiles of injured cartilage surfaces may determine if the changes observed in this study resemble, for example, similar reports of superficial zone fissuring following mechanical compression (12).

In the current study, we used immature bovine cartilage from a single anatomical site, the femoropatellar groove. It is worth noting, however, that previous studies have documented increased levels of endogenous lubricin in the superficial zone of adult bovine cartilage in comparison with tissue from younger animals (32). Other investigators have compared immature and adult cartilage from bovine and human joints in studies of injurious compression, and have

observed that certain responses vary with age and anatomical location. In experiments comparing the responses of immature bovine and adult human tissue, it was found that higher strains and faster strain rates were needed for human tissue in order to induce stresses and visible damage similar to those of immature bovine tissue, and that GAG loss in response to injury was lower in human tissue than bovine (15). Also, Patwari *et al.* (14) observed that human adult ankle cartilage is less susceptible to injurious compression than knee cartilage. Future studies may therefore examine the effect of injurious compression on lubricin biosynthesis in adult bovine and human cartilages from various anatomical locations in addition to immature bovine cartilage. Interestingly, a study using post-ACL injury human cartilage describe a disrupted surface layer with loss of GAG staining (57). In addition, another study describes the histological appearance of a human osteoarthritic cartilage sample as smooth, acellular and covered with a fibrous layer (58). A parallel could be drawn between these results and the amorphous, acellular and GAG/collagen-depleted surface layer of injured superficial zone-containing level 1 explants observed in this study (Figure 4, panels b & d).

It is worth considering that lubricin is expressed in multiple synovial tissues in addition to cartilage, including meniscus, tendon and ligament. Altered lubricin biosynthesis in response to pathophysiological biomechanical stimuli may also therefore have functional implications for these tissues. In addition, lubricin expression by both chondrocytes and synoviocytes has been shown to be affected by a variety of cytokines and growth factors (25, 42-44), and interaction with exogenous cytokines also modulates the response of articular cartilage to injurious compression (15). Factors external to cartilage may therefore modulate the response of the superficial zone to injury observed in this study, and these could be investigated by including cytokines and growth factors in the culture media post-injury, or by co-culturing cartilage with other synovial tissues as has been described previously (59).

## ACKNOWLEDGMENTS

**The histological expertise of Diane Peluso and Donna Gavin, Wyeth Research, is gratefully acknowledged. Monoclonal antibody 6-A-1 was generously provided by Dr. Clare Hughes and Prof. Bruce Caterson, Cardiff University, UK. SC, AJS, DHC and AJG acknowledge funding support from NIH Grant AR45779.**

## REFERENCES

1. Buckwalter JA, Mankin HJ, Grodzinsky AJ. Articular cartilage and osteoarthritis. *Instr Course Lect* 2005;54:465-80.
2. Kerin A, Patwari P, Kuettner K, Cole A, Grodzinsky A. Molecular basis of osteoarthritis: biomechanical aspects. *Cell Mol Life Sci* 2002;59(1):27-35.
3. Martel-Pelletier J. Pathophysiology of osteoarthritis. *Osteoarthritis Cartilage* 2004;12 Suppl A:S31-3.
4. Gelber AC, Hochberg MC, Mead LA, Wang NY, Wigley FM, Klag MJ. Joint injury in young adults and risk for subsequent knee and hip osteoarthritis. *Ann Intern Med* 2000;133(5):321-8.
5. Roos EM. Joint injury causes knee osteoarthritis in young adults. *Curr Opin Rheumatol* 2005;17(2):195-200.
6. Guilak F, Fermor B, Keefe FJ, Kraus VB, Olson SA, Pisetsky DS, et al. The role of biomechanics and inflammation in cartilage injury and repair. *Clin Orthop Relat Res* 2004(423):17-26.
7. Bendele AM. Animal models of osteoarthritis. *J Musculoskelet Neuronal Interact* 2001;1(4):363-76.
8. Feller J. Anterior cruciate ligament rupture: is osteoarthritis inevitable? *Br J Sports Med* 2004;38(4):383-4.
9. Kurz B, Lemke AK, Fay J, Pufe T, Grodzinsky AJ, Schunke M. Pathomechanisms of cartilage destruction by mechanical injury. *Ann Anat* 2005;187(5-6):473-85.
10. DiMicco MA, Patwari P, Siparsky PN, Kumar S, Pratta MA, Lark MW, et al. Mechanisms and kinetics of glycosaminoglycan release following in vitro cartilage injury. *Arthritis Rheum* 2004;50(3):840-8.
11. D'Lima DD, Hashimoto S, Chen PC, Colwell CW, Jr., Lotz MK. Impact of mechanical trauma on matrix and cells. *Clin Orthop Relat Res* 2001(391 Suppl):S90-9.
12. Ewers BJ, Dvoracek-Driksna D, Orth MW, Haut RC. The extent of matrix damage and chondrocyte death in mechanically traumatized articular cartilage explants depends on rate of loading. *J Orthop Res* 2001;19(5):779-84.
13. Kurz B, Jin M, Patwari P, Cheng DM, Lark MW, Grodzinsky AJ. Biosynthetic response and mechanical properties of articular cartilage after injurious compression. *J Orthop Res* 2001;19(6):1140-6.
14. Patwari P, Cheng DM, Cole AA, Kuettner KE, Grodzinsky AJ. Analysis of the relationship between peak stress and proteoglycan loss following injurious compression of human post-mortem knee and ankle cartilage. *Biomech Model Mechanobiol* 2007;6(1-2):83-9.

15. Patwari P, Cook MN, DiMicco MA, Blake SM, James IE, Kumar S, et al. Proteoglycan degradation after injurious compression of bovine and human articular cartilage in vitro: interaction with exogenous cytokines. *Arthritis Rheum* 2003;48(5):1292-301.
16. Torzilli PA, Grigiene R, Borrelli J, Jr., Helfet DL. Effect of impact load on articular cartilage: cell metabolism and viability, and matrix water content. *J Biomech Eng* 1999;121(5):433-41.
17. Sah RL, Doong JY, Grodzinsky AJ, Plaas AH, Sandy JD. Effects of compression on the loss of newly synthesized proteoglycans and proteins from cartilage explants. *Arch Biochem Biophys* 1991;286(1):20-9.
18. Chen CT, Bhargava M, Lin PM, Torzilli PA. Time, stress, and location dependent chondrocyte death and collagen damage in cyclically loaded articular cartilage. *J Orthop Res* 2003;21(5):888-98.
19. Thibault M, Poole AR, Buschmann MD. Cyclic compression of cartilage/bone explants in vitro leads to physical weakening, mechanical breakdown of collagen and release of matrix fragments. *J Orthop Res* 2002;20(6):1265-73.
20. Chen CT, Burton-Wurster N, Lust G, Bank RA, Tekoppele JM. Compositional and metabolic changes in damaged cartilage are peak-stress, stress-rate, and loading-duration dependent. *J Orthop Res* 1999;17(6):870-9.
21. Loening AM, James IE, Levenston ME, Badger AM, Frank EH, Kurz B, et al. Injurious mechanical compression of bovine articular cartilage induces chondrocyte apoptosis. *Arch Biochem Biophys* 2000;381(2):205-12.
22. Quinn TM, Grodzinsky AJ, Hunziker EB, Sandy JD. Effects of injurious compression on matrix turnover around individual cells in calf articular cartilage explants. *J Orthop Res* 1998;16(4):490-9.
23. Lee JH, Fitzgerald JB, Dimicco MA, Grodzinsky AJ. Mechanical injury of cartilage explants causes specific time-dependent changes in chondrocyte gene expression. *Arthritis Rheum* 2005;52(8):2386-95.
24. Charnley J. The lubrication of animal joints in relation to surgical reconstruction by arthroplasty. *Ann Rheum Dis* 1960;19:10-19.
25. Flannery CR, Hughes CE, Schumacher BL, Tudor D, Aydelotte MB, Kuettner KE, et al. Articular cartilage superficial zone protein (SZP) is homologous to megakaryocyte stimulating factor precursor and is a multifunctional proteoglycan with potential growth-promoting, cytoprotective, and lubricating properties in cartilage metabolism. *Biochem Biophys Res Commun* 1999;254(3):535-41.
26. Ikegawa S, Sano M, Koshizuka Y, Nakamura Y. Isolation, characterization and mapping of the mouse and human PRG4 (proteoglycan 4) genes. *Cytogenet Cell Genet* 2000;90(3-4):291-7.
27. Jay GD, Tantravahi U, Britt DE, Barrach HJ, Cha CJ. Homology of lubricin and superficial zone protein (SZP): products of megakaryocyte stimulating factor (MSF) gene expression by human synovial fibroblasts and articular chondrocytes localized to chromosome 1q25. *J Orthop Res* 2001;19(4):677-87.
28. Kuroda M, Wang X, Sok J, Yin Y, Chung P, Giannotti JW, et al. Induction of a secreted protein by the myxoid liposarcoma oncogene. *Proc Natl Acad Sci U S A* 1999;96(9):5025-30.
29. Marcelino J, Carpten JD, Suwairi WM, Gutierrez OM, Schwartz S, Robbins C, et al. CACP, encoding a secreted proteoglycan, is mutated in camptodactyly-arthropathy-coxa vara-pericarditis syndrome. *Nat Genet* 1999;23(3):319-22.

30. Schumacher BL, Block JA, Schmid TM, Aydelotte MB, Kuettner KE. A novel proteoglycan synthesized and secreted by chondrocytes of the superficial zone of articular cartilage. *Arch Biochem Biophys* 1994;311(1):144-52.
31. Rees SG, Davies JR, Tudor D, Flannery CR, Hughes CE, Dent CM, et al. Immunolocalisation and expression of proteoglycan 4 (cartilage superficial zone proteoglycan) in tendon. *Matrix Biol* 2002;21(7):593-602.
32. Schumacher BL, Hughes CE, Kuettner KE, Caterson B, Aydelotte MB. Immunodetection and partial cDNA sequence of the proteoglycan, superficial zone protein, synthesized by cells lining synovial joints. *J Orthop Res* 1999;17(1):110-20.
33. Schumacher BL, Schmidt TA, Voegtline MS, Chen AC, Sah RL. Proteoglycan 4 (PRG4) synthesis and immunolocalization in bovine meniscus. *J Orthop Res* 2005;23(3):562-8.
34. Sun Y, Berger EJ, Zhao C, An KN, Amadio PC, Jay G. Mapping lubricin in canine musculoskeletal tissues. *Connect Tissue Res* 2006;47(4):215-21.
35. Jay GD. Lubricin and surfacing of articular joints. *Curr Opin Orthop* 2004;15:335-359.
36. Rhee DK, Marcelino J, Baker M, Gong Y, Smits P, Lefebvre V, et al. The secreted glycoprotein lubricin protects cartilage surfaces and inhibits synovial cell overgrowth. *J Clin Invest* 2005;115(3):622-31.
37. Jay GD, Torres JR, Warman ML, Laderer MC, Breuer KS. The role of lubricin in the mechanical behavior of synovial fluid. *Proc Natl Acad Sci U S A* 2007;104(15):6194-9.
38. Jay GD, Harris DA, Cha CJ. Boundary lubrication by lubricin is mediated by O-linked beta(1-3)Gal-GalNAc oligosaccharides. *Glycoconj J* 2001;18(10):807-15.
39. Jones AR, Gleghorn JP, Hughes CE, Fitz LJ, Zollner R, Wainwright SD, et al. Binding and localization of recombinant lubricin to articular cartilage surfaces. *J Orthop Res* 2007;25(3):283-92.
40. Elsaid KA, Jay GD, Chichester CO. Reduced expression and proteolytic susceptibility of lubricin/superficial zone protein may explain early elevation in the coefficient of friction in the joints of rats with antigen-induced arthritis. *Arthritis Rheum* 2007;56(1):108-16.
41. Young AA, McLennan S, Smith MM, Smith SM, Cake MA, Read RA, et al. Proteoglycan 4 downregulation in a sheep meniscectomy model of early osteoarthritis. *Arthritis Res Ther* 2006;8(2):R41.
42. Jones AR, Flannery CR. Bioregulation of lubricin expression by growth factors and cytokines. *Eur Cell Mater* 2007;13:40-5; discussion 45.
43. Khalafi A, Schmid TA, Neu C, Reddi AH. Expression of superficial zone protein (SZP) in articular cartilage: stimulation by bone morphogenic protein-7 and growth factors. *Trans Orthop Res Soc* 2006;31:1360.
44. Ohno S, Schmid T, Tanne Y, Kamiya T, Honda K, Ohno-Nakahara M, et al. Expression of superficial zone protein in mandibular condyle cartilage. *Osteoarthritis Cartilage* 2006;14(8):807-813.
45. Grad S, Lee CR, Gorna K, Gogolewski S, Wimmer MA, Alini M. Surface motion upregulates superficial zone protein and hyaluronan production in chondrocyte-seeded three-dimensional scaffolds. *Tissue Eng* 2005;11(1-2):249-56.
46. Grad S, Li Z, Wimmer MA, Alini M. Articular motion stimulates the PRG4 gene expression in chondrocytes from both superficial and deep zone cartilage. *Trans Orthop Res Soc* 2006;31:1345.

47. Nugent GE, Aneloski NM, Schmidt TA, Schumacher BL, Voegtline MS, Sah RL. Dynamic shear stimulation of bovine cartilage biosynthesis of proteoglycan 4. *Arthritis Rheum* 2006;54(6):1888-96.
48. Nugent GE, Schmidt TA, Schumacher BL, Voegtline MS, Bae WC, Jadin KD, et al. Static and dynamic compression regulate cartilage metabolism of PRoteoGlycan 4 (PRG4). *Biorheology* 2006;43(3-4):191-200.
49. Nugent-Derfus GE, Takara T, O'Neill J K, Cahill SB, Gortz S, Pong T, et al. Continuous passive motion applied to whole joints stimulates chondrocyte biosynthesis of PRG4. *Osteoarthritis Cartilage* 2007;15(5):566-74.
50. Frank EH, Jin M, Loening AM, Levenston ME, Grodzinsky AJ. A versatile shear and compression apparatus for mechanical stimulation of tissue culture explants. *J Biomech* 2000;33(11):1523-7.
51. Schinagl RM, Gurskis D, Chen AC, Sah RL. Depth-dependent confined compression modulus of full-thickness bovine articular cartilage. *J Orthop Res* 1997;15(4):499-506.
52. Gleghorn JP, Jones AR, Flannery CR, Bonassar LJ. Boundary mode frictional properties of engineered cartilaginous tissues. *Eur Cell Mater* 2007;14:20-8; discussion 28-9.
53. Gleghorn JP, Bonassar LJ. Mapping of cartilage lubrication modes using Stribeck analyses. *Trans Orthop Res Soc* 2007;32:0613.
54. Schmidt TA, Sah RL. Effect of synovial fluid on boundary lubrication of articular cartilage. *Osteoarthritis Cartilage* 2006.
55. Schmidt TA, Gastelum NS, Nguyen QT, Schumacher BL, Sah RL. Boundary lubrication of articular cartilage: role of synovial fluid constituents. *Arthritis Rheum* 2007;56(3):882-91.
56. Schmidt TA, Sah RL. Effect of synovial fluid on boundary lubrication of articular cartilage. *Osteoarthritis Cartilage* 2007;15(1):35-47.
57. Nelson F, Billingham RC, Pidoux I, Reiner A, Langworthy M, McDermott M, et al. Early post-traumatic osteoarthritis-like changes in human articular cartilage following rupture of the anterior cruciate ligament. *Osteoarthritis Cartilage* 2006;14(2):114-9.
58. Plaas A, Osborn B, Yoshihara Y, Bai Y, Bloom T, Nelson F, et al. Aggrecanolytic in human osteoarthritis: confocal localization and biochemical characterization of ADAMTS5-hyaluronan complexes in articular cartilages. *Osteoarthritis Cartilage* 2007;15(7):719-34.
59. Lee JH, Bai Y, Flannery CR, Sandy JD, Plaas A, Grodzinsky AJ. Cartilage mechanical injury and co-culture with joint capsule tissue increase abundance of ADAMTS-5 protein and aggrecan G1-NITEGE product. *Trans Orthop Res Soc* 2006;31:214.

## FIGURE LEGENDS

**Figure 1.** Loading device used to submit bovine cartilage explants from superficial and deep zones to injurious compression. **A**, Custom incubator-housed loading apparatus and **B**, polysulfone chamber used to house cartilage explants during unconfined compression. **C**, Division of cartilage explants from the femoropatellar groove into level 1, containing superficial zone (SZ), and level 2.

**Figure 2.** Western blot analysis of soluble and cartilage-associated lubricin after 48 hours in culture post-injury, using monoclonal antibody 6-A-1. **A**, Soluble lubricin protein in conditioned media. Level 2 conditioned media was concentrated 10-fold prior to SDS-PAGE. **B**, Cartilage-associated lubricin, as assessed by analyses of 1.5 M NaCl cartilage extracts. The migration position of molecular weight standards is indicated.

**Figure 3.** Quantitative RT-PCR analyses of lubricin mRNA expression in bovine explants following injurious compression. **A**, Lubricin mRNA levels in level 1 and level 2 cartilage after 48 hours in culture post-injury. **B**, Lubricin mRNA levels in level 1 cultures 2 and 6 days post-injury. Lubricin mRNA levels were normalized to GAPDH and expressed relative to those in control cultures for each level. Values are the mean and standard deviation of 3 separate analyses. \*Values significantly different to free-swelling control levels ( $p < 0.05$ , Student's t-test).

**Figure 4.** Histological analysis of level 1 (a-d) and level 2 (e-h) articular cartilage explants, after 2 days in culture following mechanical injury. Sections were stained with Safranin O for

glycosaminoglycan (a, b, e, f) or trichrome for collagen (c, d, g, h). The articular cartilage surface is oriented at the top of each panel. Bar = 100 $\mu$ m.

**Figure 5.** Immunohistochemical detection of lubricin in injured level 1 cartilage explants and free-swelling controls after 48 hours in culture post-injury. Sections were incubated with anti-lubricin antibody G35 (a, b) or rabbit IgG negative control (c, d). The articular cartilage surface is oriented at the top of each panel and is indicated by the arrowhead. Bar = 100 $\mu$ m.

**Figure 6.** Friction testing of cartilage explants after 48 hours in culture following injurious compression to determine the coefficient of friction,  $\mu$  equilibrium ( $\mu_{eq}$ ). **A**, Friction testing of control and injured, level 1 (L1) and level 2 (L2) explants conducted in PBS (non-extracted). A second test was conducted with the same explants after 1.5 M NaCl extraction followed by a 1 hour equilibration period in PBS (1.5 M NaCl-extracted). \*Significantly different to level 1 control; \*\*significantly different to corresponding non-extracted condition ( $p < 0.05$ , Tukey's post hoc test). **B**, Friction testing of level 1 explants subsequent to 1.5 M NaCl extraction. Explants were soaked in equine synovial fluid for 1 hour and tested in PBS (ESF soak). Explants were then tested with ESF as the bathing solution (ESF). Data shown are the mean and standard deviation of 6 separate analyses. \*Significantly different to control ( $p < 0.05$ , Tukey's post hoc test).



Figure 1

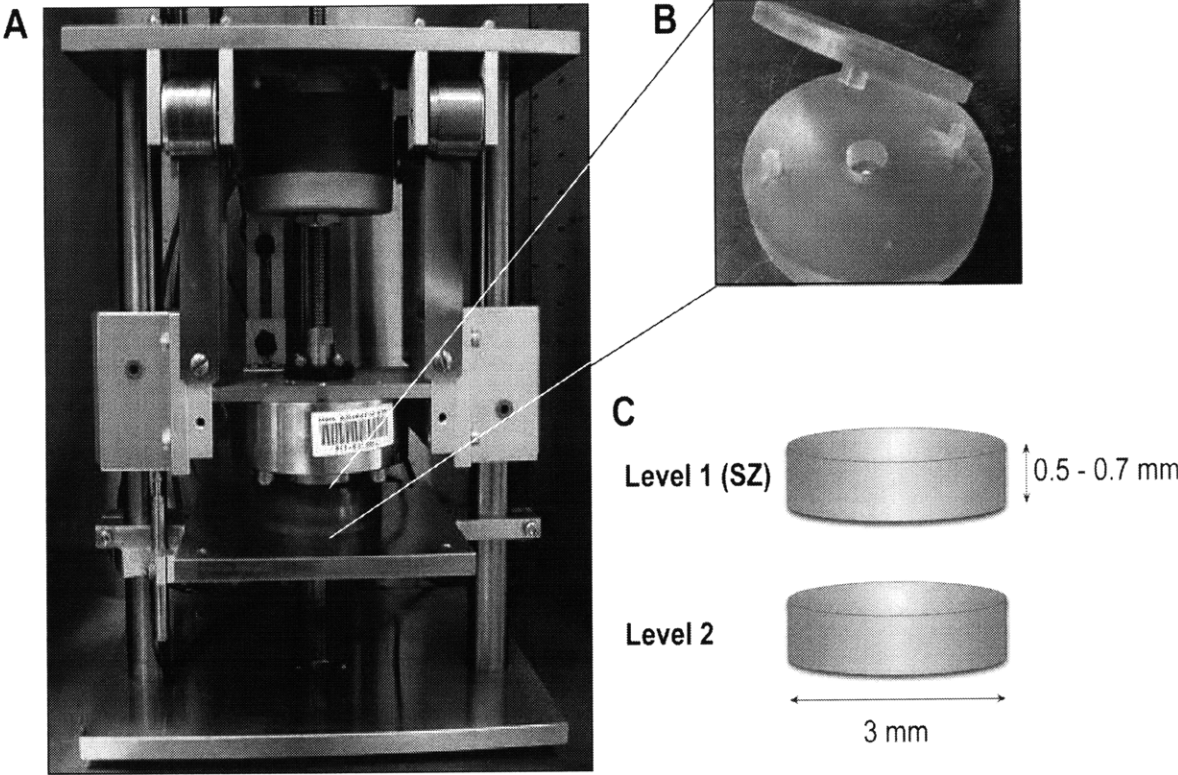


Figure 2

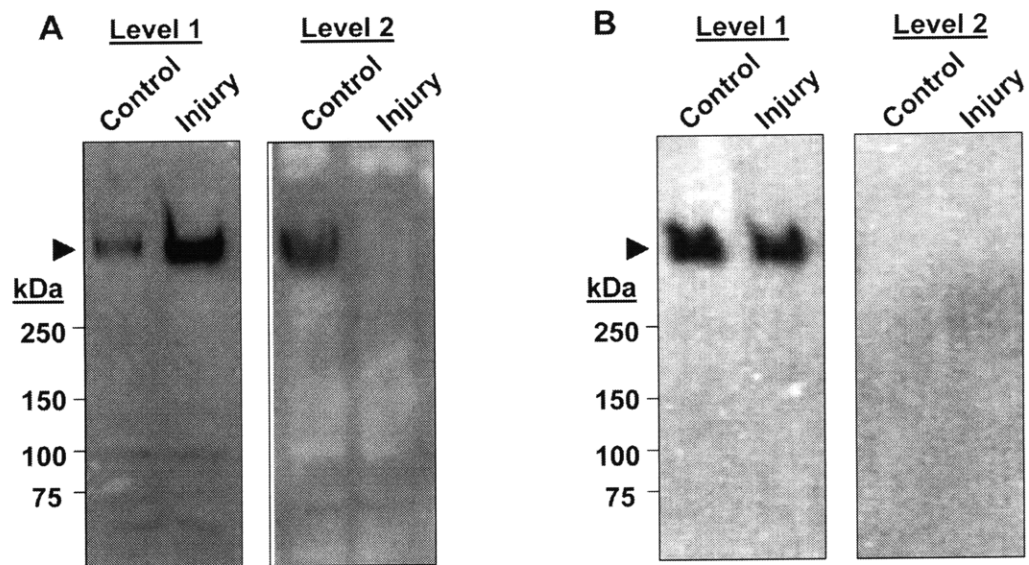
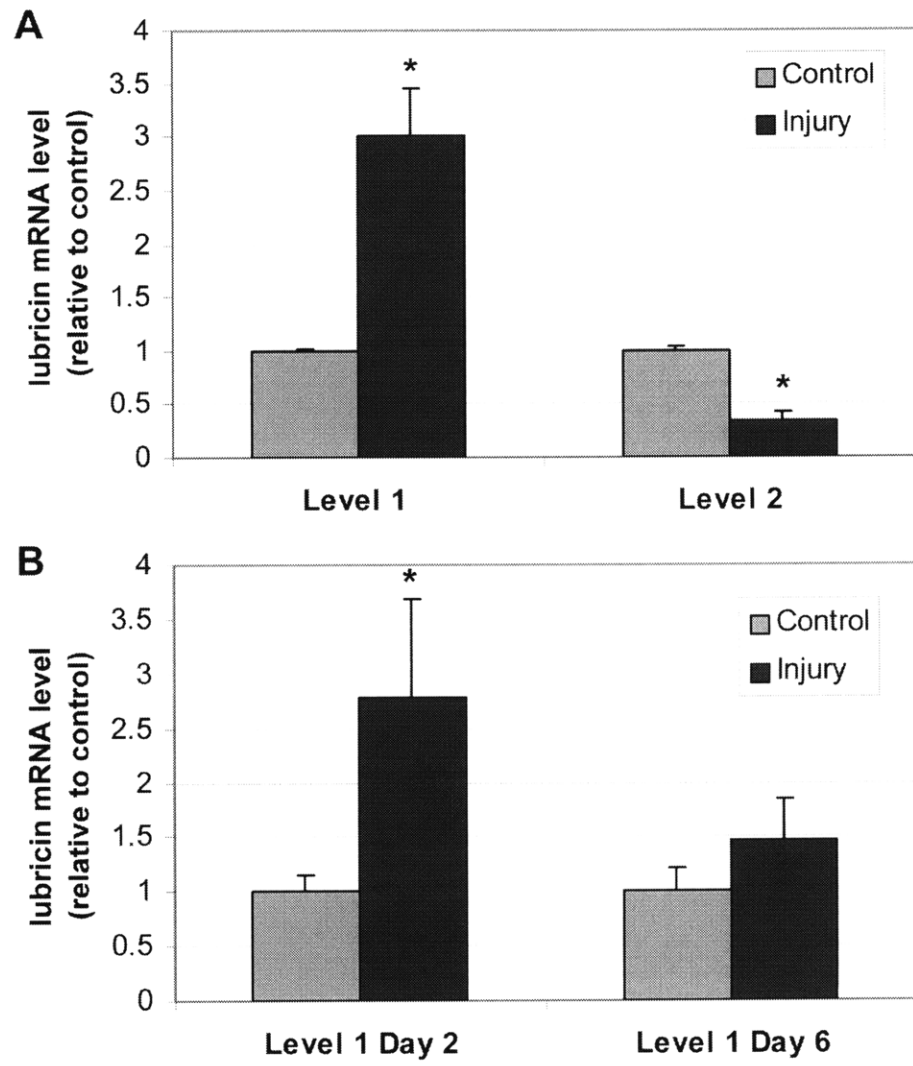
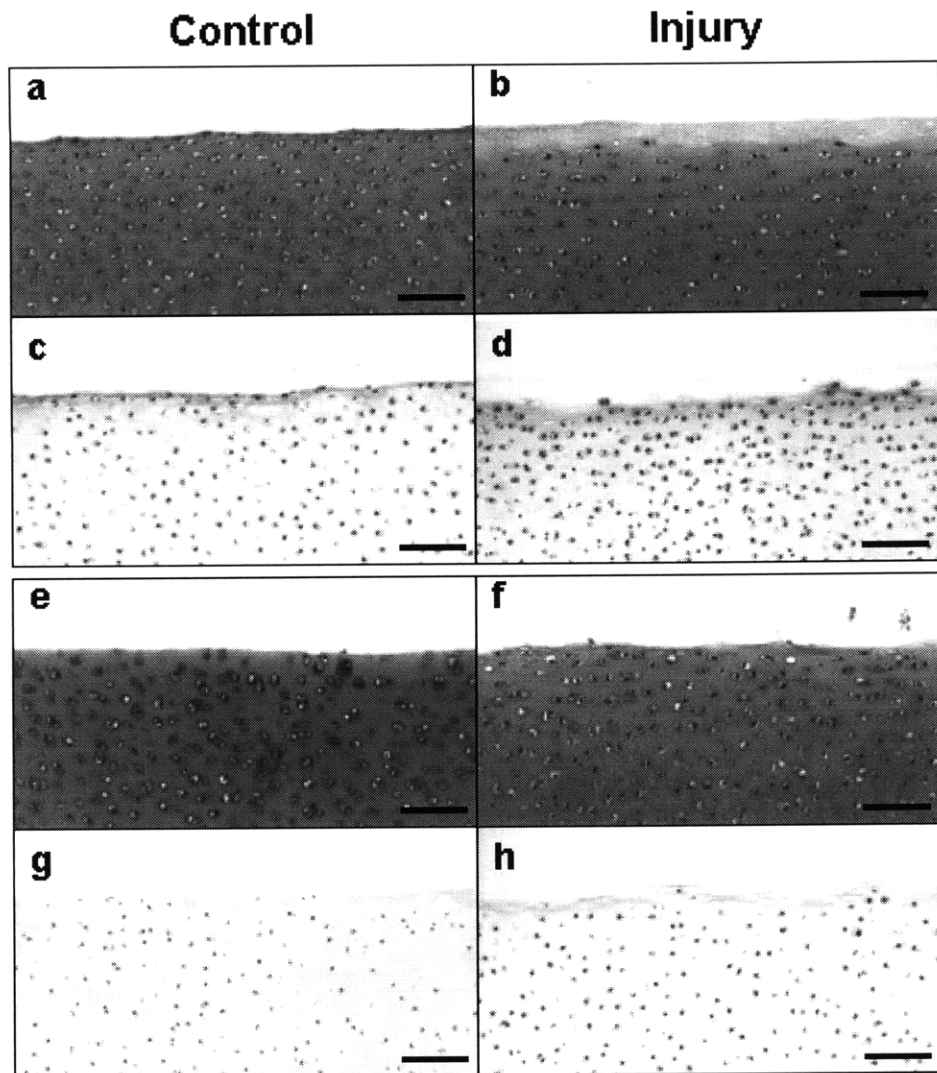


Figure 3



**Figure 4**



**Figure 5**

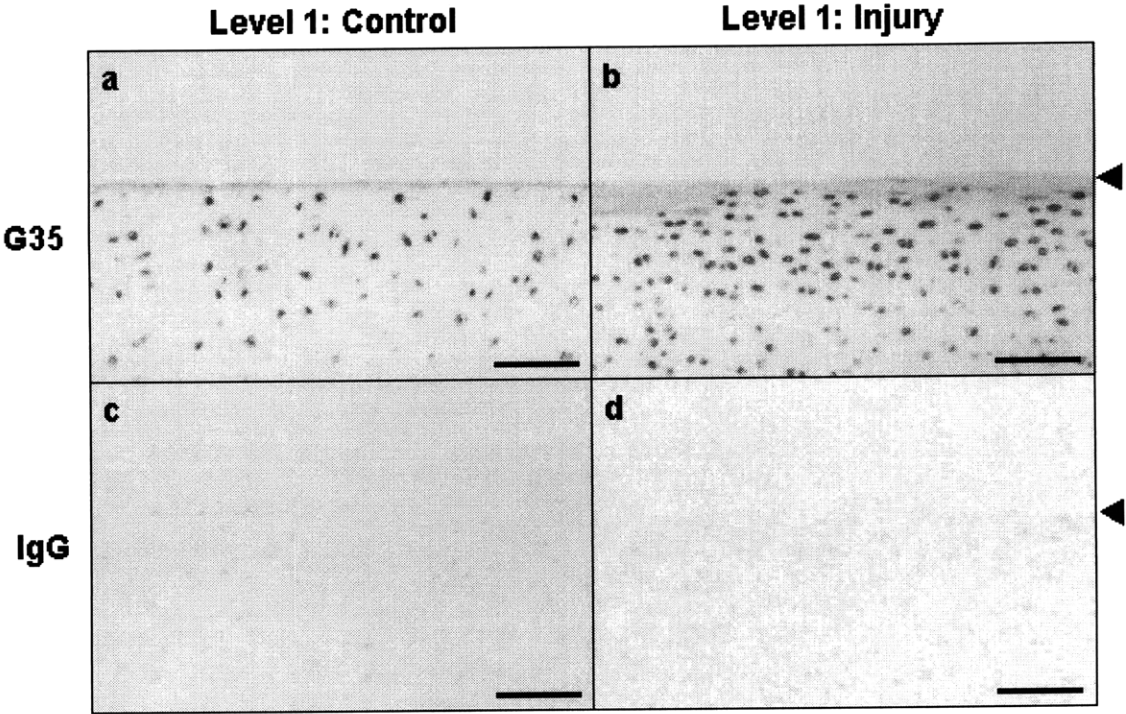
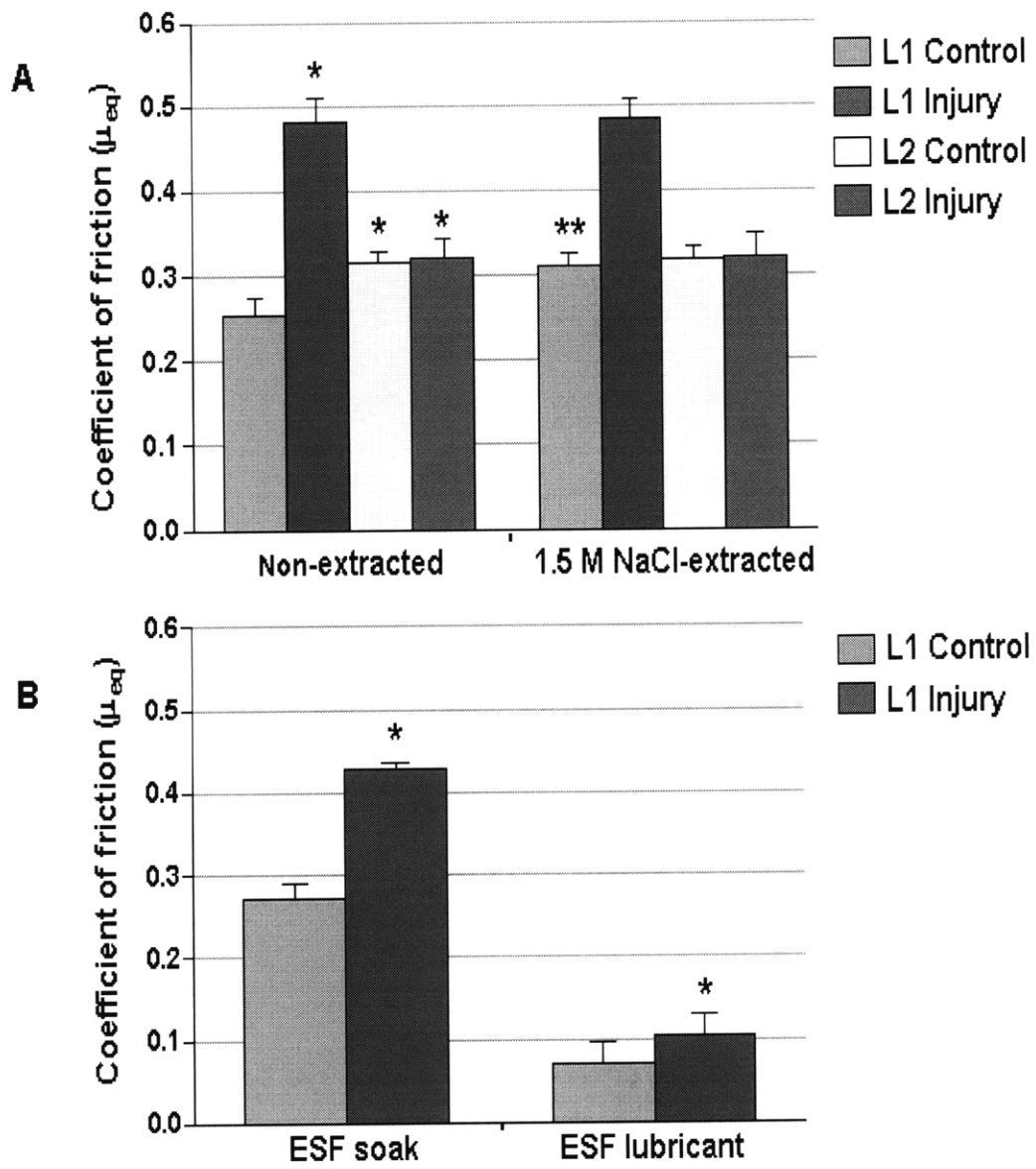
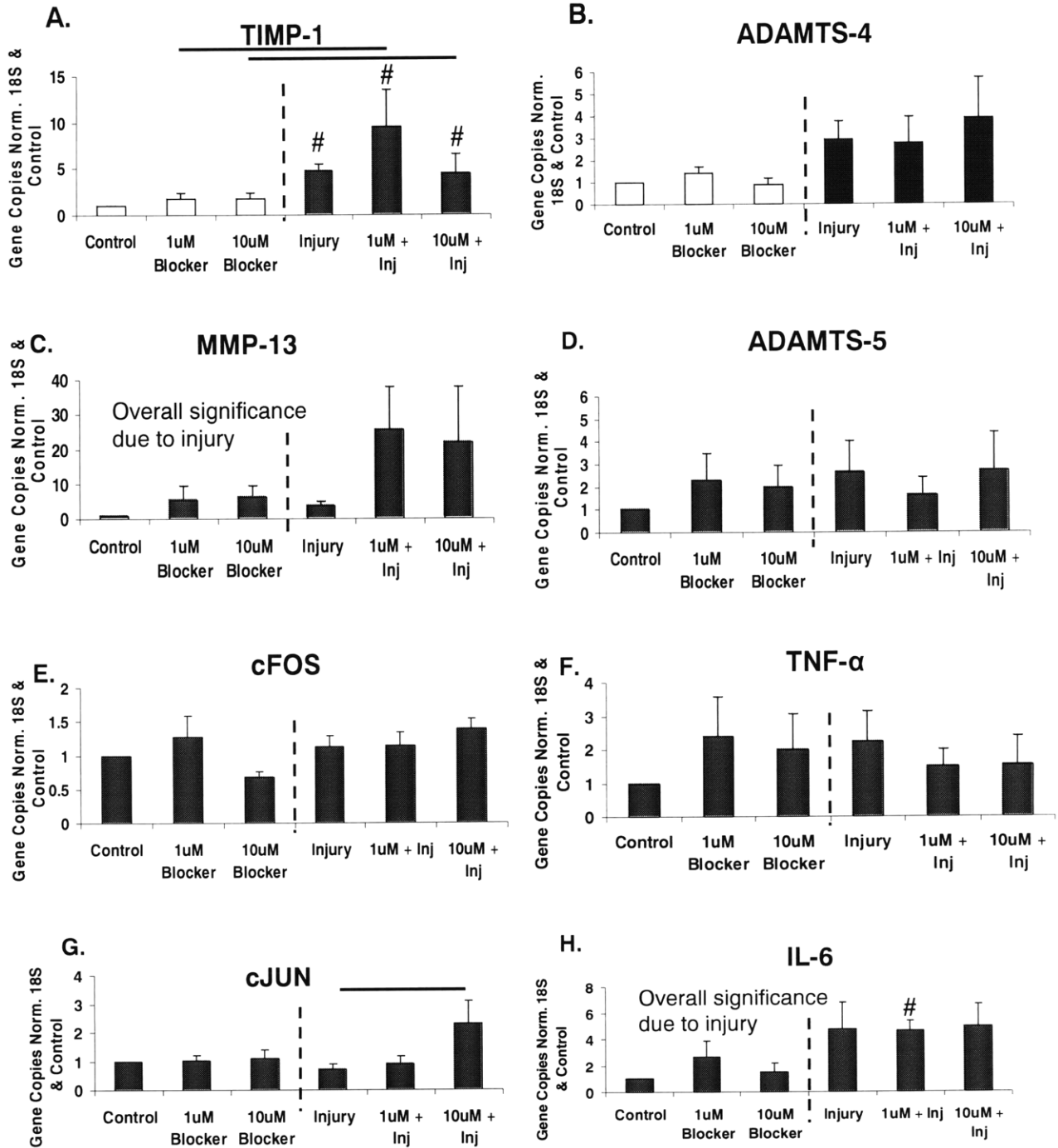


Figure 6



## B. Gene Expressions due to TGF- $\beta$ Blocker



n=4 animals; bar  $\rightarrow$  p<0.05 and #  $\rightarrow$  p<0.05 relative to control. Statistics were performed using linear mixed model with animal as the random variable and injury and the respective blocker concentration as the fixed variables.

## C. Derivation for Hydraulic Permeability

### Constants

$$L = 10\mu\text{m}$$

$$H = 1\text{kPa}$$

$$\mu = 0.001\text{Pa} \cdot \text{s} \text{ (Cytosol is mostly water)}$$

$$\xi = 15\text{nm} \quad \text{(The pore size ranges from 10~20nm)}$$

$$\phi = 0.43 \quad [50]$$

### Fiber Matrix Model

This model describes fluid flowing perpendicular to an array of cylindrical rigid rods with pore size  $\xi$ .

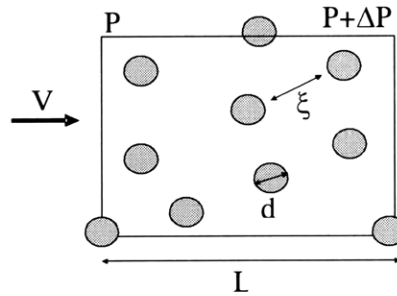


**Figure C.1.** Fluid flow with velocity  $V$  across a network of rigid rods bounded by a cubic Gaussian surface of length  $L$ .

Let  $N$  be the number of fibers contained in a cube with volume  $L^3$ , shown in Fig. 13:

$$N = \left(\frac{L}{\xi}\right)^2$$

Let  $F$  be the total fluid shear force across one rigid rod where  $\mu$  is the fluid viscosity:

$$F = \left(\frac{\mu V}{d}\right) \pi dL$$

A force balance on either side yields the following:

$$\Delta PL^2 \approx NF = \left(\frac{L}{\xi}\right)^2 \mu V \pi L$$

Since  $V = -k\nabla P$ ,

$$k = \frac{VL}{\Delta P} = \frac{\xi^2}{\mu\pi} = 7.162 * 10^{-14} \frac{\text{m}^4}{\text{N} \cdot \text{s}}$$

$$\therefore \tau = \frac{L^2}{Hk} = 1.4\text{s}$$



### Poiseuille's Flow through Parallel Capillary Tubes Model:

Let  $q$  be the volume flow rate through one cylinder according to the Poiseuille's Flow:

$$q = \frac{\pi \xi^4}{128\mu} \frac{dp}{dx}$$

Let  $\phi$  be the porosity:

$$\phi = \frac{\pi \xi^2 L N_A}{4AL}$$

Fluid velocity,  $V$ , is the total flow rate per cross-sectional area where  $N_A$  is the # of cylinders per unit area

$$\begin{aligned} V &= \frac{qAN_A}{A} = \frac{\pi \xi^4 N_A}{128\mu} \frac{dp}{dx} \\ k &= \frac{\pi \xi^4 N_A}{128\mu} = \frac{\xi^2 \phi}{32\mu} = 3.02 * 10^{-15} \frac{m^4}{N \cdot s} \\ \therefore \tau &= \frac{L^2}{Hk} = 33.07s \end{aligned}$$

### Charras Model

This model concept closely resembles A2 except it states that the actual fluid velocity through the media is  $V_{ACT} \sim \frac{\xi^2 \partial_x p}{\mu}$ , but the apparent velocity through the porous media is  $V_{APP} \sim \frac{\xi^2 \partial_x p}{\mu \phi^{1/3}}$ .

$$\begin{aligned} \therefore k &\sim \frac{\xi^2}{\mu \phi^{1/3}} = 2.98 * 10^{-13} \frac{m^4}{N \cdot s} \\ \therefore \tau &= \frac{L^2}{Hk} = 0.34s \end{aligned}$$

However, according to Salem,  $V_{APP} \sim \frac{\xi^2 \partial_x p}{\mu}$  and  $V_{ACT} \sim \frac{\xi^2 \partial_x p}{\phi \mu}$  [51].

$$\begin{aligned} \therefore k &\sim \frac{\xi^2}{\mu} = 2.25 * 10^{-13} \frac{m^4}{N \cdot s} \\ \therefore \tau &= \frac{L^2}{Hk} = 0.44s \end{aligned}$$

### Kozeny-Carman Model

The Kozeny-Carman equation developed from the Hagen-Poiseuille equation describes the relationship between porosity and permeability while incorporating the geometry of the grain or fiber. Therefore, it has many applications in transport through granular and fibrous structures. If the cell is modeled as a fiber matrix media, then the general Kozeny-Carman equation reduces to the following where  $c$  is the Kozeny constant that depends on the arrangement and packing density and  $r_f$  is the fiber radius [52]:

$$k = \frac{r_f^2}{\mu c} \frac{\phi^3}{(1-\phi)^2}$$

If the cell is assumed to be a porous media with overlapping fibers distributed randomly in 3-D space, then the empirical permeability is determined to be the following where  $\varepsilon_p$  is 0.037, and  $\alpha$  is 0.661 [53].

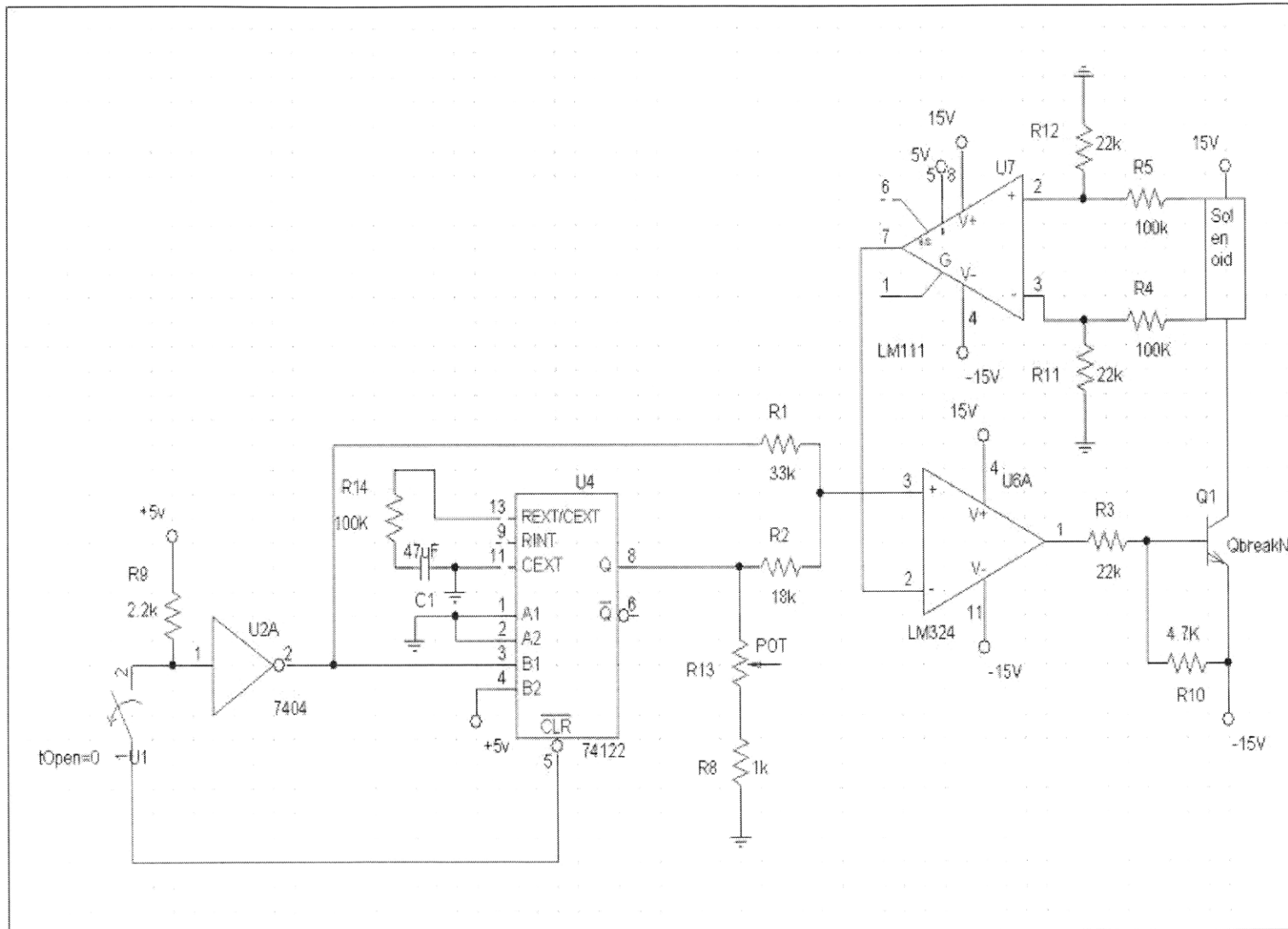
$$k = \frac{\phi_f^2}{8\mu \ln^2 \phi} \frac{(\phi - \varepsilon_p)^{\alpha+2}}{(1 - \varepsilon_p)^\alpha [(\alpha + 1)\phi - \varepsilon_p]^2}$$

$R_f$  for the cytoskeleton fibrils is around 7.5 nm on average. Therefore, the permeability and the corresponding time constant are given by the following:

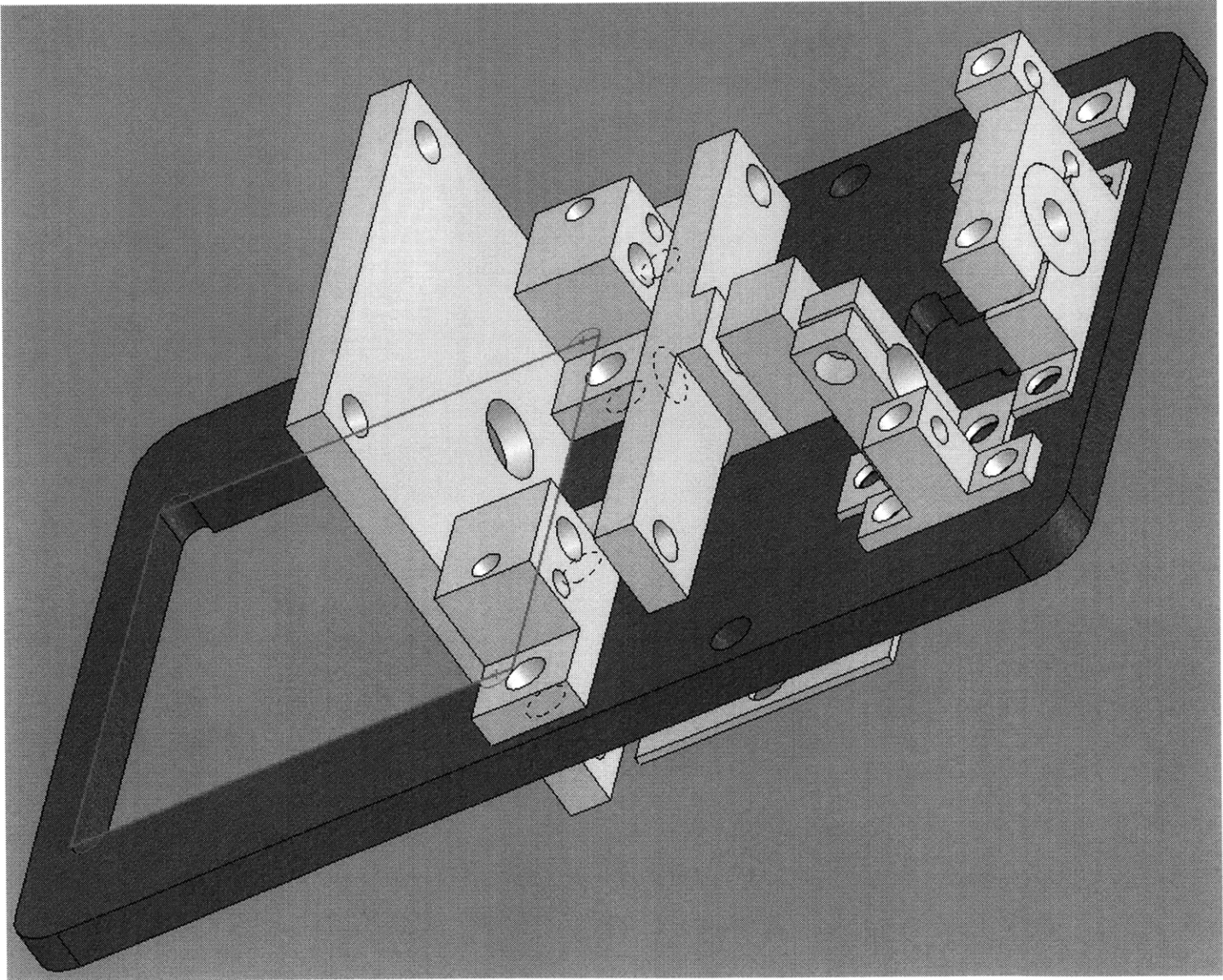
$$k=9.614*10^{-16} \text{ m}^4/\text{N*s}$$

$$\tau=104 \text{ s}$$

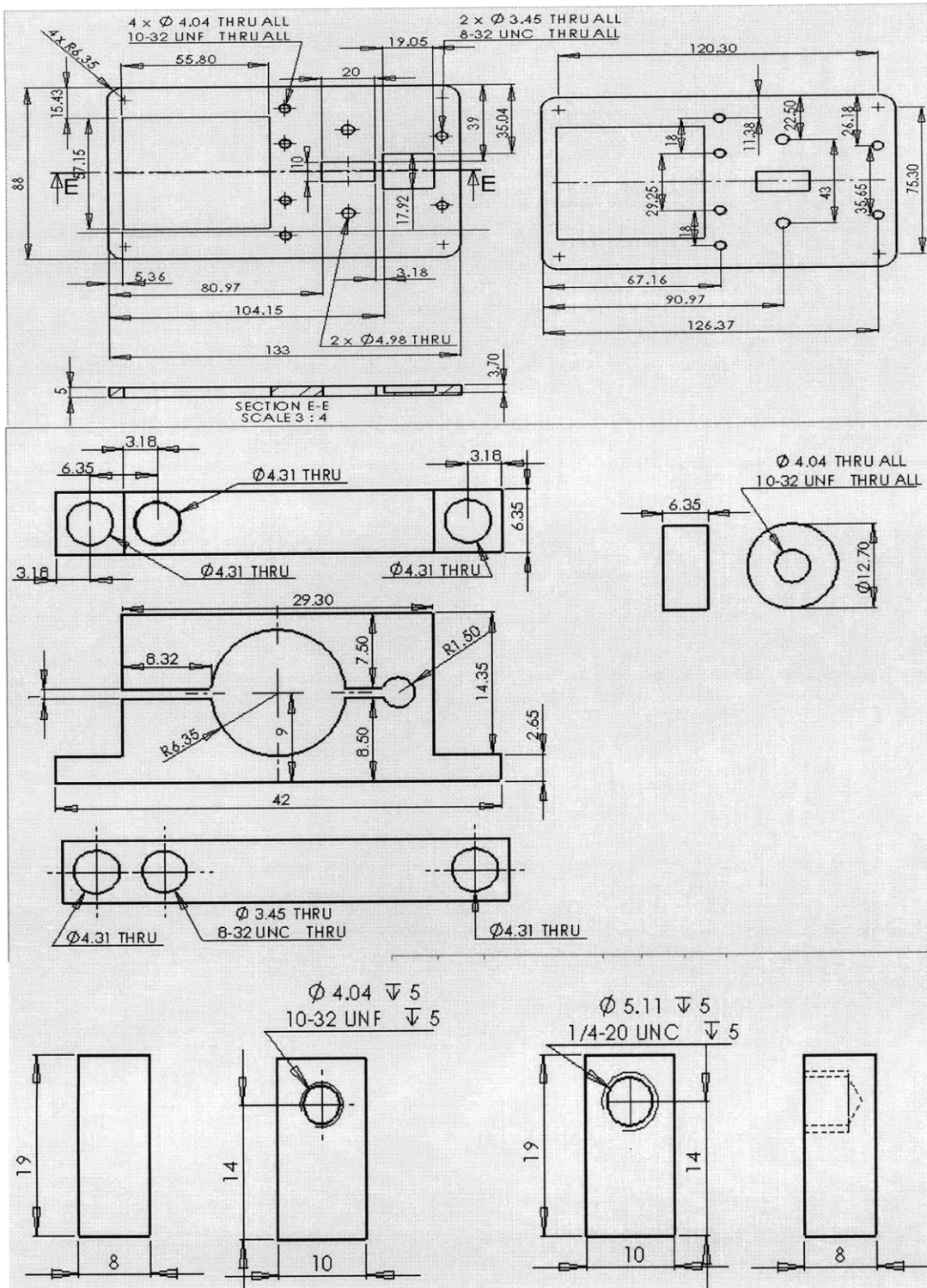
## D. Schematic of the Solenoid Output Circuit for Actuator Design



**E. Illustration of Mechanical Actuator 2.0 Platform**



# F. Blueprint of Selected Parts



Sheet3

